Characterisation of the synergistic vancomycin-furazolidone action against *Escherichia coli*.

A thesis presented in partial fulfilment of the requirements for the degree of

Masters

in

Biochemistry

at Massey University, Manawatū,

New Zealand.

Raveen Marlon Weerasinghe

2017

Abstract

The use of antibiotic combinations is garnering increased interest in the recent years due to the spread of antibiotic-resistant bacteria. The shortage of antibacterial therapy options is particularly severe for infections caused by Gram-negative bacteria, due to the formidable barrier to molecules > 600 Da imposed by the outer membrane. Vancomycin is a large glycopeptide antibiotic to which the outer membrane is poorly permeable, hence the minimal inhibitory concentration of this antibiotic for *Escherichia coli* is very high (~500 mg/L). Due to the resistance of *E. coli* and other Gram-negative pathogens to an increasing number of < 600 Da antibiotics including beta lactams, aminoglycosides and quinolones, enabling vancomycin use on Gram-negative bacteria would be valuable. Furazolidone was reported to increase sensitivity of *E. coli* to vancomycin, and this interaction has been investigated in this thesis in order to explore the potential of the vancomycin-furazolidone combination for clinical applications. The initial analysis of the vancomycin-furazolidone synergy demonstrated that their interaction is synergistic rather than merely additive. Furthermore, effectiveness of this combination for growth inhibition and eradication of *E. coli* biofilm was investigated. However, despite the synergy between vancomycin and furazolidone, the concentration of vancomycin in combinations required for growth inhibition and killing of *E. coli* in a planktonic mode and as a biofilm was above the nephrotoxicity (toxicity in the kidneys) threshold and therefore too high to treat infections with this organism systemically. However, by adding deoxycholic acid to the combination, the bactericidal vancomycin concentration was decreased below the nephrotoxicity threshold. The mechanism of synergy in the planktonic mode of growth was investigated through the analysis of *E. coli* gene-knock-out mutants and it was observed that TolC, the outer membrane channel common to a number of efflux systems (exporting enterobactin, xenobiotics and metabolites) is likely to be involved in vancomycin-furazolidone synergy. However, it was not possible to reliably pinpoint any particular efflux pump or enterobactin accumulation as factors in synergy. Using the genetic approach, it was found that DNA excision repair endonuclease UvrABC was ruled out as a factor involved in synergy. Overall this study characterised the synergy between vancomycin and furazolidone, initiated the enquiry into the mechanisms of interaction between these two antibiotics and examined its effectiveness against biofilms.

Acknowledgements

I would first like to thank my supervisor, Associate Professor Jasna Rakonjac for giving me the opportunity to do this MSc under her on such short notice and for all the guidance and patience that she has shown me over this past year. Her knowledge and expertise in this field has been of tremendous help during this study and has prevented many headaches.

I would also like to thank my fellow lab mates from Helipad/D4.01: Vuong, Sofia, Stefanie, Fabian, Georgia and Marina. Thank you, guys, for all the assistance and help you have given me and for making my time at Massey a great and a memorable experience. I'll miss you guys! I would like to extend my thanks to IFS in Massey University as a whole. It is a truly wonderful place to study and the skills that I have gained here will no doubt be extremely useful for later in life.

Also to my friends in Otago: Aran, Will, Shirley, Chris and Jithendra. Thank you, guys, for all your support during my years at Otago and in my decision to move to Massey and for being good mates throughout all these years.

Finally, I would like to thank my parents, Raja and Manel. I could not have done this year without either of you and words cannot express all the love and support you have shown me. I would also like to apologise to you for putting up with me during my whinging sessions which were enough to last a lifetime.

Abbreviations

%	Percentage
$	Dollars
°C	Degrees Celsius
µL	Microlitre
µm	Micrometre
8-OHdG	8-hydroxydeoxyguanosine
ABC	Adenosine triphosphate binding cassette
AMR	Antimicrobial resistance
ATP	Adenosine triphosphate
$CaCl_2$	Calcium chloride
CAUTI	Catheter associated infections
CDC	Centres for Disease Control and Prevention
CFU/mL	Colony forming units per millilitre
Da	Daltons
DMSO	Dimethyl sulfoxide
DNA	Deoxyribonucleic acid
DOC	Sodium deoxycholate
ECM	Extracellular matrix
ESBL	Extended-spectrum beta-lactamase
FICI	Fractional Inhibitory Concentration Index
g	Grams
g/L	Grams per litre
HepG2	Hepatoma

kDa	Kilodaltons
Km^R	Kanamycin resistance marker
kPa	Kilopascals
LPS	Lipopolysaccharide
MATE	Multidrug and toxic efflux
MBC	Minimal Bactericidal Concentration
MBEC	Minimal Biofilm Eradication Concentration
MBIC	Minimal Biofilm Inhibitory Concentration
mg/kg	Milligram per kilogram
mg/kg/day	Milligram per kilogram per day
mg/L	Milligram per litre
$MgSo_4$	Magnesium sulfate
MIC	Minimal Inhibitory Concentration
mL	Millilitre
mM	Millimolar
MRSA	Methicillin resistant *S. aureus*
Na	Sodium
nm	Nanometre
NO	Nitric oxide
NZ	New Zealand
OD	Optical density
ORF	Open reading frame
PMF	Proton motive force
RND	Resistance nodulation division

Rpm	Revolutions per minute
ROS	Reactive oxygen species
SOC	Super Optimal broth with Catabolite repression
SMR	Small multidrug resistance
USA	United States of America

Table of Contents

List of Figures

List of tables

1 Introduction

1.1 Antimicrobial resistance

Antimicrobial resistance (AMR) is a global phenomenon in which bacteria becomes resistant to current antibiotic treatments. Antibiotics have been described as one of the greatest advances of modern medicine and surgery. They are typically used to treat bacterial infections in patients and animals and are widely used in the agricultural industry (Carey and McNamara, 2014, Ventola, 2015). Additionally, it has been reported in the United States, that the use of antibiotics has resulted in a significant increase in life expectancy from 56.4 years in 1920 in the pre-antibiotic era to 80 years (Ventola, 2015). The recent rise in AMR impacts greatly on the health of the patients and the economic burden on governments (Cosgrove and Carmeli, 2003).

The period from 1930 – 1960 was described as the 'golden age' of antibiotics with most of the currently used antibiotics being discovered in this period (Davies, 2006). However, in the past few decades, pathogen resistance to antibiotics started to emerge, including most notably methicillin-resistant *Staphylococcus aureus* (MRSA) and extended-spectrum beta-lactamase (ESBL) producing bacteria. It has been reported that over 2 million people are infected with antibiotic resistance bacterial strains in the US alone each year and from this, over 25 000 people die and this is further exacerbated in developing countries (Carey and McNamara, 2014, Planta, 2007). In New Zealand, 2.6% of the isolated blood culture samples were tested as ESBL positive in 2006, however, in 2011 this had increased to 3.8% (Thomas *et al.*, 2014).

In addition to patient mortality, AMR is a major clinical and economic burden. When facing AMR infections, healthcare professionals are more likely to use more toxic and expensive treatments as a result of the frontline treatments being inefficient at treating these infections. In the US, it has been found that the average cost for treating patients with AMR infections ranges from $18 500 - $29 000 (Ventola, 2015). Annually in the US alone, it is estimated by the Centres for Disease Control and Prevention (CDC) that approximately $20 billion is used for health care costs of AMR and an additional $35 billion is lost in antimicrobial production (Littmann, 2015). AMR has been in particular a large concern to developing countries as the rates of AMR are generally higher and many second or third line drugs are inaccessible or are too expensive for most patients (Littmann, 2015).

1.2 Antimicrobial resistance in Gram-negative bacteria

While AMR is a big issue with both Gram-positive and Gram-negative bacteria, it has been reported that successful development of novel drugs to treat Gram-negative infections lags behind that of Gram-positive infections (WHO, 2014). Many frontline antibiotics such as vancomycin and bacitracin that are effective against Gram-positive bacteria are shown to be very ineffective against Gram-negative bacteria due to the difference in cell envelope structure (Zhou *et al.*, 2015). The main difference between the two different groups is that Gram-negative bacteria have an outer membrane that acts as a selective barrier for molecules whose molecular weight is above 600 Da. Studies have shown that antibiotics can either penetrate the outer membrane by diffusion through porin channels for hydrophilic antibiotics or through a lipid-mediated pathway for hydrophobic antibiotics (Delcour, 2009, Yarlagadda *et al.*, 2016). A large issue is that many frontline antibiotics that are used to treat successfully Gram-positive infections are too big to pass through the porins and many cannot diffuse through the lipid bilayer of the outer membrane (Delcour, 2009, Yarlagadda *et al.*, 2016, Zhou *et al.*, 2015). As such, there is a need for new treatments against Gram-negative bacteria whether it be through drug combinations or through novel discoveries.

1.3 Efflux pumps

Efflux pumps are transport proteins that are localised in the cytoplasmic membrane and are involved in the transport of toxic compounds from the cytoplasm of the cell into the external environment (Sun *et al.*, 2014, Webber, 2002). Many different classes of efflux pumps exist in both Gram-negative and Gram-positive bacteria such as the multidrug and toxic efflux (MATE), small multidrug resistance (SMR), adenosine triphosphate (ATP) binding cassette (ABC) and the major facilitator superfamily (MFS). However, in addition to these classes of efflux pumps, is the resistance nodulation division (RND) pump that is exclusively found in Gram-negative bacteria (Sun *et al.*, 2014, Webber, 2002). The RND family of pumps has been found to be associated with extensive antibiotic resistance in *E. coli*, *Pseudomonas aeruginosa* and *Salmonella enterica sv. Typhimurium*. In *E. coli*, the most prominent of the RND pumps is the AcrAB pump which works together with the outer membrane partner-channel, TolC, forming together the AcrAB-TolC variant of the transenvelope Type I secretion system (Sun *et al.*, 2014).

1.3.1 **Structure of the AcrAB-TolC system**

The AcrAB-TolC is a tripartite system that is comprised of a channel in the outer membrane (TolC), a periplasmic protein adaptor (AcrA) and an inner membrane efflux protein that is extended from the cytoplasm into the periplasm (AcrB) (Blair and Piddock, 2009, Raczkowska *et al.*, 2015) (Figure 1).

AcrB is comprised of three subunits which form a complex spanning the cytoplasmic membrane. The cytoplasmic domains of AcrB can exist in the three different conformational states; access, binding and extrusion. The shift from one conformational state to the other is responsible for the pumping action of AcrB (Murakami *et al.*, 2006, Seeger *et al.*, 2006). This tripartite complex is also comprised of the periplasmic head and the transmembrane region. The periplasmic head in addition to connecting with the TolC outer channel contains a pore region (Sun *et al.*, 2014). Crystallography results have shown that all the subunits of AcrB, contains phenylalanine residues and it has been proposed that it is through these residues that the substrate is bound (Murakami *et al.*, 2006, Seeger *et al.*, 2006, Sun *et al.*, 2014). The monomer labelled as the "access monomer" contains a smaller binding site and a vestibule (Figure 2). The third monomer labelled as the "extrusion monomer" contains an α-helix that is normally inclined which prevents the exit of the substrate from the binding site to the periplasmic head (Littmann, 2015, Nakashima *et al.*, 2011, Seeger *et al.*, 2006, Sun *et al.*, 2014, Yarlagadda *et al.*, 2016) (Figure 2). Inactivation of any one of the monomers inhibited the activity of this complex suggesting that all the monomers work cooperatively (Takatsuka and Nikaido, 2009).

AcrA is a periplasmic adaptor protein that is primarily comprised of the three distinct domains: α-helical domain, lipoyl domain and a β-barrel domain. In the AcrAB-TolC efflux pump system, there are two copies of AcrA. Studies have shown that AcrA associates with TolC through the α-helical domain and the β-barrel domain binds to AcrB (Fernandez-Recio *et al.*, 2004) (Figure 1). While AcrA is not directly involved in the export of substrates out of the cell, it is primarily involved in coordinating the interaction between AcrB and the TolC channel (Mikolosko *et al.*, 2006). However, studies have shown that in response to fluctuations in the pH during drug efflux, AcrA undergoes reversible conformational rearrangements. It has been proposed that these

conformational arrangements bring both the inner and outer membranes closer together and induce conformational changes in AcrB and TolC through protein-protein interactions (Ip *et al.*, 2003). Deletion mutants in the AcrA gene were shown to have increased susceptibility to many drugs including nitrofurantoin, ampicillin and erythromycin (Ayhan *et al.*, 2016, Liu *et al.*, 2010).

The outer membrane channel, TolC, is a trimer that is comprised of three subunits, each containing β-strands and α-helices (Koronakis *et al.*, 2000). Each of the three protomers contributes 4 β-strands to form the β-barrel domain that is anchored to the outer membrane of the cell. Similarly, each of the protomers contributes 4 α-helices in order to form the α-helix barrel that spans the periplasm and interacts physically with AcrB (Koronakis *et al.*, 2000). On the β-barrel side, TolC is constitutively open, however, on the periplasmic side, the opening and closing of TolC are mediated through the action of AcrA. Mutations causing the constitutive opening of the TolC channel in the periplasmic side were found to be more sensitive to antibiotics due to a greater influx of antibiotics entering the cell in comparison to the efflux of antibiotics going out of the cell (Augustus *et al.*, 2004).

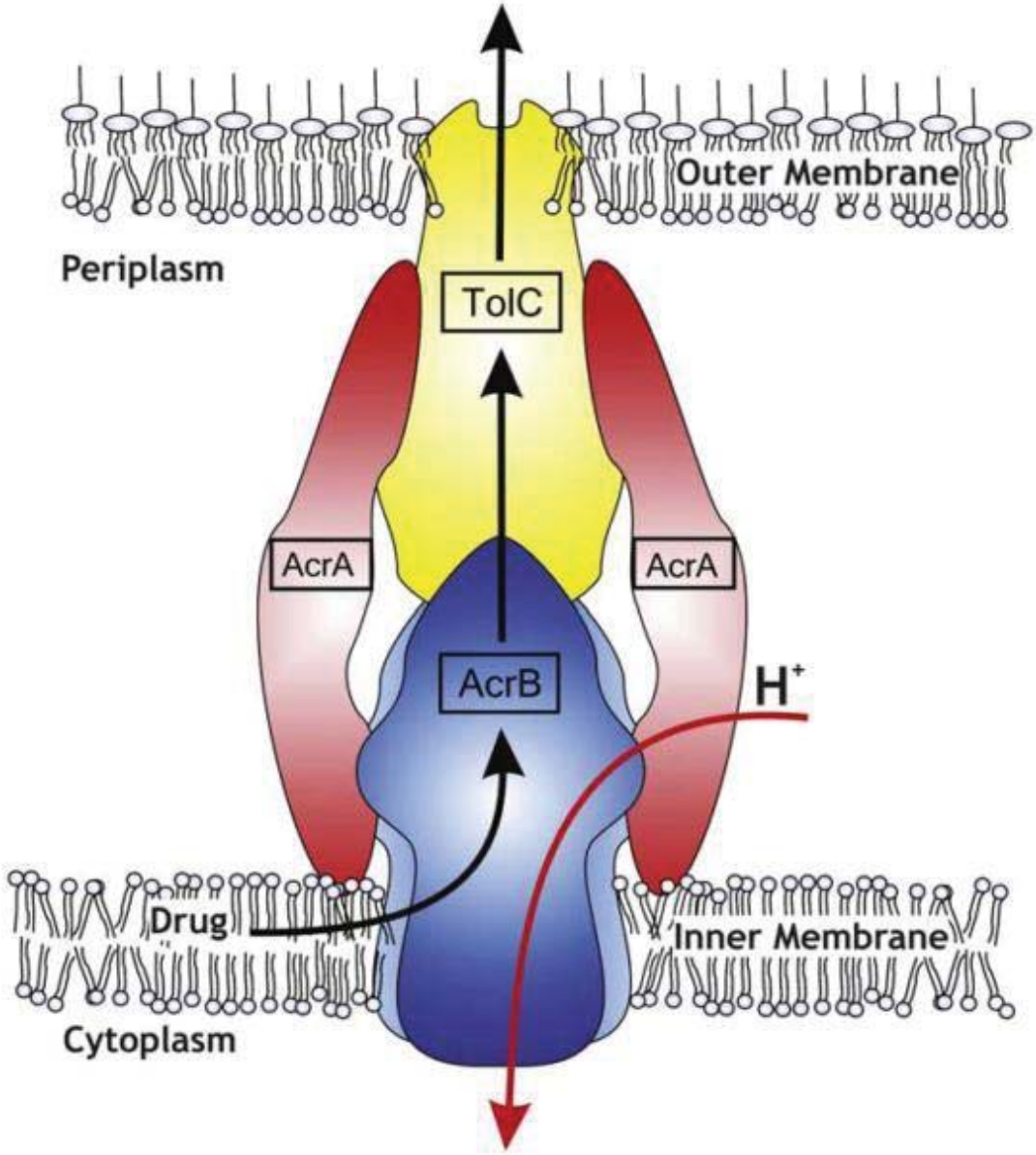

Figure 1: Diagram of the AcrAB-TolC efflux system

AcrAB-TolC is an RND class efflux pump found in *E. coli* that span from the inner membrane across the periplasm and into the outer membrane. AcrB, the inner membrane component, is associated with the two AcrA adaptor proteins and the outer membrane channel, TolC. This figure was taken with permission from Blair and Piddock, (2009).

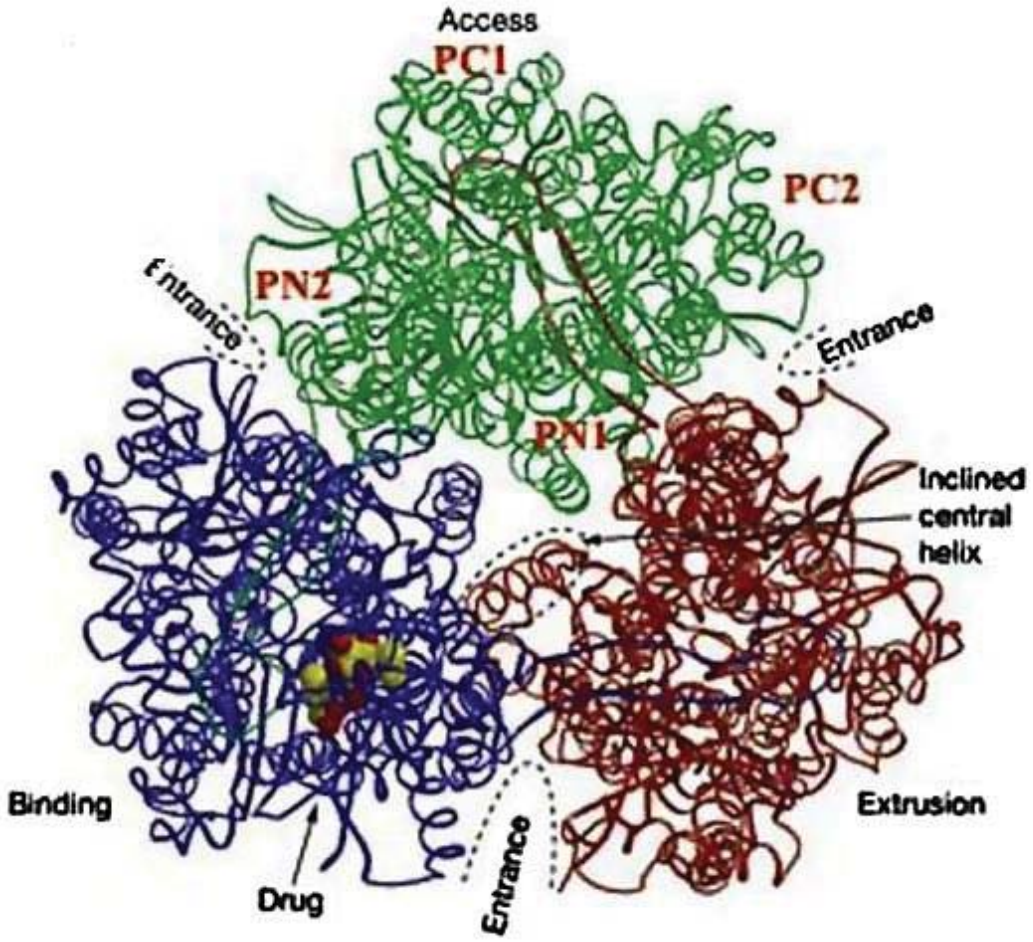

Figure 2: Structure of the AcrB trimer

AcrB is a component of the AcrAB-TolC complex that is comprised of 3 different subunits. The substrate enters and binds to the binding site in the access monomer. Through interactions with the phenylalanine residues, the substrate travels into the binding monomer. Changes in the positioning of the central α-helix causes the extrusion of the substrate into the TolC channel. This figure was taken with permission from Sun *et al.,* (2014).

1.3.2 Function of the AcrAB-TolC system

It has been proposed based on the atomic resolution structures, that the AcrAB-TolC efflux pump transports substrates through a functionally rotating mechanism (Takatsuka and Nikaido, 2009). During the access state, the substrate travels through the vestibule of the access monomer of AcrB and binds to the transmembrane domain (Figure 2). During the binding state, the substrate is transported and binds to the substrate binding domain through interactions with the phenylalanine residues (Nakashima *et al.*, 2011, Sun *et al.*, 2014). During the extrusion state, the α-helix changes positioning thus opening the exit and coupled with the shrinking of the binding site, the substrate is pushed through the funnel-like exit towards the TolC channel (Murakami *et al.*, 2006, Seeger *et al.*, 2006, Sun *et al.*, 2014) (Figure 2). Due to conformational changes induced through AcrA, the TolC channel on the periplasmic side opens and the substrate travels through the TolC channel into the external environment (Weeks *et al.*, 2010). This process of substrate efflux is thought to be powered by the proton motive force (PMF) generated from the electron transport chain (Seeger *et al.*, 2006).

1.4 Vancomycin

Vancomycin is a currently used antibiotic that belongs to the glycopeptide class and was previously referred to as the drug of last resort (Zhou *et al.*, 2015). Vancomycin was initially discovered in the 1950s but was replaced with new antibiotics discovered concurrently that were more efficient and less toxic. With the emergence of MRSA, vancomycin was brought back to treat MRSA and enterococci and ever since it has been the most successful glycopeptide used to date (Levine, 2006, Yarlagadda *et al.*, 2016). Similarly to other glycopeptides, vancomycin is hydrophilic with a high molecular weight structure of 1.486 kDa (Yarlagadda *et al.*, 2016).

1.4.1 Mechanism of action

Vancomycin kills bacteria by targeting peptidoglycan synthesis (Weeks *et al.*, 2010, Yarlagadda *et al.*, 2016). During peptidoglycan synthesis, 2 D-Ala molecules are joined together by ligases to form the D-Ala-D-Ala motif. This motif is then added to uracil diphosphate-N-acetylmuramyl-tripeptide to form uracil disphosphate-N-acetylmuramyl-pentapeptide which, while bound to a lipid carrier, translocates into the cell wall where it

is incorporated into the peptidoglycan via transglycosylation (Figure 3). This allows for the formation of cross-bridges by transpeptidation (Courvalin, 2006). Vancomycin inhibits peptidoglycan synthesis by binding to the D-Ala-D-Ala complex which is stabilised by a combination of hydrogen bonds and van der Waals forces (Figure 4). As a consequence of this, cross-bridge formation by transpeptidation does not occur, thereby preventing the formation of the cell wall (Courvalin, 2006, Xie *et al.*, 2011) (Figure 2).

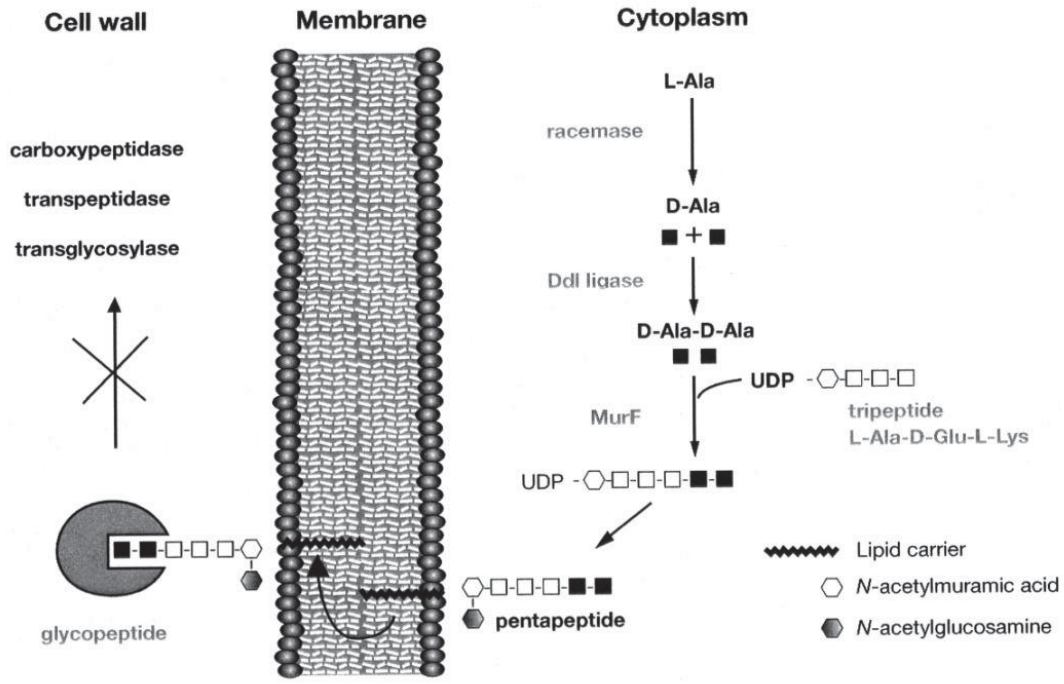

Figure 3: Mechanism of the peptidoglycan biosynthesis inhibition by vancomycin.

The peptidoglycan precursors are translocated across the cell membrane from the cytoplasm into the cell wall where vancomycin binds to the D-Ala-D-Ala complex at the end of the precursors, thereby inhibiting peptidoglycan biosynthesis. This figure was taken with permission from Courvalin, (2006).

Resistance to vancomycin may occur in Gram-positive bacteria through the acquisition of the mutations in various *van* genes (*vanA, vanB, vanD, vanC, vanE* and *vanG*) (Courvalin, 2006, Levine, 2006, Xie *et al.*, 2011). All of these *van* genes target the binding between vancomycin and D-Ala-D-Ala by modifying the binding sites. Strains containing *vanA, vanB* and *vanD* mutations if applicable have been reported to synthesize the peptidoglycan precursors with a D-Ala-D-Lac. Unlike the D-Ala-D-Ala

complex, the D-Ala-D-Lac lacks the central hydrogen bond and as a result of this, the binding affinity to vancomycin has been found to be lower by a thousand-fold thus resulting in resistance (Courvalin, 2006, Wright, 2011, Xie *et al.*, 2011) (Figure 4). *vanC, vanE* and *vanG*, in contrast, have been reported to synthesise precursors with D-Ala-D-Ser at the ends. As with the lac substitution, the presence of serine instead of alanine results in a steric hindrance, hence reducing the efficiency of vancomycin binding (Courvalin, 2006, Xie *et al.*, 2011). The MICs for vancomycin against the Gram-positive bacteria harbouring these genes were recorded to be from up to 1000-fold higher than those of the wild-type *E. coli* (4 mg/L – 1000 mg/L); (Courvalin, 2006).

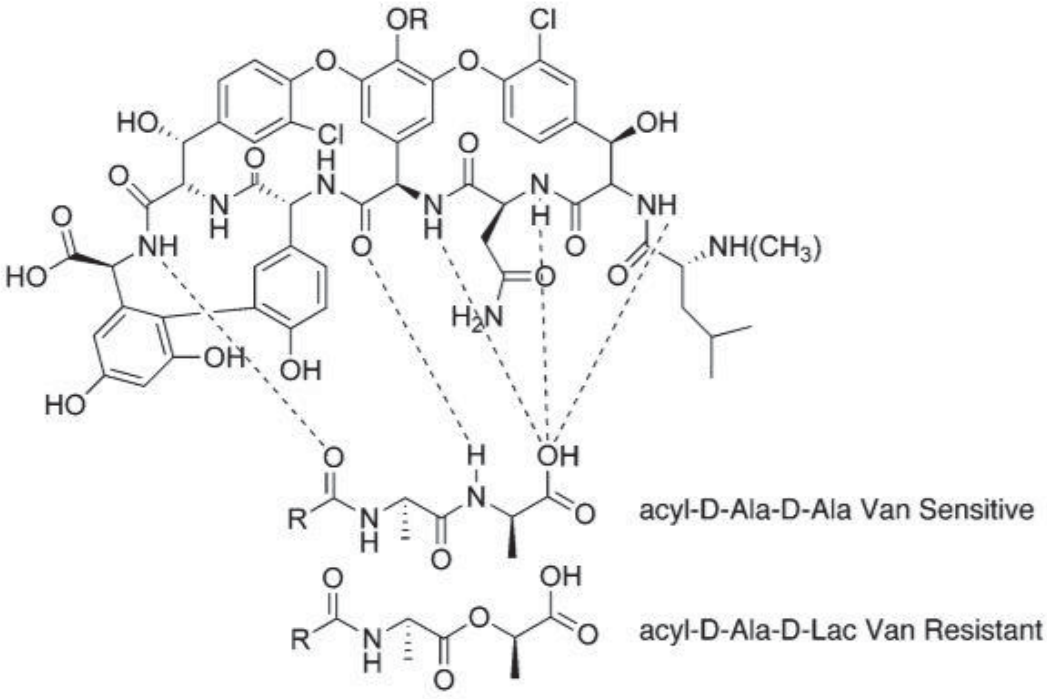

Figure 4: Vancomycin binding sites.

Vancomycin binds to the D-Ala-D-Ala complex of the peptidoglycan precursors through a series of hydrogen bonds in order to stabilise the interaction. In vancomycin-resistant strains, vancomycin binds to the D-Ala-D-Lac complex of the peptidoglycan precursors with significantly less affinity due to the loss of the central hydrogen bond. This figure was taken with permission from (Wright, 2007).

Unlike Gram-positive bacteria, Gram-negative bacteria are intrinsically resistant to vancomycin due to the presence of the outer membrane. In order for vancomycin to reach the D-Ala-D-Ala complex, it must cross the outer membrane. As vancomycin is

hydrophilic, however, it cannot diffuse through the lipid bilayer of the outer membrane. In addition to this, vancomycin cannot diffuse through the porins in the outer membrane as it is too large (Delcour, 2009, Yarlagadda *et al.*, 2016). Due to this, many studies have found that the MIC (minimal inhibitory concentration) for vancomycin against Gram-negative bacteria can be as high as 400 mg/L as opposed to ≤ 2 mg/L for Gram-positive bacteria (Holmes *et al.*, 2012, Zhou *et al.*, 2015). Mutations in *E. coli* involving outer membrane assembly reduced the MIC for vancomycin to as low as 8 mg/L, confirming the role of the outer membrane in the resistance of vancomycin to Gram-negative bacteria (Zhou *et al.*, 2015). Vancomycin sensitivity profiles of the Keio collection (*E. coli* K-12 deletion mutants for each non-essential gene) showed that mutations involved in both the assembly of the outer membrane as well as in protein synthesis caused an increase in sensitivity. This suggests that vancomycin may also have additional targets instead of just targeting peptidoglycan biosynthesis (Tamae *et al.*, 2008, Liu *et al.*, 2010). In another study vancomycin was tested against various *E. coli* mutants in combination with nitrofurantoin. Based on these findings it was suggested that in addition to protein synthesis, vancomycin may cause DNA damage through oxidative stress (Zhou *et al.*, 2015).

1.4.2 Implications

A significant issue with vancomycin is that it is associated with nephrotoxicity, i.e. toxicity to kidneys (Elyasi *et al.*, 2012). While the exact mechanism as to why vancomycin is associated with nephrotoxicity is yet to be elucidated, several studies have shown that this may arise through induction of oxidative stress (Oktem *et al.*, 2005, Elyasi *et al.*, 2012). Studies that were carried out using animal models have shown that after administering vancomycin to rats there was a decrease in the antioxidant enzyme activity found in the rat renal tissue sample. This in turn suggests that the rats were subject to oxidative stress (Nishino *et al.*, 2009, Elyasi *et al.*, 2012). In addition, patients that were treated with vancomycin at concentrations used above 32 mg/L had a strong correlation with nephrotoxicity. This study also recommended that treatments should be no more than 30 mg/L and no less than 15 mg/L which further supports the hypothesis that vancomycin is ineffective at treating Gram-negative infections (Alvarez *et al.*, 2016).

1.5 Furazolidone

Furazolidone is an antimicrobial compound that belongs to the nitrofuran class. In Europe, furazolidone was initially used as an antibiotic for veterinary applications, aquacultures and for food additives for livestock (Vass, 2008). Due to its property as a mutator in *E. coli* and possibility that it could be a carcinogen, furazolidone was banned in the EU in 1995 as a treatment in livestock due to safety concerns and in addition, furazolidone is also banned for treatment in livestock in other countries such as Australia, USA and the Philippines (Khong *et al.*, 2004, Vass, 2008). However, despite its ban, furazolidone and the other nitrofurans are readily available as treatments and in South America, where furazolidone is commonly used as treatment for the children with diarrhoea due to the resistance to other antibiotics (Martinez-Puchol *et al.*, 2015, Vass, 2008). Nitrofurantoin is widely used as a second-line antibiotic for recurrent urinary tract infections, including New Zealand,

1.5.1 Mechanism of action

Like other nitrofurans, furazolidone is a prodrug with a molecular weight of approximately 200-300 Da and its antimicrobial activity is related to its 5-nitro furan ring (Walzer *et al.*, 1991). While the full mechanism of furazolidone is currently not fully understood, studies have shown that under aerobic conditions, furazolidone activation is catalysed by two nitroreductases, NfsA and NfsB (Chatterjee *et al.*, 1983, Martinez-Puchol *et al.*, 2015). Both of these enzymes are type I oxygen insensitive nitroreductases that are involved in the reduction of the nitro groups found on the 5-nitro furan ring through the addition of two electrons from NAD(P)H in order to produce a nitroso intermediate that is further reduced to form hydroxylamine and amino derivatives (Paterson *et al.*, 2002, Roldan *et al.*, 2008, Walzer *et al.*, 1991). Deletions in *nfsA* reduce the activity of furazolidone, however, deletions in the only *nfsB* in the presence of *nfsA*, showed no loss in activity although deletions in both *nfsA* and *nfsB* showed a larger decrease in furazolidone activity (Martinez-Puchol *et al.*, 2015, Whiteway *et al.*, 1998). While the exact mechanisms are yet to be elucidated, it has been proposed that the hydroxylamine intermediates produced are what causes furazolidone's antibacterial activity as the intermediates have been found to interact with DNA and induce DNA

damage (Roldan *et al.*, 2008). Furthermore, furazolidone may act through the cross-linking of DNA which can lead to the formation of DNA lesions thus ultimately inhibiting DNA biosynthesis (Chatterjee *et al.*, 1983).

Another proposed mechanism is that DNA damage is induced by the upregulation of intracellular reactive oxygen species (ROS) (Jin *et al.*, 2011). ROS are molecules or ions that contain an unpaired electron that can induce DNA damage through the modification of guanine through many mechanisms such as oxidation, alkylation, halogenation and nitration (Jena, 2012, Roldan *et al.*, 2008). Using 8-hydroxydeoxyguanosine (8-OHdG) as a biomarker for oxidative stress, studies have shown that mitochondrial DNA is affected by ROS significantly more than that of nuclear DNA due to mitochondria being the major site of intracellular ROS generation, (Jin *et al.*, 2011). Furthermore, the effects of furazolidone and the level of intracellular ROS was shown to be mitigated by the addition of catalase and superoxide, supporting the proposed mechanism of DNA damage by ROS (Jin *et al.*, 2011).

Due to the lower molecular weight and different antimicrobial targets, furazolidone, unlike vancomycin possesses broad spectrum activity against both Gram-negative and Gram-positive bacteria. Minimal inhibitory concentrations for furazolidone against *E. coli* is in the 0.25-2 mg/L range and at 6 mg/L it has been shown to inhibit the growth of *Staphylococci* (Eady *et al.*, 2000, Martinez-Puchol *et al.*, 2015).

1.5.2 Implications

Despite its broad spectrum antimicrobial activity, there have been concerns regarding the use of furazolidone primarily due to its carcinogenic nature. Despite its carcinogenic activity, at lower concentrations furazolidone are considered safe to use against diarrhoea, however at higher concentrations, furazolidone is known to be cytotoxic (Jin *et al.*, 2011, Martinez-Puchol *et al.*, 2015, Vass, 2008). It has been shown in a rat model, that at higher concentrations (100 mg/kg and above), adverse symptoms occur as opposed to the group that was treated with lower concentrations at 50 mg/kg/day which experienced no adverse effects (Walzer *et al.*, 1991). The implications of using furazolidone at higher concentrations are further highlighted when tested for cell viability on HepG2 cells at concentrations between 25 mg/L and 50 mg/L was shown to cause a significant reduction in cell viability (Jin *et al.*, 2011).

1.6 Sodium Deoxycholate

Sodium deoxycholate (DOC) is an amphipathic secondary bile salt that is found in the enterohepatic circulation of humans and most animals (Shefer *et al.*, 1995). In addition, DOC possesses antimicrobial activity against Gram-positive bacteria, however, it has been found to be ineffective against Gram-negative bacteria due to the presence of the outer membrane and the RND efflux pump systems. Due to this, DOC is commonly used as a detergent and as a selective agent in media to select for Gram-negative bacteria (Begley *et al.*, 2005, D'Mello and Yotis, 1987). While the full antimicrobial mechanism of action is not fully elucidated, it has been proposed that DOC possesses many targets and is involved in the induction of oxidative stress, protein misfolding, DNA damage and disruption of the cell membrane (Bernstein *et al.*, 1999, Cremers, 2014, Merritt and Donaldson, 2009).

1.7 Drug combinations

In order to counter the global antibiotic resistance phenomenon, there is a need for the synergistic combination of drugs or for the discovery and the development of new novel treatments (Worthington and Melander, 2013). In the case of Gram-negative bacteria, the identification of new drug combinations is crucial as they are generally more difficult to treat than Gram-positive bacteria and so the development of novel antimicrobials against Gram-negative bacteria is lagging behind (Tangden, 2014).

The main objective for the use of different antibiotic combinations is to try and identify a synergistic response from both drugs (Rahal, 2006). Synergy is achieved when normally sub-inhibitory concentrations (lower than the MICs) of both drugs successfully inhibit bacterial growth (Mitosch and Bollenbach, 2014, Rahal, 2006). This may provide many benefits such as increased efficacy, reduced levels of toxicity and the lower likelihood of antibiotic resistances emerging as opposed to single antibiotic treatments. Interestingly, recent *in vitro* studies have argued that the use of synergistic antibiotic combinations may potentially exacerbate the antimicrobial resistance phenomenon due to increased evolutionary rates of resistance emerging (Hegreness *et al.*, 2008, Pena-Miller *et al.*, 2013). This, however, may be due to the added selection pressure for resistance mutations, however, it is shown that extremely inhibitory synergistic interactions where the bacteria are cleared quickly may mitigate this (Hegreness *et al.*, 2008, Pena-Miller *et al.*, 2013).

1.7.1 Evaluation of interactions

Two antibiotics, when combined may interact synergistically, antagonistically or indifferently and these interactions between two different drugs are commonly evaluated using the Bliss independence method, Fractional Inhibitory Concentration Index (FICI) and time-kill curves (Mitosch and Bollenbach, 2014). The Bliss independence method is derived from the idea where two drugs contribute towards a common result but do not directly interact with one another (Lee, 2010, Tang *et al.*, 2015). This model predicts the interaction between the drugs by using four growth measurements with one being the growth of the bacteria without any drugs, the growth of the bacteria in the presence of drug A, the growth of the bacteria in the presence of drug B and the growth of the bacteria in the presence of drug A and drug B in combination (Bliss, 1939) .While the Bliss independence model is a very popular for the quantification of interaction, it is not without its disadvantages, with the key disadvantage being the assumption that the dose-effect curves are exponential. This can lead to potential underestimations or overestimations regarding the interaction between the drugs. (Foucquier and Guedj, 2015, Mitosch and Bollenbach, 2014, Tang *et al.*, 2015).

In addition to the Bliss independence method, FICI can be used to quantify interactions between different drugs. FICI is based off the Loewe's additivity theory which uses a FIC index of 1 to determine whether a drug is either synergistic or antagonistic (Meletiadis *et al.*, 2010, Singh *et al.*, 2013). The Bliss independence method only tests one given concentration of the two drugs in combination. In contrast, the FICI method tests multiple different combinations and provides significantly more information regarding the drug to drug interaction (Berenbaum, 1989, Meletiadis *et al.*, 2010).

1.7.2 Targets and mechanisms

Different antibiotics may act through direct interaction where both physically interact with each other at the targets to elicit their response or conversely they may act indirectly where one antibiotic facilitates the uptake of the other antibiotic. The antibiotics can either inhibit different targets through different pathways, inhibit the same target through different pathways or inhibit different targets through the same pathway (Worthington and Melander, 2013, Bollenbach, 2015). It has also been hypothesised that interactions between bactericidal and bacteriostatic antibiotics may be antagonistic because

bactericidal antibiotics work on growing cells, while bacteriostatic antibiotics serve to inhibit cell growth thus resulting in an antagonistic interaction between the two (Mitosch and Bollenbach, 2014). A common example of this is the combination between protein synthesis inhibitors and penicillin. Protein synthesis inhibitors act bacteriostatically and inhibit bacterial cell growth, thus limiting the bactericidal activity of penicillin through the lack of a target (Tuomanen, 1986). It is also understood that aminoglycoside antibiotics work synergistically with beta-lactams as the beta-lactams make the cell more permeable to aminoglycosides (Davis, 1982). Despite the use of many antibiotic combinations, the exact mechanisms of their interacttions are not fully elucidated at this point (Mitosch and Bollenbach, 2014, Tangden, 2014, Bollenbach, 2015). While basic targets and mechanisms are understood, the more complex mechanism such as the exact changes in the physiology of the cells and the effects at the molecular level are still unknown for many antibiotic combinations (Mitosch and Bollenbach, 2014).

1.8 Biofilms

1.8.1 Structure

Biofilms are defined as populations of bacteria that grow as a sessile multicellular colony that provides bacteria with survival advantages (Hoiby *et al.*, 2010).

Normally bacteria may exist in either a planktonic or in a sessile state, which are physiologically and phenotypically distinct from each other (Coenye and Nelis, 2010). Biofilm formation is initiated when bacteria sense a set of environmental cues such as temperature, osmolarity, pH and iron. Studies have found that different conditions are required the biofilm formation of different bacterial species, for example, *E. coli* O157:H7 only forms biofilms in low nutrient media whereas *E. coli* K-12 only forms biofilms in minimal media when supplemented with amino acids (O'Toole, 2000).

The multistep process of biofilm formation is initiated by planktonic bacteria in which bacterial cells initially attach to a surface using cell surface structures, such as fimbriae, in a reversible manner that is mediated through the weak van der Waals forces (Dufour, 2010, Rendueles and Ghigo, 2012) (Figure 5). The bound colonies on the surface produce an extracellular matrix that is comprised of exopolysaccharides, proteins and extracellular DNA which is used to complex between the cell surface structures and the surface (Figure 5). This allows bacteria to be irreversibly bound to the surface in the

absence of physical or chemical interventions. Furthermore, the extracellular matrix has been reported to be involved in the communication between bacteria through quorum-sensing and this is a key factor regarding the interference of the penetration of antimicrobials (Coenye and Nelis, 2010, Vasudevan, 2014). Production of the extracellular matrix is followed by the maturation phase of the biofilms.

During the maturation phase, the bacteria begin to actively replicate and the overall density of the biofilm increases. Based on early evidence, it was initially thought that biofilms were comprised of cells stacked on top of each other. However, based on advances in microscopy techniques over the years, studies have found that the biofilms are hydrated with water channels that provide the bacteria within the biofilm with nutrients and ions (O'Toole, 2000). The maximum growth of the biofilm is limited due to factors such as nutrients present on the surface, the ability to remove waste products and for the delivery of nutrients to the cells within the biofilm (Dunne, 2002). At the maximal population within the biofilm, some bacterial cells may detach from the biofilm in order to colonise a new niche (Dufour, 2010, Rendueles and Ghigo, 2012, Vasudevan, 2014) (Figure 5). It has been found that, depending on the bacterial species and strains, there are multiple ways in which the biofilm dispersal may occur. This includes swarming dispersal, clumping dispersal and surface dispersal (Hall-Stoodley *et al.*, 2004). It has also been suggested that population dependent gene expression, controlled by cell to cell signalling drives the formation, maturation and the dispersal of biofilms (Dunne, 2002).

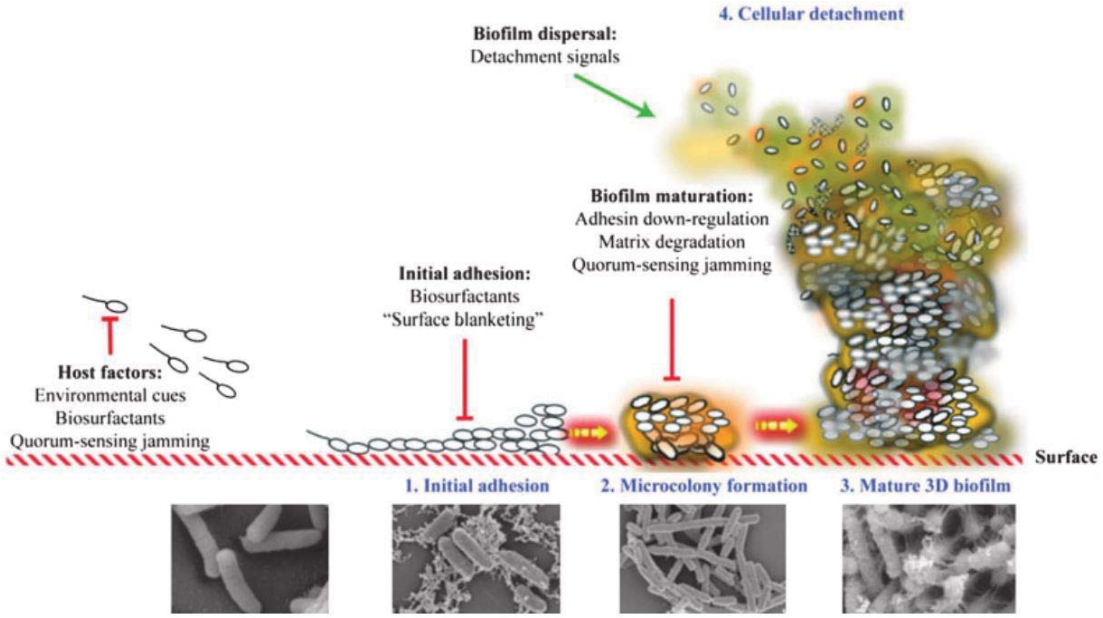

Figure 5: Steps involved in biofilm formation.

Initially, planktonic bacteria adhere to surfaces using cell surface structures. Following the initial attachment, the bound colonies produce the extracellular matrix which enables the biofilm to be bound irreversibly and provides important survival properties that ensures its maturation. Once fully matured, cells disperse from the biofilm to colonise new niches. Scanning electron microscopy images show the initial attachment, formation and the full maturation of the biofilm. This figure was taken with permission from Rendueles and Ghigo, (2012).

1.8.2 Clinical significance

The key issue caused by the presence of biofilms is that they are significantly more difficult to treat as they are highly resistant to many antibiotics. It has been reported that in biofilms, different genes are expressed that confer resistance to antibiotics such as increasing the expression of resistance nodulation division (RND) efflux pumps and the presence of the extracellular matrix that acts as a protection barrier against antibiotics (Dufour, 2010, Vasudevan, 2014). Additionally, it has been proposed that due to the slow growth rates of the bacteria within the biofilm, they are not as susceptible to many antibiotics as opposed to fast growing planktonic bacteria (Trautner and Darouiche, 2004, Vasudevan, 2014). Within the biofilms, a very small percentage (0.1-1%) of cells, termed as persister cells, become metabolically dormant and can escape the activity of the antibiotics. Once conditions are favourable, the persister cells are resuscitated to their normal physiological state and can act as initiator cells and reform the biofilm. This factor is also very common in chronic biofilm infections (Dufour, 2010, Vasudevan, 2014). Many studies have found that the minimal inhibitory concentrations (MICs) and the minimal bactericidal concentrations (MBCs) of bacteria growing in a biofilm are significantly greater than that of planktonic bacteria of the same strain and with the same genome, with some being as high as up to 1000-fold higher (Dufour, 2010, Dunne, 2002, Vasudevan, 2014).

The presence of biofilms poses a large problem within the health care and hospital settings. In hospitals, catheter associated infections (CAUTI) are highly prevalent and are primarily caused by the biofilms present on the surface of the catheters (Nicolle, 2014). The prevalence of these infections is very high and it has also been reported that the duration of a patient is in contact with a catheter, is correlated with the risk of developing an infection (Nicolle, 2014). Studies conducted by the National Institute of Sciences in India, have shown that biofilms are the main cause of infection for approximately 60% of infections in hospitals (Vasudevan, 2014). As a preventative measure, hospitals treat catheters with antibiotics or with antibiotic combinations in order to prevent the formation of biofilms, however, it has been noted that current antibiotic treatments cannot completely eradicate a biofilm (Hoiby *et al.*, 2010).

1.9 Hypothesis and aims

The key issue in the use of antibiotic combinations is that the underlying mechanisms of actions are unclear. Unpublished work in the Rakonjac Laboratory has identified the synergism between nitrofurans and vancomycin (JR, unpublished). Furthermore, recent studies have found that there is synergism between vancomycin and another nitrofuran, nitrofurantoin, against *E. coli*, although the mechanisms of this antibiotic interaction are not yet elucidated (Zhou *et al.*, 2015).

We hypothesised that furazolidone enters the cell and through the intermediates formed through the reduction of the 5-nitro furan ring, disrupts the generation of the PMF. This would prevent the AcrAB-TolC system from functioning normally and while TolC is in its open state, vancomycin would be able to bypass the outer membrane of the cell.

Another potential hypothesis was that furazolidone freely diffuses into the cell through the porins and vancomycin would enter the cell through the outer membrane channel, TolC, activated by the transport of enterobactin out of the periplasm of *E. coli*. The biosynthesis of enterobactin and its export would in turn be upregulated by oxidative stress induced by furazolidone.

This thesis aims to characterise the vancomycin-furazolidone synergy in E. coli K12 planktonic cells and biofilm. The second aim waws to investigate the mechanism of this synergy exploiting the genetic tools available for E. coli K12.

Unpublished work done in the Rakonjac Laboratory has found that there is synergy between furazolidone and DOC against *E. coli* (Vuong Le, unpublished). Based on this, it was hypothesised that there would be a highly synergistic interaction of the triple combination containing vancomycin, furazolidone and DOC. Therefore, the third aim of the thesis was to determine whether there is a triple-synergy among these three molecules against *E. coli* K12.

2 Materials and methods

2.1 Media preparation

All media were prepared and stored according to the manufacturer's instructions.

All *E. coli* strains were grown in 2xYT rich media (BD Difco™) or in 2xYT media supplemented with antibiotics, kanamycin at 50 mg/L or chloramphenicol at 25 mg/L or ampicillin at 100 mg/L or chemicals, 10 mM $CaCl_2$ (Sigma-Aldrich ®) or 10 mM Na-citrate. Sterile broths were obtained by autoclaving at 121°C at 100 kPa for 15 minutes. Antibiotics and chemicals were added after autoclaving.

The agar plates were solidified using 2xYT media and bacteriological agar (Acumedia) at 1% or Bacto-agar (BD) at 1.5%

2.2 Bacterial strains

All strains that were used were laboratory *E. coli* and are listed in Table 1. All strains of *E. coli* were streaked on to 2xYT agar and were incubated overnight at 37°C with the exception of *E. coli* K1466 which was incubated at 30°C. A single isolated colony was inoculated in 2xYT rich media which was incubated at 37°C (30°C for *E. coli* K1466) while shaking overnight. Frozen stocks were produced by adding dimethyl sulfoxide (DMSO) to fresh bacterial overnight cultures at a final concentration of 7% and were subsequently frozen at -80°C. Overnight cultures were obtained by inoculating 5 mL of 2xYT media with a single colony from the *E. coli* strain of interest which was incubated at 37°C shaking at 200 rpm overnight.

Table 1: List of *E. coli* strains used.

Strain	Parent	Genotype	Source
BW25113		*F-, Δ(araD-araB)567, ΔlacZ4787(::rrnB-3), λ-, rph-1, Δ(rhaD-rhaB)568, hsdR514*	(Baba *et al.*, 2006)
K1508	MC4100	*MC4100 ΔlamB106*	(Baneyx, 1991)
K2404	BW25113	*BW25113, ΔtolC732*	(Baba *et al.*, 2006)
K2427	BW25113	*BW25113, ΔtolC732, ΔentC731*	(This work)
K2428	BW25113	*BW25113, ΔacrA726*	(Baba *et al.*, 2006)
K2430	BW25113	*BW25113, ΔentC731*	(Baba *et al.*, 2006)
K2431	BW25113	*BW25113, ΔuvrA753*	(Baba *et al.*, 2006)
K2414	BW25113	*BW25113, ΔtolC732, ΔentC731::kan*	(This work)
JW0585-2	BW25113	*BW25113, ΔentC731::kan*	(Baba *et al.*, 2006)
JW5503-1	BW25113	*BW25113, ΔtolC732::kan*	(Baba *et al.*, 2006)
JW0862-1	BW25113	*BW25113, ΔmacA779::kan*	(Baba *et al.*, 2006)
JW0863-1	BW25113	*BW25113, ΔmacB780::kan*	(Baba *et al.*, 2006)
JW3481-1	BW25113	*BW25113, ΔmdtE768::kan*	(Baba *et al.*, 2006)
JW3482-1	BW25113	*BW25113, ΔmdtF769::kan*	(Baba *et al.*, 2006)
JW0452-3	BW25113	*BW25113, ΔacrA726::kan*	(Baba *et al.*, 2006)
JW0451-2	BW25113	*BW25113, ΔacrB747::kan*	(Baba *et al.*, 2006)
JW2454-1	BW25113	*BW25113, ΔacrD790::kan*	(Baba *et al.*, 2006)
JW3233-2	BW25113	*BW25113, ΔacrE783::kan*	(Baba *et al.*, 2006)
JW3234-1	BW25113	*BW25113, ΔacrF784::kan*	(Baba *et al.*, 2006)
JW5338-1	BW25113	*BW25113, ΔmdtA773::kan*	(Baba *et al.*, 2006)
JW2060-1	BW25113	*BW25113, ΔmdtB774::kan*	(Baba *et al.*, 2006)
JW2660-1	BW25113	*BW25113, ΔemrA766::kan*	(Baba *et al.*, 2006)
JW2661-1	BW25113	*BW25113, ΔemrB767::kan*	(Baba *et al.*, 2006)
JW2365-1	BW25113	*BW25113, ΔemrK777::kan*	(Baba *et al.*, 2006)
JW2364-1	BW25113	*BW25113, ΔemrY776::kan*	(Baba *et al.*, 2006)

2.3 Antibiotics

All antibiotics that were used are listed in Table 2. Antibiotics were suspended in solvents at concentrations and storage conditions according to the manufacturer's instructions.

Table 2: List of antibiotics and concentrations used.

Antibiotic	Supplier	Stock concentration and solvent	Storage	Concentration range (mg/L)
Vancomycin	Goldbio	100 g/L in DMSO	-20 °C	64 000 – 3.9
Furazolidone	Goldbio	10 g/L in DMSO	-20 °C	1250 – 0.078
Tetracycline	Boehringer Mannheim	10 g/L in 50% ethanol and 50% distilled water	-20 °C	10
Kanamycin	Goldbio	50 g/L in distilled water	-20 °C	25
Ampicillin	Goldbio	100 g/L in distilled water	-20 °C	100
Chloramphenicol	Sigma	50 g/L in 100% ethanol	-20 °C	25

2.4 Minimal inhibitory concentration (MIC)

2.4.1 Checkerboard assay

For combined antibiotic assays, appropriate vancomycin or furazolidone dilutions were added sequentially (12.5 µL each) to the wells of a flat-bottom 384 microtitre well plate (Corning®, USA). Each concentration combinations were made in triplicate. For the MICs of each antibiotic alone or for the positive control, 25 µL of each of the vancomycin and furazolidone concentrations, or tetracycline at 10 mg/L was added. No antibiotic was added to the negative controls. The final concentration of DMSO in all of the wells was 4%.

Fresh overnight cultures of the *E. coli* strain of interest were diluted 1:100 and incubated at 37 °C for 1.5 hours while shaking at 200 rpm. Following the 1.5-hour incubation, the optical density of the bacteria was measured on a spectrophotometer (Thermo Fisher Mutiskan™ GO Microplate spectrophotometer) at 600 nm and the cultures were diluted down to 2×10^6 CFU/mL. From this bacterial inoculum, 25 µL was added into the wells containing the antibiotics and the controls. Following this, the 384 microtitre well plate was spun at 1000 rpm for a few seconds (Heraeus Labofuge 400R) to eliminate bubbles. The microtitre plate was incubated at 30°C and readings were taken every hour for 24 hours at 600 nm on a plate reader (Thermofisher Multiskan^{TM} GO). Each experiment was performed in triplicate.

The OD readings for the 24-hour time point was chosen to calculate the percentage of inhibition. The percentage of inhibition was calculated using the formula:

$$\%\ of\ inhibition = 100 - \frac{(OD_{Sample} - OD_{positive})}{(OD_{negative} - OD_{positive})} \times 100$$

From this, the minimal concentration of the antibiotic causing 90% inhibition (IC90) can be determined (Campbell, 2010). Following this, the Fractional Inhibitory Concentration Index (FICI) was calculated using the formula:

$$FICI = \frac{FICI_{Vancomycin}}{IC90_{Vancomycin}} + \frac{FICI_{Furazolidone}}{IC90_{Furazolidone}}$$

FICI is the minimal concentration of an antibiotic that causes 90% growth inhibition when used in combination with another antibiotic.

MIC is the minimal concentration of each antibiotic when applied alone that causes 90% inhibition.

An FIC index of ≤ 0.5 indicates a synergistic relationship, additive if the FIC index is from 0.5-2.0 and antagonistic if the FIC index is >2.0 (Singh *et al.*, 2013).

2.4.2 Minimal Bactericidal Concentration (MBC)

Following the 24 hours incubation of the checkerboard assay, from the triplicate wells with no visible growth, 10 µL were plated on 2xYT plates. The 2xYT plates were incubated overnight at 37 °C and to determine whether any colonies were formed. Given that the starting bacterial count was million per mL, hence thousand per 10 µL, 10 colonies corresponded to 99% killing. The combinations that yielded less than 10 colonies were chosen for the time-kill assay.

2.5 Time-kill assay

This method was adapted from Petersen *et al.* (2006). Antibiotic dilutions in 500 µL tubes were prepared, with vancomycin being diluted to as shown in Table 2. In the combination groups, vancomycin was diluted down to 62.5 mg/L and was added to 1.25 mg/L and 0.625 mg/L of furazolidone.

Overnight cultures of the appropriate strain were diluted 100-fold into sterile 2xYT and were incubated on a shaker at 37°C for 1.5 hours. The optical density of the bacterial suspension was read on a spectrophotometer at 600 nm and was subsequently diluted down to 2×10^6 CFU/mL. To each of the tubes containing 500 µL of antibiotics, 500 µL of the diluted bacterial suspension was added in triplicates and was incubated at 30°C for 0, 2, 4, 6 and 24 hours on a shaker. At each time point, the tubes containing the antibiotics and bacteria were serially diluted 1:10 (10^0-10^{-5}) and from each of the dilutions, 10 µL was spread on to 2xYT plates and for 12-16 hours with the exception of the tetracycline dilutions which was incubated for 18 hours at 37°C. The colonies were counted and the CFU/mL was determined using this equation:

$$Colony\ forming\ units/ml = \frac{Average\ number\ of\ colonies\ \times\ dilution\ factor}{volume\ plated}$$

2.6 Competent cells

This method was adapted from (Jacobsson *et al.*, 2003). The *E. coli* mutant strain of interest was suspended in 2xYT media supplemented with kanamycin at 50 mg/L and was grown overnight at 37 °C with medium shaking. From the overnight culture, 500 µL was inoculated into 25 mL of 2xYT media and was incubated at 37 °C until the OD reading was 0.2 – 0.4 (0.15 – 0.2 for chemically competent cells) at 600 nm. The bacterial inoculum was incubated on ice for 30 minutes and was subsequently centrifuged at 4000 × g for 10 minutes at 4 °C. Following centrifugation, the supernatant was removed and the cells were resuspended in 10% glycerol and were incubated on ice for 10 minutes three times. The pellet was resuspended in 0.5 mL of 10% glycerol and was stored at -80 °C.

2.7 FLP recombination in *E. coli*

This method was adapted from (Baba *et al.*, 2006, Datsenko and Wanner, 2000) and is based on the plasmid, pCP20 that expresses the FLP recombinase under a temperature sensitive promoter pL and has a temperature-sensitive origin of replication and Amp resistance marker. This plasmid is transformed into strains containing the Keio collection Km cassettes that replace the specific ORFs and are flanked by frt sequences (targets of FLP recombinase) and incubated under the conditions that are permissive to pCP20 replication (30°C). The transformation was performed by electroporation. Briefly, pCP20 DNA (100 ng) was added to a microtube containing the electrocompetent cells and the mix was further added into 0.2 cm electroporation cuvettes (Bio-Rad). The electroporation cuvettes were placed into the electroporation apparatus (Bio-Rad MicroPulser^{TM}) and electroshocked at 2.5 kV for 5.8 milliseconds followed immediately by adding 1 ml of Super Optimal broth with Catabolite repression (SOC). The cell suspension was transferred to a microfuge tube and incubated at 200 rpm for 1 hour at 30°C. Of this culture, 20 µL was plated on a 2xYT plate supplemented with ampicillin at 100 mg/L and was incubated overnight at 30°C. From the 2xYT + ampicillin plate, a single colony was inoculated into 5 mL of 2xYT broth and was incubated at 43°C overnight. A dilution series of 1:10 from 10^0 – 10^{-6} was prepared of which 50 µL was streaked on to 2xYT plates that were incubated at 30°C overnight. From the 2xYT plate, 10 single colonies were patch plated on to 2xYT supplemented with kanamycin at 50 mg/L, 2xYT supplemented with ampicillin at 100 mg/L and 2xYT plates. The 2xYT and

kanamycin plates were incubated at 37 °C overnight while the ampicillin plate was incubated at 30°C overnight. Patches on the 2xYT plate that were sensitive to both kanamycin and ampicillin corresponded to the FLP recombinants from which the Km^R marker was removed and which lost the pCP20 plasmid. Cells from one such patch were deletion mutants without the Km^R cassette and were used in further experiments.

2.8 P1 transduction

An overnight culture of a donor *E. coli* strain was prepared. From this overnight culture, 50 µL along with 100 µL of prewarmed 2xYT media supplemented with 10 mM $CaCl_2$ and 50 µL of the P1 phage master stock (titre 10^7 – 10^8) was added to a preheated flask which was subsequently incubated for 5 minutes at 39°C. Following incubation, 10 mL of prewarmed 2xYT media supplemented with 10 mM $CaCl_2$ was added to the flask and was incubated at 39°C while shaking at 200 rpm for 6 hours for lysis to occur. Following cell lysis, chloroform was added and the remaining cell debris was centrifuged at 4500 rpm for 10 minutes at 4 °C. The supernatant was filtered through a 0.45 µm filter and was titred on a 2xYT plate supplemented with 25 mg/L chloramphenicol and soft agar. Fresh overnight cultures of the recipient *E. coli* strain was prepared and 1 mL was centrifuged at 10 000 rpm for 3 minutes. The supernatant was discarded and the pellet was resuspended in 1 mL of 10 mM $MgSO_4$ and was spun twice. Mixtures containing 2, 10 and 20 µL of P1 lysate of the donor strain and 100 µL of 10 mM $MgSO_4$ and 50 µL of the recipient cells was incubated at 39°C for 10 minutes to allow the phage to enter the cells. Prewarmed 2xYT containing 10 mM of Na-citrate was added in 1 mL quantities into each of the mixtures and was incubated at 39°C for 1 hour while shaking at 200 rpm. Following incubation, the mixtures were centrifuged at 12 000 rpm for 2 minutes at room temperature and the supernatant was discarded and was resuspended in an equal volume of 10 mM $MgSO_4$ and spun again. Following the second round of centrifugation, each of the mixtures were resuspended in 50 µL of 10 mM $MgSO_4$ of which 30 µL was streaked on 2xYT plates supplemented with kanamycin at 50 mg/L and 10 mM Na-citrate. The plates were incubated at 39°C and the transductants were streaked on to a 2xYT plate supplemented with kanamycin at 50 mg/L. Colonies resistant to kanamycin were streaked on to a fresh 2xYT plate containing kanamycin were subjected to removal using transient transformation with pCP20 as described above.

2.9 Biofilms

2.9.1 Growing biofilms

This method was adapted from (Moskowitz *et al.*, 2004). The optical density of the overnight culture of *E. coli* BW25113 was measured on a spectrophotometer (Thermo Fisher Mutiskan™ GO Microplate spectrophotometer) at 600 nm and the culture was diluted down to 1×10^7 CFU/mL in 2xYT media. From the diluted bacterial culture, 150 µL was added into the wells of a 96 well plate (Nunc 269787) which were subsequently covered with a peg lid (Nunc Immuno-TSP 445497). For the sterility control, 2xYT media was added. The 96 well plate and the peg lid was incubated on a shaker at 37 °C for 24 hours at 120 rpm. Following the 24 hours incubation, the lid containing pegs was transferred into a new 96 well antibiotic challenge plate. For this plate, 200 µL of antibiotic dilutions or the combination of vancomycin and furazolidone dilutions was prepared and for the growth and the sterility controls, 200 µL of 2xYT media was added. The antibiotic challenge plate with the inserted peg lid containing the biofilms was incubated at 30°C for 24 hours. Following the incubation, the peg lid was washed in rinse plates containing 200 µL of sterile 2xYT media for one minute in order to rinse off non-attached or loosely attached cells. Following the rinsing, the peg lid was inserted into a recovery plate containing 150 µL of sterile 2xYT media which was centrifuged at 2000 rpm for 20 minutes (Heraeus Labofuge 400R) in order to dislodge the biofilm and collect the cells in the recovery plate.

2.9.2 Minimal biofilm inhibition concentration (MBIC)

This method was adapted from (Moskowitz *et al.*, 2004). The OD of the cells collected in the recovery plate in the previous step was measured at 600 nm. The minimal inhibitory concentration was determined as the lowest concentration to cause 90% of biofilm inhibition.

2.9.3 Minimal biofilm eradication (killing) concentration (MBEC)

The contents in the recovery plate were serially diluted (10-fold 10^0 to 10^{-4}). From each dilution, 25 µL was subsequently spread on to 2xYT plates. The plates were incubated overnight at 37 °C. The following day, the colonies were counted and the viable titre (CFU/mL) was calculated using the formula:

$$Colony\ forming\ units/ml = \frac{Average\ number\ of\ colonies \times dilution\ factor}{volume\ plated}$$

3 Results

3.1 Quantifying synergy between vancomycin and furazolidone for *E. coli*

3.1.1 MICs for vancomycin and furazolidone against *E. coli*

Initially the MICs for both vancomycin and furazolidone against the *E. coli* strains, BW25113 and K1508 were determined in order to establish the concentration range needed for the checkerboard assay and to help quantify the synergy. BW25113 is closely related to MG1655, whose genome has been sequenced as a model *E. coli* K-12 strain and was the "wild type" strain used to construct a collection of *E. coli* knock-out mutations for all non-essential genes (Baba *et al.*, 2006). Another strain used in this study, K1508, is related to a widely used laboratory strain, MC4100, apart from a mutation of the gene encoding the maltoporin, LamB.

Both *E. coli* strains at a titre of 2×10^6 CFU/mL were challenged by both vancomycin and furazolidone individually across wide concentration ranges (1000 mg/L – 3.9 mg/L for vancomycin and 5 mg/L – 0.078 mg/L for furazolidone). The growth was assessed by measuring OD_{600} after a 24-hour incubation at 30°C and the MICs were determined as the minimal concentration causing 90% of growth inhibition. By itself, the MIC for vancomycin against both strains was very high, 500 mg/L (Table 3). For furazolidone, the MIC was 2.5 mg/L (Table 3). The positive control, tetracycline, inhibited the growth of both *E. coli* strains at 10 mg/L (Table 3).

3.1.2 Interaction between vancomycin and furazolidone in growth inhibition of *E. coli*

After obtaining the MICs for each of the antibiotics, in order to observe whether the vancomycin and furazolidone interacted synergistically, a checkerboard assay was performed. Both *E. coli* strains, BW25113 and K1508 at 2×10^6 CFU/mL, were challenged with a range of concentration combinations as described in the materials and methods section (Table 2). Following the 24 hours of antibiotic exposure at 30°C, OD measurements at 600 nm were taken and the % of survival of the cells and the FICI scores were calculated in order to determine whether the interaction was synergistic or not. For both of the *E. coli* strains that were tested, the FICI scores suggested an additive interaction between vancomycin and furazolidone. However, for *E. coli* BW25113, the combination of vancomycin at 62.5 mg/L and furazolidone at 0.3125 mg/L showed a

synergistic interaction based on its FICI score of 0.25. Vancomycin at 31.25 mg/L and furazolidone at 1.25 mg/L was another notable combination that showed a very strong additive effect, as its FICI score of 0.5625 was marginally above the FICI synergistic cut-off point (Table 4). Other combinations of vancomycin and furazolidone against *E. coli* BW25113 yielded FICI scores from 1.0078 to 1.0312, suggesting an additive interaction at these concentrations. Similarly, *E. coli* K1508 showed a similar trend to that of BW25113 although the vancomycin-furazolidone combination was slightly less synergistic (Figure 6). Two important combinations consisting of vancomycin at 62.5 mg/L and furazolidone at 0.625 mg/L and vancomycin at 125 mg/L and furazolidone at 0.3125 mg/L showed synergy based on their FICI scores of 0.375 (Figure 6). Other notable combinations include vancomycin at 31.25 mg/L and furazolidone at 1.25 mg/L and the combination containing vancomycin at 250 mg/L and furazolidone at 0.156 mg/L that have FICI scores of 0.5625 and 0.56104 respectively (Figure 6). Overall these findings suggest that there is a synergistic relationship between the two antibiotics.

Table 3: FICI scores for the vancomycin and furazolidone antibiotic combinations against *E. coli* laboratory strain BW25113 obtained from the checkerboard assay.

Van [a]	500	250	125	62.5	31.25	15.6	7.8	3.9	0
Fur [a]									
2.5	2	1.5	1.25	1.125	1.0625	1.0312	1.0156	1.0078	1
1.25	0.5	1	0.75	0.625	0.5625	0.5312	0.5156	0.5078	0.5
0.625	0.254	0.75	0.5	0.375	0.3125	0.2812	0.2656	0.2578	0.25
0.3125	0.126	0.625	0.375	0.25	0.1875	0.1562	0.1406	0.1328	0.125
0.156	0.0629	0.56	0.31	0.1874	0.1249	0.0936	0.078	0.0702	0.0625
0.078	0.0315	0.53	0.28	0.1562	0.0937	0.0624	0.0468	0.039	0.03125
0	1	0.5	0.25	0.125	0.0625	0.03125	0.015625	0.007813	0.015625

[a] All concentrations are expressed in mg/L. Numbers in the body of the table correspond to FICI's for each concentration combination, calculated as described in the Materials and Methods section. Unshaded and shaded areas correspond, respectively, to the wells that demonstrated greater than or less than 90% inhibition. Only the FICI's of the first concentration combinations above 90% inhibition were given.

Table 4: FICI scores for vancomycin and furazolidone antibiotic combinations against *E. coli* laboratory strain KI508 obtained from the checkerboard assay.

Van [a]	500	250	125	62.5	31.25	15.6	7.8	3.9	0
Fur [a]									
2.5	2	1.5	1.25	1.125	1.0625	1.0312	1.0156	1.0078	1
1.25	0.5	1	0.75	0.625	0.5625	0.5312	0.5156	0.5078	0.5
0.625	0.0254	0.75	0.5	0.375	0.3125	0.2812	0.2656	0.2578	0.25
0.3125	0.126	0.625	0.375	0.25	0.1875	0.1562	0.1406	0.1328	0.125
0.156	0.0629	0.56104	0.3124	0.1874	0.1249	0.0936	0.078	0.0702	0.0625
0.078	0.0315	0.5312	0.2812	0.1562	0.0937	0.0624	0.0468	0.039	0.03125
0	1	0.5	0.25	0.125	0.0625	0.03125	0.015625	0.007813	0.015625

[a] All concentrations are expressed in mg/L. Numbers in the body of the table correspond to FICI's for each concentration combination, calculated as described in the Materials and Methods section. Unshaded and shaded areas correspond, respectively, to the wells that demonstrated greater than or less than 90% inhibition. Only the FICI's of the first concentration combinations above 90% inhibition were given.

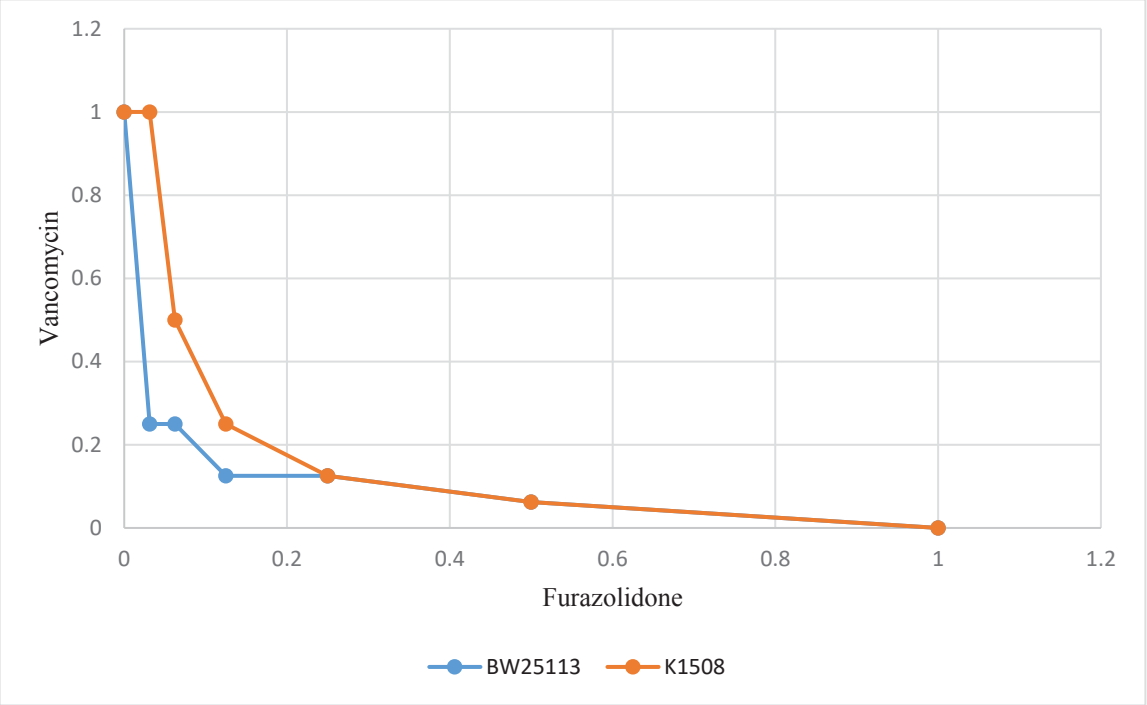

Figure 6: Isobologram comparing the synergy of the vancomycin furazolidone combination against the laboratory strains, BW25113 and KI508.

FICI values for vancomycin were plotted against the FICI values of furazolidone (see Tables 3 and 4).

3.2 Bactericidal effect of vancomycin and furazolidone in combination

Strain BW25113 was used in further experiments given that the isogenic mutant collection of non-essential *E. coli* genes (Keio collection) was available from the Japan National Genetics Centre (Baba *et al.*, 2006). Cultures of the wells of the checkerboard assays containing combinations with no detectable growth were titrated in order to determine the concentrations that not only inhibited growth but have killed bacteria from the initial inoculum. Given that the starting viable titre was $1x10^6$/mL, hence $1x10^4$/10 µL, concentration combinations giving < 10 colonies from 10 µL cultures underwent > 99% killing. Two combinations; vancomycin at 125 mg/L with furazolidone at 0.625 mg/L and vancomycin at 62.5 mg/L with furazolidone at 0.625 mg/L both, fulfilled this criterion (no colonies detected) suggesting bactericidal activity (Table 5). However, due to the concerns about vancomycin toxicity, the combination of a lower concentration of vancomycin (62.5 mg/L) with furazolidone (0.625 mg/L) was chosen for the time-kill assay. Another notable combination of vancomycin at 62.5 mg/L and furazolidone at 1.25 mg/L gave no colonies and had a FICI score marginally above the synergy threshold at 0.625, hence it was also chosen for the time-kill assay (Table 5).

In the time-kill assay, *E. coli* BW25113 at 2×10^6 CFU/mL was challenged with vancomycin and furazolidone in combination at bactericidal concentrations in combination. The bacterial cell counts were obtained at 0, 2, 4, 6 and 24 hours. For the two concentration combinations tested, there were three orders of magnitude reduction of the bacterial cell counts after 6 hours. However, the bacteria challenged with the combination containing vancomycin at 62.5 mg/L and furazolidone at 0.625 mg/L showed an increase of about 10-fold in the titre at the 24-hour time point, indicating that cells which remained alive after 6 hours of incubation may have grown and divided up to 3 to 4 times over the remaining 18 hours. In contrast, the combination containing vancomycin at 62.5 mg/L and furazolidone at 1.25 mg/L did not allow growth of surviving bacteria (if any). The bacterial cell count in this culture was reduced to below 100 CFU/mL at the 24-hour point which was the lowest possible detected number possible in this experiment (Figure 7). When challenged with vancomycin at 500 mg/L, the rate of killing was greater than that of both of the combinations and within 2 hours the bacterial cell count had dropped by 4 orders of magnitude and then below the level of detection at the 4-hour time-point (Figure 7). Furazolidone at 5 mg/L, in contrast, did not display the rapid rate of killing matching that of vancomycin at 500 mg/L or even match

the rate of killing displayed by the two combinations tested. Like the combination containing vancomycin at 62.5 mg/L and furazolidone at 0.625 mg/L, following the 6-hour time point, the bacterial cell counts in the culture containing 5 mg/L of furazolidone, started to increase again although not to the level of the 0-hour time point (Figure 7). The positive control, tetracycline at 10 mg/L, showed no killing, in agreement with its well-recognised bacteriostatic activity. These findings suggest that both vancomycin/furazolidone combinations possess bactericidal activity.

Table 5: Titres of viable cells in the inhibitory vancomycin and furazolidone concentration combinations.

Vancomycin (mg/L)	Furazolidone (mg/L)	FICI	CFU/10 µL[a]
250	2.5	1.5	0
250	1.25	1	0
250	0.625	0.75	0
250	0.3125	0.625	TMTC [b]
250	0.1526	0.56	TMTC
250	0.078	0.53	TMTC
125	2.5	1.25	0
125	1.25	0.75	0
125	0.625	0.5	3
125	0.3125	0.375	TMTC
125	0.1526	0.31	TMTC
125	0.078	0.28	TMTC
62.5	2.5	1.125	0
62.5	1.25	0.625	0 [c]
62.5	0.625	0.375	0
62.5	0.3125	0.25	28
31.25	2.5	1.0625	8
31.25	1.25	0.5625	TMTC
15.6	2.5	1.0312	TMTC
15.6	1.25	0.5312	TMTC
7.8	2.5	1.0156	TMTC
3.9	2.5	1.0078	TMTC

[a] Number of BW25113 colonies from 10 µL cultures containing the indicated combinations of antibiotics.

[b] TMTC, too many to count.

[c] Highlighted rows correspond to the combinations that were used for the time-kill assay.

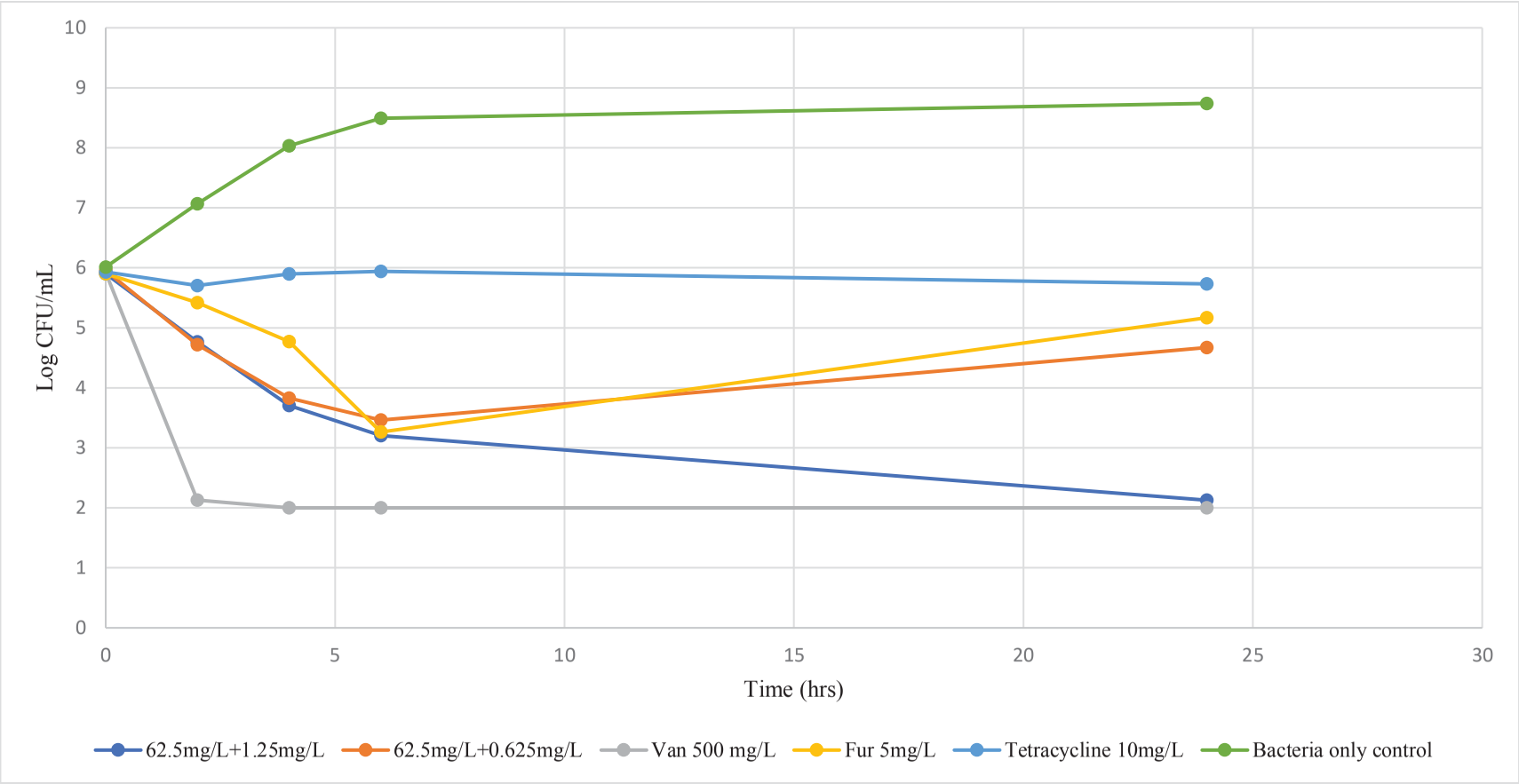

Figure 7: Time-kill assay for the vancomycin and furazolidone combination against *E. coli* BW25113.

Logarithmic phase BW25113 was added at 2×10^6 CFU/mL to different combinations of vancomycin and furazolidone or each antibiotic alone. After 0, 2, 4, 6 and 24 hours of incubation at 37 °C, the combinations were titred on 2xYT (antibiotic-free) plates. Bacterial counts were carried out and the viable titres (CFU/mL) of bacteria from each combination was determined. For the positive control, bacteria were challenged with 10 mg/L of tetracycline. For the negative control, no antibiotics were added to the media. The limit of detection of this assay was 100 CFU/mL.

3.3 Investigation of the synergy mechanism: the role of efflux pumps

3.3.1 Efflux pump mutant screen

We hypothesised that the mechanism of synergy between vancomycin and furazolidone could be based on inhibition of efflux out of the cells. An MIC screen of the Keio collection of deletion mutants in genes encoding the efflux pump subunits was performed. Each mutant was challenged with a series of vancomycin concentrations ranging from 1000 mg/L to 125 mg/L and furazolidone ranging from 5 mg/L to 1.25 mg/L individually (Table 6). A deletion mutant lacking the gene encoding the outer membrane channel TolC, was more sensitive to furazolidone (MIC was half that of the wild-type parent). No difference in the MIC, however, was detected for vancomycin compared to the parental wild-type strains (Tables 3, 6). The strain containing a deletion of the *acrA* gene encoding a transenvelope protein connecting the outer membrane channel TolC to the inner membrane components of several efflux pumps showed a twofold decrease in MIC for both vancomycin and furazolidone when assayed separately (Table 6). Increased resistance or susceptibility to furazolidone was not observed in any of the other mutants. Mutants of the genes; *macB, acrF, emrA, emrB, emrK* and *emrY* showed greater susceptibility to vancomycin (Table 6). Similarly, to *E. coli* BW25113, all the mutants were inhibited by the tetracycline positive control at 10 mg/L.

Table 6: MICs for vancomycin and furazolidone against *E. coli* mutants involved in the TolC efflux systems.

E. coli strain	Mutation/comment	Vancomycin (mg/L)	Furazolidone (mg/L)
BW25113	No deletion	500	2.5
JW5503-1	*ΔtolC::kan*	500	1.25
K2404	*ΔtolC*	500	1.25
JW0452-3	*ΔacrA::kan*	250	1.25
K2428	*ΔacrA*	250	1.25
JW2454-1	*ΔacrD::kan*	250	2.5
JW0862-1	*ΔmacA::kan*	250	2.5
JW0863-1	*ΔmacB::kan*	500	2.5
JW3481-1	*ΔmdtE::kan*	250	2.5
JW3482-1	*ΔmdtF::kan*	250	2.5
JW0451-2	*ΔacrB::kan*	250	2.5
JW3233-2	*ΔacrE::kan*	500	2.5
JW3234-1	*ΔacrF::kan*	500	2.5
JW5338-1	*ΔmdtA::kan*	250	2.5
JW2060-1	*ΔmdtB::kan*	250	2.5
JW2660-1	*ΔemrA::kan*	500	2.5
JW2661-1	*ΔemrB::kan*	500	2.5
JW2365-1	*ΔemrK::kan*	500	2.5
JW2364-1	*ΔemrY::kan*	500	2.5

Each mutant was challenged at 2×10^6 CFU/mL with vancomycin from 1000 mg/L to 125 mg/L or furazolidone from 5 mg/L to 1.25 mg/L. OD readings at 600 nm were taken following 24 hours of exposure at 30°C. The MIC was determined as a minimal concentration required to inhibit bacterial growth (measured by OD) by 90%.

3.3.2 Checkerboard analysis of TolC efflux pump system mutants

TolC is an outer membrane channel that is involved in many efflux pump systems and it was hypothesised that it could be involved in the interaction between vancomycin and furazolidone, based on two-fold decrease in the MIC of the *ΔacrA* mutant. Therefore, the checkerboard assays were performed on strains JW5503-1 and JW0452-3, harbouring deletions in the TolC outer membrane channel and the AcrA periplasmic subunit-encoding genes, respectively. These two strains contained a *kan* cassette inserted in the place of the corresponding ORFs (Baba *et al.*, 2006). To preclude potential polar effect of the *kan*-encoding gene insertion (including the translational stop codon) on downstream genes within the respective operons (Appendix 1, 2, 3), the *kan* cassette (which was flanked by *frt* sites) was removed by transient expression of the site-specific recombinase FLP (acting on the *frt* sites). The resulting strains containing "in frame" scarless deletions of the respective genes, K2404 (*ΔtolC*) and K2428 (*ΔacrA*) were also tested using the checkerboard assays (Figure 8). When comparing the effects on the vancomycin/furazolidone interaction in *ΔtolC* mutants with or without the *kan* cassette on an isobologram, it was observed that there was a minimal, if any, difference in the synergy (Figure 8A). Unlike the *ΔtolC* mutants, a slight decrease in synergy between the vancomycin and furazolidone was observed on isobologram in the presence *vs*. absence of the *kan* cassette in the *ΔacrA* allele (Figure 8B).

Comparisons of isobolograms between the wild-type parent strain BW25113 and mutants *ΔtolC* and *ΔacrA* showed that the deletion of the *tolC* gene results in a greater decrease in synergy compared to the deletion *acrA* gene. The latter mutant, by comparison, shows an extremely slight loss in synergy compared to that of the parental BW25113 strain (Figure 9A.). These findings suggest that despite some decrease in synergy between the two antibiotics in the strains lacking the *tolC* and *acrA* genes, the combination is still overall synergistic. The isobolograms of these mutants relative to wild-type parent show some decrease in synergy although this is more so for *ΔtolC* than for *ΔacrA*. Therefore, the TolC unit may contribute to the synergy, but are not involved in the main mechanism of the vancomycin and furazolidone synergistic interaction.

(A)

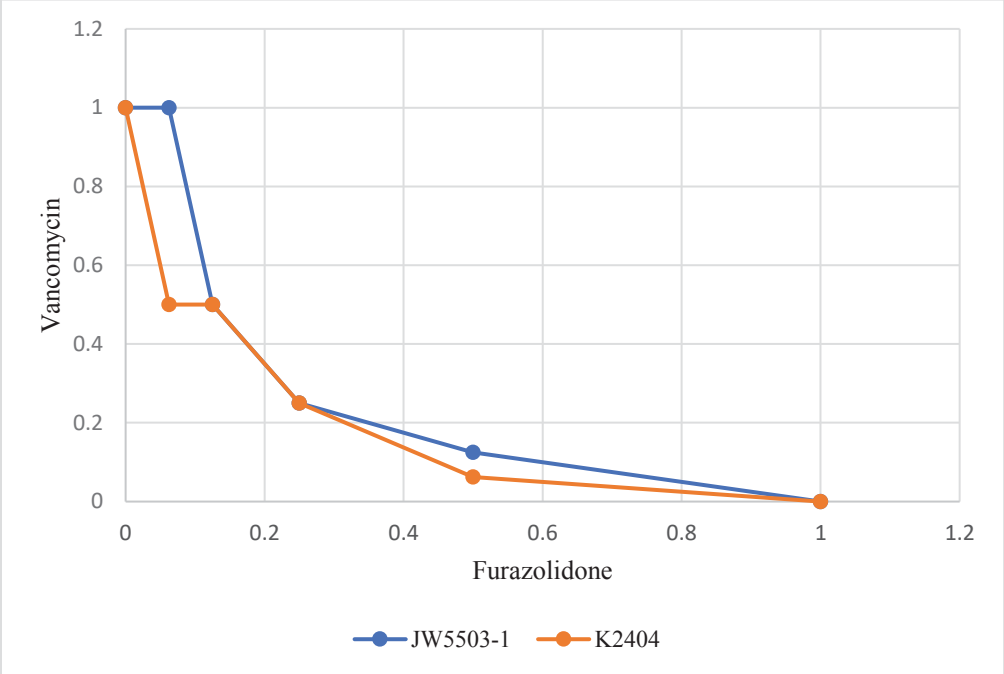

(B)

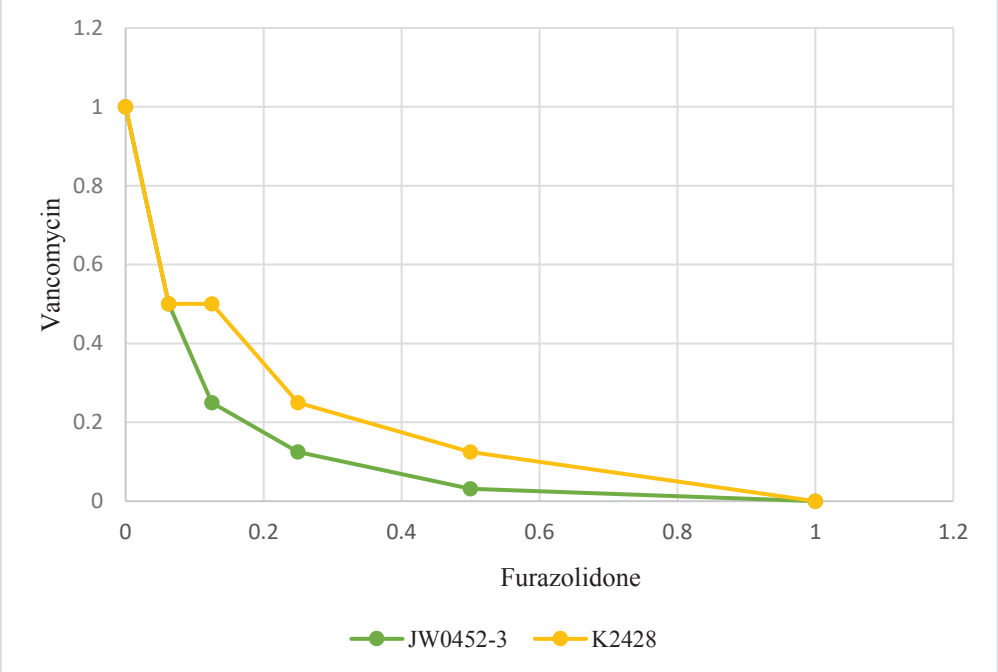

Figure 8: Effects of the kanamycin resistance marker in the *ΔtolC* and *ΔacrA* alleles on vancomycin and furazolidone interaction.

(A), strains JW5503-1 and K2404 containing the *ΔtolC::kan* and *ΔtolC* alleles respectively. **(B)**, strains JW0452-3 and K2428 containing the *ΔacrA::kan* and *ΔacrA* alleles, respectively. Isobologram was derived from checkerboard assays of each strain, performed as described in the Materials and Methods section.

(A)

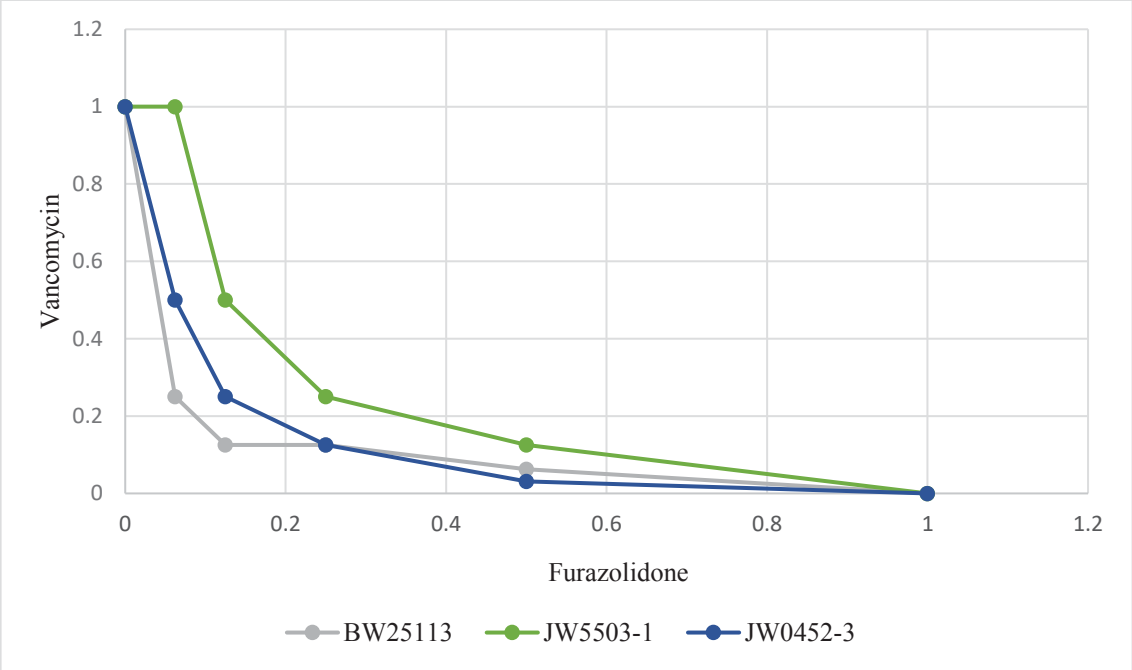

(B)

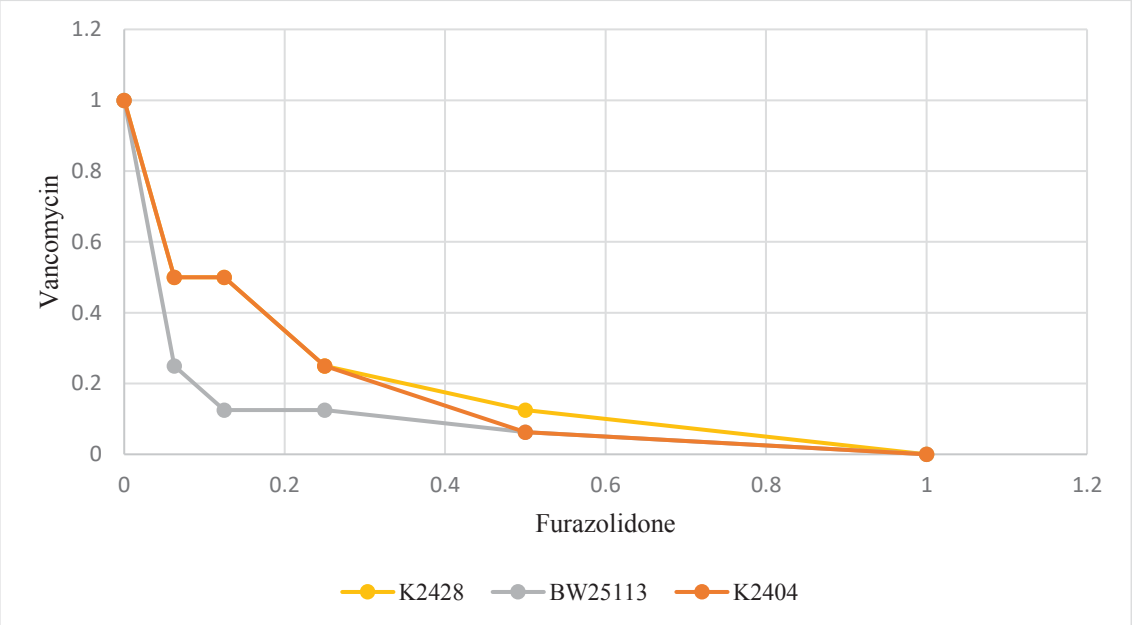

Figure 9: Effect of the *ΔtolC* and *ΔacrA* mutations on the interaction between vancomycin and furazolidone.

(A), strains JW5503-1 and JW0452-3 containing the *ΔtolC::kan* and *ΔacrA::kan* alleles respectively compared to strain, BW25113. **(B)**, strains K2404 and K2428 containing the *ΔtolC* and *ΔacrA* alleles respectively from which the *kan* cassette was removed and compared to strain, BW25113. Isobologram was derived from checkerboard assays of each strain, performed as described in the Materials and Methods section.

3.4 Enterobactin synthesis and transport

Given a potential role of TolC in the vancomycin-furazolidone synergy determined in the previous section and potential oxidative stress that furazolidone may induce in the host cells (Jin *et al.*, 2011), one possible mechanism of how TolC is involved in synergy could be related to decrease of its function due to furazolidone-induced oxidative stress and iron starvation response, part of which is overproduction of enterobactin which activates the TolC opening to the periplasm thus allowing the entry of vancomycin into the periplasm. The effect of enterobactin synthesis and transport on the interaction between vancomycin and furazolidone was investigated by combining *ΔtolC* and *ΔentC* mutations and observing their effect on the vancomycin and furazolidone synergy using checkerboard assays and graphically presented by isobolograms (Figures 10 and 11).

The MICs for *ΔentC* with vancomycin and furazolidone alone were first compared to those of the wild-type and Δ*tolC* mutant (Table 7). Prior to analysing the double mutants, the effect of the presence or absence of the *kan* cassette in *ΔentC* on the synergy was monitored. Strain JW0858-2 contains the *ΔentC::kan* mutation whereas K2430 contains *ΔentC* without the kanamycin cassette, which was removed by FLP recombination starting from strain JW0858-2. When the FICI scores were compared on an isobologram, it was observed that the removal of the kanamycin resistance marker resulted in a somewhat decreased synergy (Figure 10A).

Double mutants K2414 and K2427 (*ΔtolC ΔentC::kan* and *ΔtolC ΔentC*, respectively) were prepared by P1 transduction. K2427 was subsequently subjected to FLP recombination in order to remove the *frt*-flanked *kan* cassette. Both of these strains were compared with respect to vancomycin-furazolidone interaction using the checkerboard assay and the derived isobologram. No change or a marginal gain in synergy was observed in the kanamycin-marker-negative mutants (Figure 10B).

More importantly, the wild-type, *ΔtolC, ΔentC,* and double *ΔtolC ΔentC* mutant were compared for their effect on the synergy between vancomycin and furazolidone. When compared overall, it was found that the deletion of the TolC channel caused the greatest decrease in synergy in the comparison between the three mutants; *ΔtolC, ΔentC*, and the *ΔtolC ΔentC* double mutant (Figure 11A). *E. coli* JW0585-2 containing the *ΔentC* mutation was found to have an isobologram similar to that of the wild-type parent strain

BW25113 (Figure 11A) which suggests that it had no effect on the synergy. The mutants that had the *kan* cassette removed showed a slightly different trend. The double mutant, K2427, showed no loss or gain in synergy in that it was almost identical to the wild-type parent strain BW25113 (Figure 11B). Furthermore, the *ΔentC* mutant strain K2430 was found to have a greater effect on the synergy in comparison to the double mutant *ΔtolC ΔentC* strain as shown on the isobologram (Figure 11B). While minor differences between the different groups were shown, overall these findings suggest that the mechanism of vancomycin and furazolidone synergy was not related to the enterobactin synthesis or transport pathways.

Table 7: MICs for vancomycin and furazolidone against the *E. coli* mutants involved in the enterobactin synthesis and transport system.

E. coli strain	Mutation/Comment	Vancomycin (mg/L)	Furazolidone (mg/L)
BW25113	No deletion	500	2.5
K2404	*ΔtolC*	500	1.25
JW0585-2	*ΔentC::kan*	250	2.5
K2430	*ΔentC*	250	2.5
K2414	*ΔtolC ΔentC::kan*	500	1.25
K2427	*ΔtolC ΔentC*	500	1.25

Each mutant was challenged at 2×10^6 CFU/mL with vancomycin from 1000 mg/L to 125 mg/L or furazolidone from 5 mg/L to 1.25 mg/L. OD readings were taken following 24 hours of exposure at 30°C at 600 nm. The MIC was determined as a minimal concentration required to inhibit bacterial growth (measured by OD) by 90%.

(A)

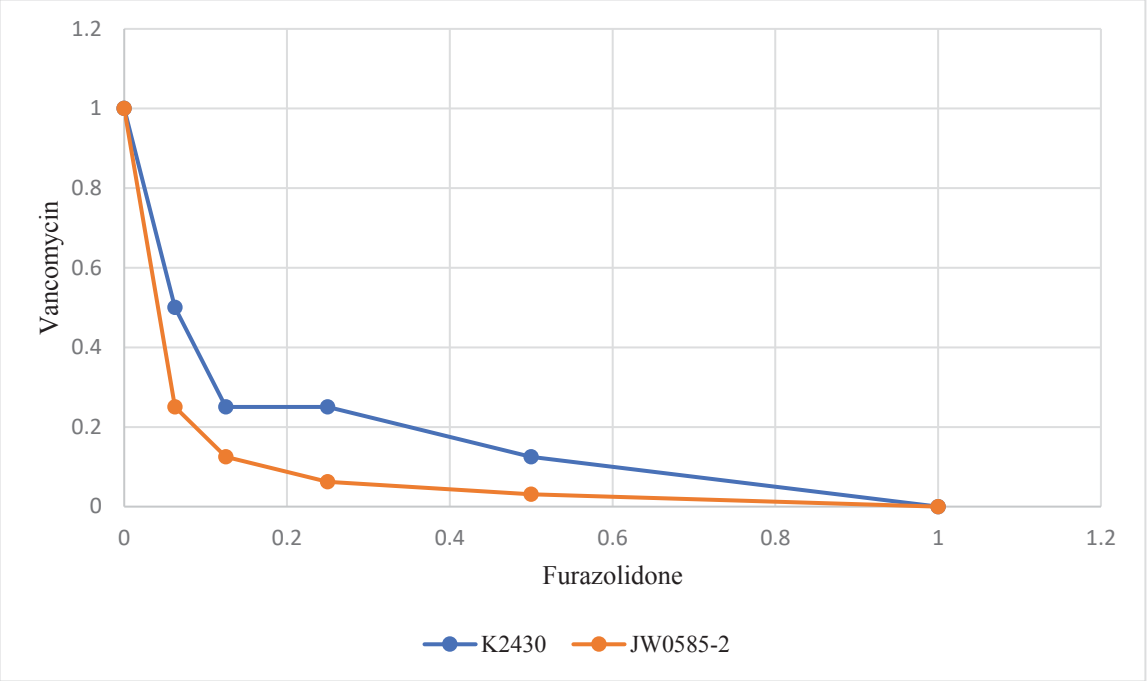

(B)

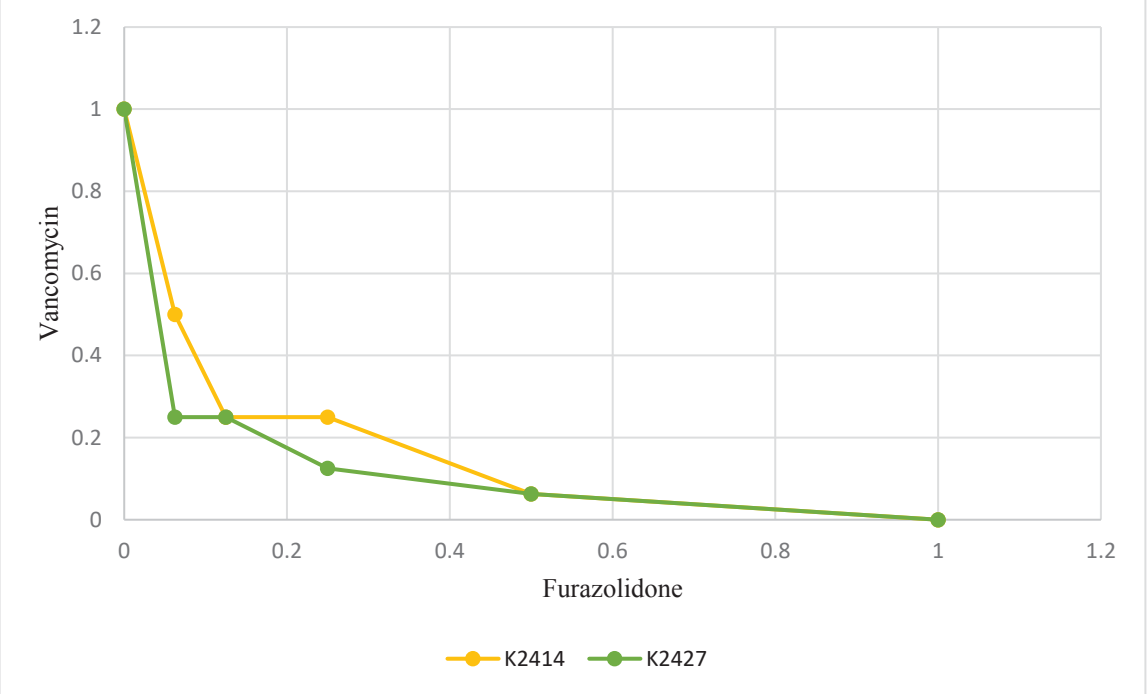

Figure 10: Effects of the kanamycin resistance marker on the synergy changes in the *ΔentC* single and *ΔtolC ΔentC* double mutant strains.

Isobologram comparisons between the wild-type *E. coli* and *ΔtolC ΔentC* mutant enterobactin synthesis and export system. (**A**), strains JW0585-2 and K2430 harbouring *ΔentC::kan* and *ΔentC* mutations, respectively. (**B**), strains K2414 and K2427 harbouring the double mutations *ΔtolC ΔentC::kan and ΔtolC ΔentC*, respectively.

(A)

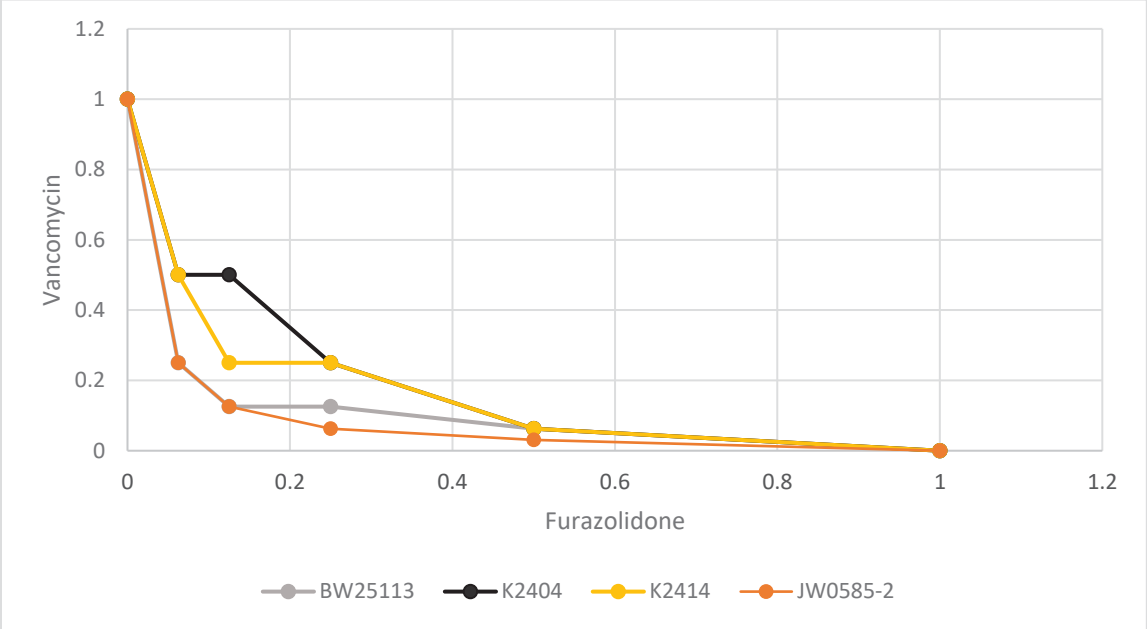

(B)

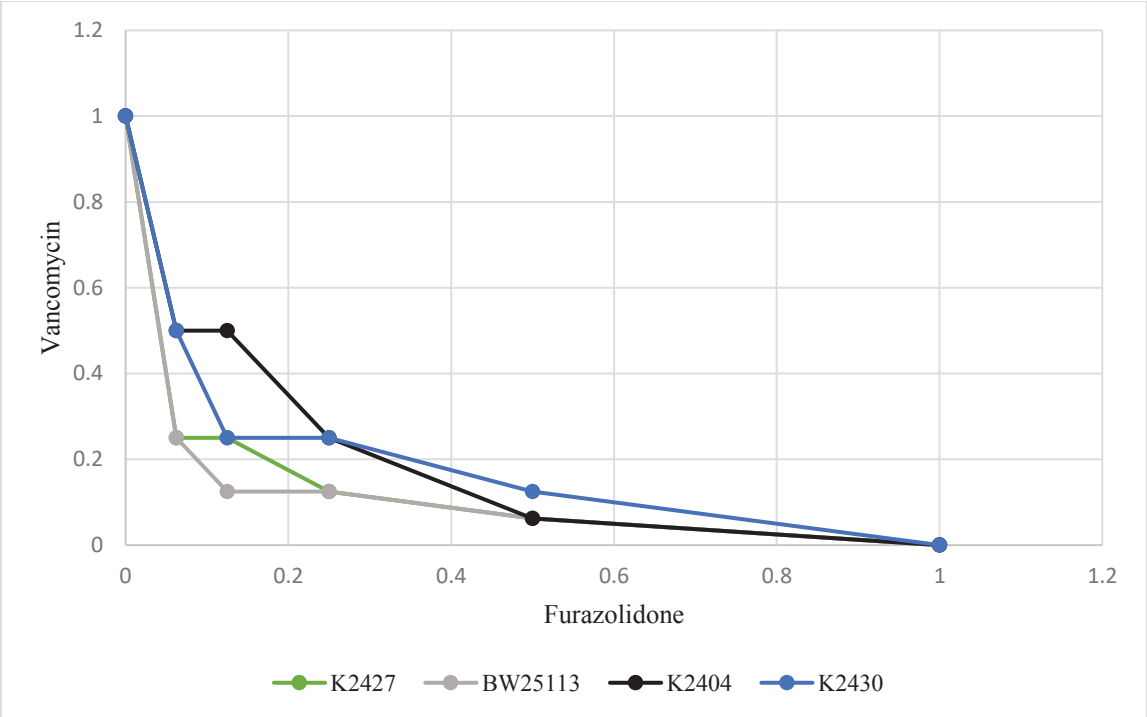

Figure 11: Effects of *ΔtolC ΔentC* single and double *ΔtolC ΔentC* mutants on the interaction between vancomycin and furazolidone.

Isobologram of the wild-type strain BW25113 was compared to derived mutants. **(A)**, mutants where either allele contains the kanamycin resistance cassette; K2404 (*ΔtolC*), JW0585-2 (*ΔentC::*kan) and K2414 (*ΔtolC ΔentC::kan*) **(B)**, strains from which the kanamycin cassettes were removed; K2404 (*ΔtolC*), K2430 (*ΔentC*) and K2427 (*ΔtolC ΔentC*).

3.5 DNA repair

A hypothesis was formulated that the potential mechanism of the vancomycin and furazolidone synergy could be through the pathways for DNA damage repair. DNA damage, in turn, could be caused by the synergistic effect of the stresses (envelope and oxidative) that vancomycin and furazolidone, respectively, impose on the *E. coli* cells. In order to further investigate this, strain K2431 which contains a deletion of a gene encoding a protein in the nucleotide excision repair system, UvrA, was challenged with the vancomycin and furazolidone antibiotic combination and was compared to the wild-type parental strain BW25113. Before performing the checkerboard assay, an MIC test for both vancomycin and furazolidone was performed in order to obtain the MIC breakpoints for strain K2431 in order to calculate the FICI scores. MICs for vancomycin and furazolidone alone were 250 mg/L and 0.3125 mg/L, the former 2-fold and the latter 8-fold lower relative to the wild-type parent strain BW25113. Despite being highly sensitive to furazolidone, the checkerboard analysis showed that deletion of the nucleotide excision does not modify the synergy when compared to BW25113 strain (Figure 12). Overall these findings suggest that DNA repair through the UvrABC nucleotide excision repair system is not the target of the vancomycin and furazolidone synergy.

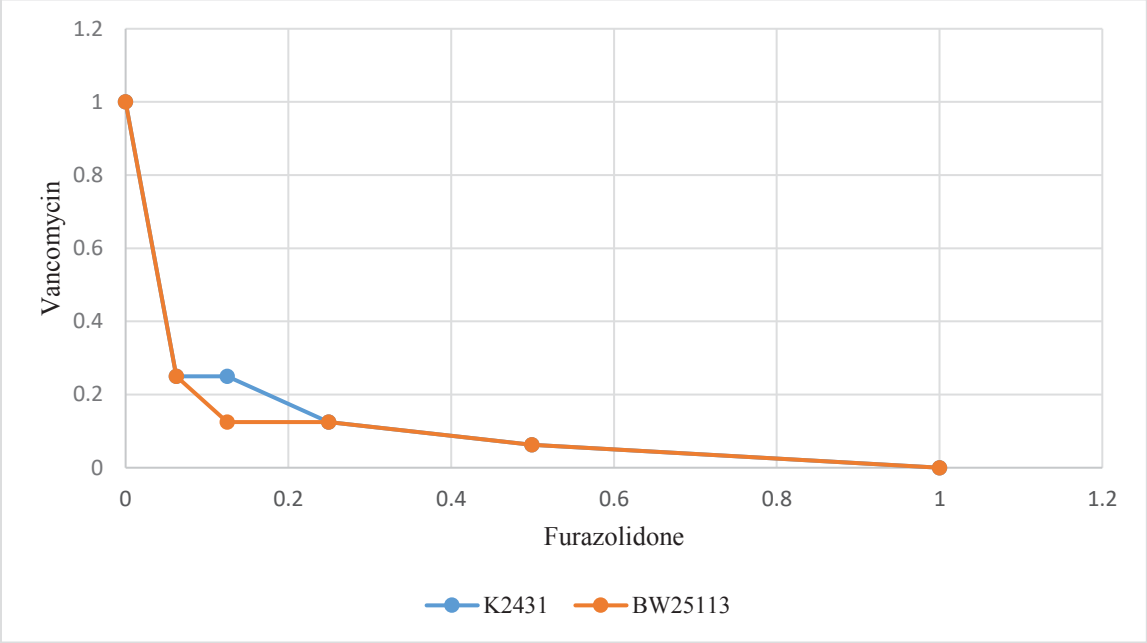

Figure 12: Effect of the excision repair system mutant *ΔuvrA* on the vancomycin and furazolidone interaction.

Isobologram of K2431 (*ΔuvrA*) as compared to that of the wild-type strain BW25113.

3.6 Biofilms

To investigate whether the vancomycin-furazolidone combination is suitable for commercial or medical applications that involve *E. coli* growth as a biofilm, the Minimal Biofilm Inhibitory Concentration (MBIC) and Minimal Biofilm Eradication Concentration (MBEC) were determined using the wild-type *E. coli*.

3.6.1 Minimal Biofilm Inhibitory Concentration (MBIC)

The BW25113 biofilms were formed using a biofilm peg lid system. The biofilm grown on the pegs in the absence of antibiotic for 24 hours at 37 °C was exposed to each antibiotic alone and their combinations. The MBIC was measured after detachment of cells into the medium without antibiotics (by centrifugation), through OD readings at 600 nm. Interestingly, when the BW25113 biofilms were challenged by vancomycin, 500 mg/L was observed to inhibit the biofilm growth, the same concentration needed to inhibit BW25113 in a planktonic mode of growth. In comparison, furazolidone concentration of as much as 19.5 mg/L was required to inhibit the biofilm growth, as opposed to 2.5 mg/L for planktonic cultures. In combination, both antibiotics appeared to be more effective than individually; a combination of vancomycin at 250 mg/L and furazolidone at 9.75 mg/L was required to inhibit 90% of the biofilm growth. The antibiotic combination was therefore much less effective in inhibiting the growth of the biofilms than that of the planktonic cultures (vancomycin at 62.5 mg/L and furazolidone at 0.3125 mg/L; Table 3).

3.6.2 Minimal Biofilm Eliminating (cell killing) Concentration (MBEC)

To determine the concentrations of antibiotics required to eliminate (kill) bacteria in the biofilm, the cells dislodged by centrifugation into antibiotic-free 2xYT media were titrated to determine the viable titre (CFU/mL), for cultures from those concentrations of antibiotics where the growth was inhibited (above the MBIC).

BW25113 biofilms were first challenged by a dilution series of vancomycin ranging from 64 000 mg/L to 62.5 mg/L. At 500 mg/L, there is a 5-log reduction in the titre of viable bacteria relative to the biofilm grown in the absence of antibiotic (Figure 13A). Interestingly, at the higher concentrations of vancomycin (from 1000 mg/L to 32 000 mg/L), there is a marked increase in the viable titres compared to that of the 500 mg/L

group, with the greatest titres of up to 3.75×10^4 CFU/mL present in the biofilms challenged with vancomycin at 16 000 mg/L and 32 000 mg/L (Figure 12A). No colonies were formed in the titration of biofilms that were challenged by vancomycin at 64 000 mg/L, suggesting that the biofilm was completely eradicated at this concentration (Figure 13A). These results show that in order to achieve a 3-log reduction of biofilm numbers, 500 mg/L of vancomycin is sufficient. In order to completely eradicate a biofilm, however, 64 000 mg/L of vancomycin would have to be used.

E. coli BW25113 biofilms were also challenged against a furazolidone dilution series ranging from 1250 mg/L to 4.875 mg/L (Figure 13B). When the biofilms are challenged with furazolidone at the MBIC concentration (19.5 mg/L), the biofilm cell count was reduced down to 1.82×10^5 CFU/mL (Figure 13B). Unlike with vancomycin, furazolidone did not display an increase in cell numbers at greater concentrations. At concentrations of 39 mg/L and above the biofilm was completely eradicated (Figure 13B). These findings overall show that the MBEC was 39 mg/L for furazolidone against BW25113. Like vancomycin, it was far less effective at clearing biofilms in comparison to the planktonic cells. It is worth mentioning that the time-kill curve analysis with planktonic cells showed that at higher concentrations, killing almost eradicates bacteria over 6 hours, however, extended incubation results in the outgrowth of a small number of surviving cells that presumably became resistant to the antibiotic. However, in contrast to the biofilm, this behaviour was observed in planktonic cultures challenged with furazolidone and combinations of vancomycin and furazolidone. High concentrations of antibiotics, however, were not analysed in the planktonic culture time-kill assays.

To investigate how effective the antibiotic combination is against biofilms, a checkerboard kill assay was performed BW25113 biofilms using the peg lid system. Similar to the single antibiotic tests, the biofilms were exposed to the vancomycin and furazolidone combination for 24 hours at 30°C. Higher concentrations than the MBEC for both vancomycin and furazolidone were analysed in this experiment as it was plausible that the interaction may potentially act antagonistically in a biofilm-based setting as opposed to the planktonic setups tested previously. Vancomycin at concentrations 4000 mg/L, 2000 mg/L and 1000 mg/L which showed an increased titre of surviving cells growth when challenged alone completely eradicated the biofilms when combined with the furazolidone dilutions (Figure 14). Vancomycin at 500 mg/L,

when combined with furazolidone at all concentrations with the exception of 9.75 mg/L, was successful in eradicating the biofilms (Figure 14). Interestingly, the combination containing 500 mg/L of vancomycin and 9.75 mg/L of furazolidone had a biofilm cell count of 3.6×10^2 CFU/mL which was higher than vancomycin at 500 mg/L alone, 8.0×10^1 CFU/mL (Figure 14). When sub-inhibitory concentrations of vancomycin (250 mg/L) was combined with furazolidone at concentrations above its MBEC, no viable cells were detected. When vancomycin at 250 mg/L was combined with sub-inhibitory concentrations of furazolidone, while more effective than either of these antibiotics alone, it was relatively ineffective at eradicating biofilms. This is observed when vancomycin at 250 mg/L was combined with furazolidone at 19.5 mg/L and 9.75 mg/L, the biofilm cell counts were found to be 2.0×10^3 CFU/mL and 2.56×10^3 CFU/mL respectively (Figure 14). The most prominent benefit of the combination is the elimination of long-term bacterial outgrowth at vancomycin concentrations above 500 mg/mL.

(A)

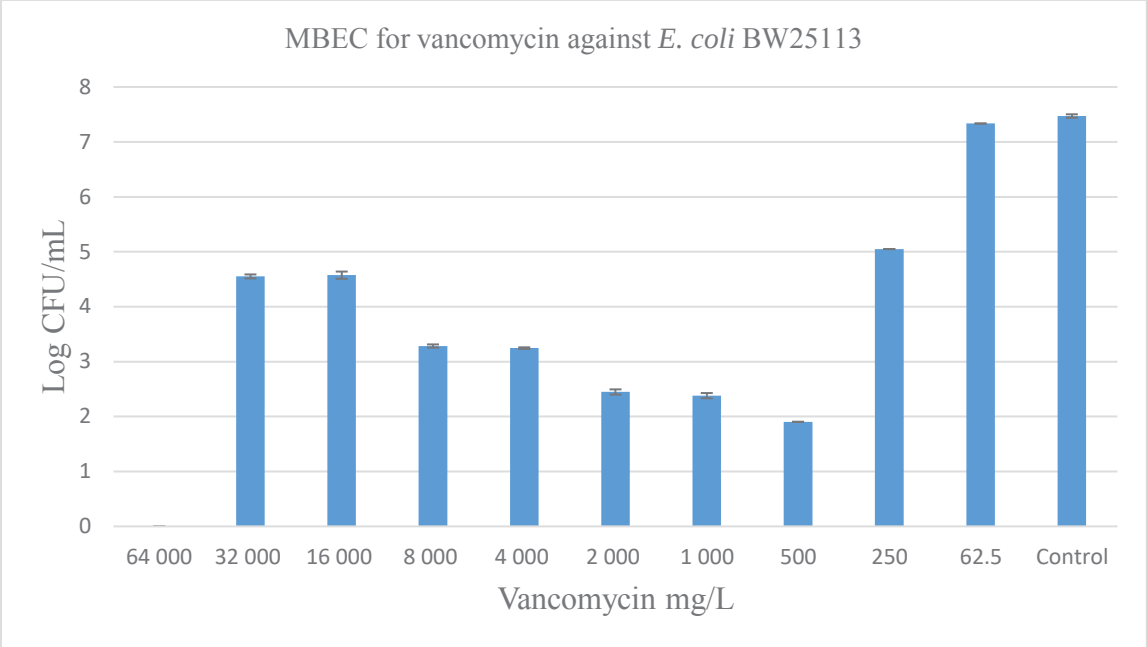

(B)

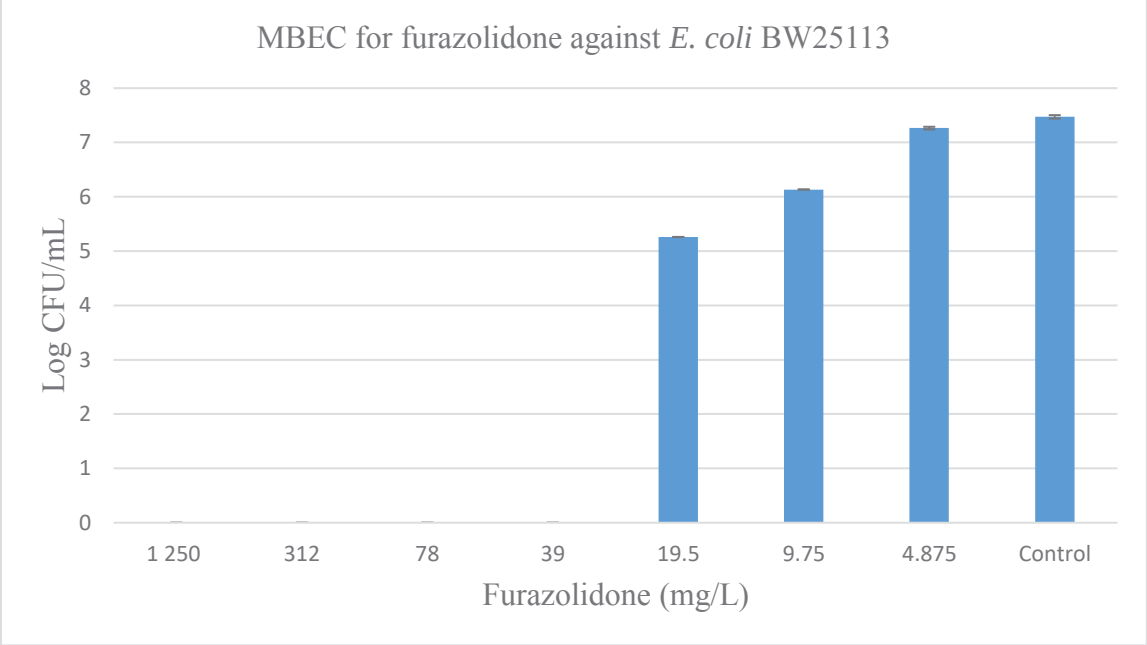

Figure 13: Susceptibility of *E. coli* BW25113 biofilms against vancomycin and furazolidone.

E. coli BW25113 at 1×10^7 CFU/mL was inoculated on to a 96-well plate containing a peg lid at 37 °C. The peg lid containing the biofilm was challenged with **(A)** vancomycin and **(B)** furazolidone dilutions for 24 hours at 30°C. Following exposure, the biofilm was centrifuged at 2000 rpm for 20 minutes to dislodge it on to 2xYT media and was titred and grown at 37 °C in order to determine the CFU/mL. The biofilm with no exposure to any antibiotics was used as the negative control and no bacteria was used as the sterility control. Error bars represent the standard deviation of the mean.

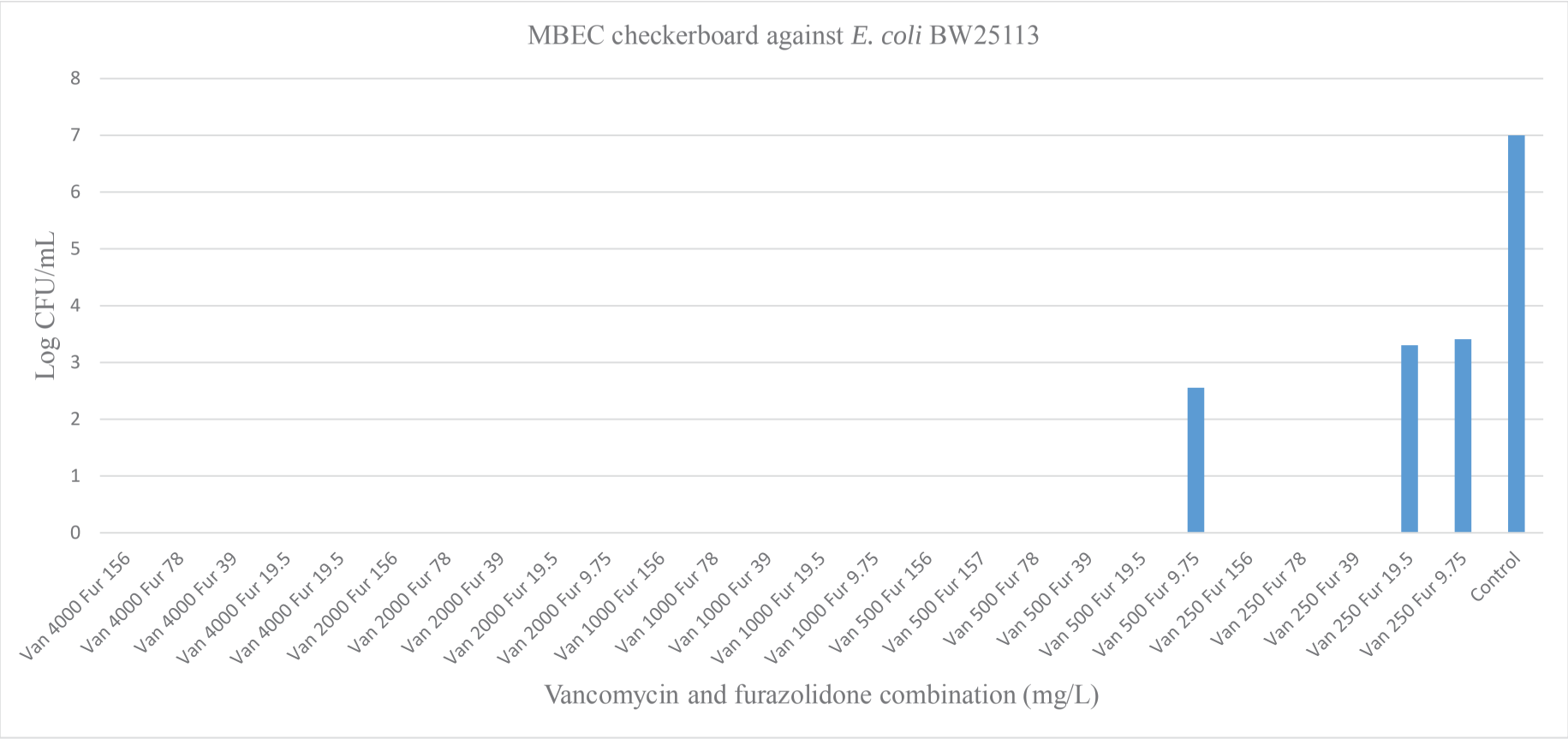

Figure 14: Checkerboard analysis of the BW25113 (wild type) biofilm killing (eradication) by vancomycin and furazolidone combinations.

BW25113 at 1×10^7 CFU/mL was inoculated on to a 96-well plate containing a peg lid at 37 °C. The peg lid containing the biofilm was challenged with combinations of vancomycin and furazolidone concentrations for 24 hours at 30°C. Following exposure to the antibiotics, the biofilm was dislodged into the antibiotic-free medium and titrated. Concentrations of antibiotics are indicated on the X-axis. For the control, the biofilm was exposed to no antibiotics. The limit of detection is 40 (1.4 log) CFU/mL.

3.7 Addition of DOC to the vancomycin-furazolidone combination

In order to see if it is possible to reduce the concentration of vancomycin to sub-nephrotoxic levels, DOC was added into the vancomycin-furazolidone antibiotic combination. Strain BW25113 was further used in experiments to look at the effects on synergy from the addition of DOC into the vancomycin-furazolidone combination. From strain BW25113, 2×10^6 CFU/mL was challenged with concentrations of vancomycin and furazolidone (500 mg/L – 3.9 mg/L for vancomycin and 2.5 mg/L – 0.078 mg/L for furazolidone) in the presence of DOC at 5 g/L, 2.5 g/L and 1.25 g/L respectively. By itself the MICs for vancomycin when combined with DOC at 5 g/L, 2.5 g/L and 1.25 g/L was 500 mg/L for all three of the different concentrations. The MICs for furazolidone when combined with DOC at 5 g/L, 2.5 g/L and 1.25 g/L was 1.25 mg/L, 2.5 mg/L and 2.5 mg/L respectively which suggests that DOC is not synergistic with either vancomycin or furazolidone against strain BW25113. When compared to the double vancomycin-furazolidone combination, the triple combination at all three concentrations of DOC appeared to be more synergistic based on the lower concentrations of vancomycin and furazolidone required for inhibiting bacterial growth. When DOC is added at 5 g/L, in the presence of furazolidone at 0.156 mg/L and 0.3125 mg/L, vancomycin at 31.25 mg/L and 15.6 mg/L was found to inhibit bacterial growth. Vancomycin at 31.25 mg/L and 15.6 mg/L was found to inhibit strain BW25113 when combined with 0.3125 mg/L of furazolidone and 2.5 g/L of DOC. The addition of DOC at 1.25 g/L proved efficacious so that vancomycin at 15.6 mg/L was still enough to inhibit bacterial growth, however, higher concentrations of furazolidone up to 0.625 mg/L was required. Overall these results show that the addition DOC to the vancomycin-furazolidone combination is more synergistic and it allows for vancomycin to be used at sub-nephrotoxic concentrations (at concentrations below 30 mg/L).

4 Discussion

Emerging antibiotic resistant Gram-negative bacteria are becoming more and more common and are difficult to treat, so the use of antibiotic combinations is garnering interest. Traditionally Gram-negative bacteria have always been highly resistant to the potent and successful antibiotic, vancomycin (Delcour, 2009, Yarlagadda *et al.*, 2016). This thesis has explored the possibility of potentially using vancomycin against Gram-negative bacteria in combination with furazolidone. This was based on unpublished work by J. Rakonjac's group that demonstrated synergy between several nitrofurans and vancomycin on growth inhibition of *E. coli* K-12 strains, which was corroborated by a published study that reported synergy between vancomycin and a nitrofuran, nitrofurantoin (Zhou *et al.*, 2015).

This study set out to explore possible mechanisms of synergy between vancomycin and the nitrofuran, furazolidone against *E. coli*. Furthermore, the effect of this antibiotic combination on *E. coli* biofilms was investigated.

4.1 Synergy between vancomycin and furazolidone

In this study, the MIC breakpoints of furazolidone, vancomycin and their combinations were characterised through the use of the broth microdilution method. Consistent with findings from other studies of *E. coli*, the MICs for vancomycin found in this study (500 mg/L) is in agreement with the known intrinsic resistance of Gram-negative bacteria to > 600 Da hydrophilic antibiotics (Zhou *et al.*, 2015) (Table 3) due to the presence of the outer membrane. The porin channels in the outer membrane only allow the diffusion of molecules that are 600 Da into the *E. coli* periplasm. The molecular weight of vancomycin is 1486 kDa which means that vancomycin cannot simply diffuse through the porins and reach its target, the peptidoglycan synthesis machinery (Delcour, 2009, Yarlagadda *et al.*, 2016).

Prior studies have found that in *E. coli* mutations involving defects in the lipopolysaccharide core resulted in increased susceptibility to vancomycin through the destabilisation of LPS, the outer leaflet of the outer membrane which maintains the resilience of this envelope layer (Shlaes *et al.*, 1989, Nikaido, 2005). Furthermore, mutations in the gate of the large outer membrane channels of the secretin family,

reported reduced MICs of vancomycin, comparable to that of the MICs reported for Gram-positive bacteria (Spagnuolo *et al.*, 2010).

Furazolidone, however, was observed to inhibit the growth of Gram-negative bacteria at significantly lower concentrations than vancomycin. Having a molecular weight of 225.16 Da, furazolidone can diffuse freely through the porin channels and exert its effect on the cell (Walzer *et al.*, 1991).

It is thought in general that when two bactericidal or two bacteriostatic drugs work in combination, that the interaction will be synergistic (Mitosch and Bollenbach, 2014). A recent study has shown that vancomycin was proven to interact synergistically with the nitrofuran, nitrofurantoin (Zhou *et al.*, 2015). Despite being different, due to the high structural similarities between nitrofurantoin and furazolidone, it was predicted that furazolidone would also interact with vancomycin in a synergistic manner (Khong *et al.*, 2004). In this thesis, the synergy between vancomycin and furazolidone was characterised through the use of checkerboard assays and FICI scores (Table 4, Figure 5).

A key limitation that is associated with the checkerboard growth inhibition assay used to determine whether synergy was present is that the limit of detection by optical density is about 10^6 bacterial cells per mL of culture, equivalent to the starting titre in the growth inhibition experiment. It was therefore not possible to determine, using optical density measurements, whether this combination acts in a bactericidal or in a bacteriostatic manner. It is important to distinguish whether the combinations act in a bactericidal or in a bacteriostatic manner because some medical conditions such as meningitis and endocarditis require bactericidal treatments whereas bacteriostatic treatments are superior for treating toxic shock syndrome (Pankey and Sabath, 2004). A time-kill assay was performed in intervals over a 24-hour period. As both combinations were chosen based on their FICI scores and were bactericidal, it was hypothesised that both combinations would display consistent bactericidal activity throughout the whole 24 hours (Table 5). This, however, was not the case for one of the combinations which, while it reduced bacterial cell numbers, it could not maintain its bactericidal effect for the whole duration of the 24-hour period (Figure 6). This contradicts with the titrations of the checkerboard cultures where no surviving cells remained after 24 hours at the same concentration of antibiotics. Unexpectedly furazolidone displayed a similar trend

despite having a concentration at twice the MIC required to kill *E. coli* in the preliminary titration of the checkerboard cultures (Table 5). It is plausible that while 1×10^6 CFU/mL bacteria were challenged by the antibiotics in the experiments, because the volume used in the time-kill assay was 20-fold greater and so the probability of the emergence of potential antibiotic-tolerant of mutants or cells emerging would be greater. Alternatively, better aeration of the time-kill experiment culture could have resulted in the emergence of tolerant mutants.

The combination comprised of vancomycin at 62.5 mg/L and furazolidone at 1.25 mg/L showed bactericidal activity throughout the full 24-hour period, consistent with the findings from the titrations from the checkerboard assay (Figure 7). Prior studies have shown that when two bactericidal drugs are used in combination, the effect will be bactericidal (Ocampo, 2014).

Overall the results obtained from the checkerboard assays and the time-kill assays support the hypothesis that both vancomycin and furazolidone interact synergistically and show that the synergistic effect is bactericidal. While the concentration of vancomycin in combination may be still too high to treat patients, other applications such as the treatment and the prevention of biofilms in urinary tract catheters may be a possibility.

4.2 Investigation of the mechanisms of synergy

4.2.1 Efflux pump system

It was hypothesised that the TolC efflux pump system may be involved in the interaction between vancomycin and furazolidone. As it is known that vancomycin cannot enter *E. coli* cells through the outer membrane, it was thought that this antibiotic could potentially enter the cell through the TolC channel while it is in its open state conformation, due to its wide diameter (3 nm); (Augustus *et al.*, 2004). As the efflux pump system is powered by the proton motive force, it was thought that one of the intermediates formed when furazolidone was activated by the nitroreductases would be nitric oxide (NO) (Korobko *et al.*, 2014). It has been reported that NO can inhibit some components of the electron transport chain which would decrease generation of the proton motive force (pmf) that acts as an energy source for the efflux pumps

(McCollister *et al.*, 2011, Yu *et al.*, 1997). This disruption of the efflux pumps would potentially divert vancomycin to the periplasm after entry through the TolC channel.

Previous studies found that the deletion of the TolC channel had no effect on the cell susceptibility to vancomycin. In contrast, mutants containing the TolC deletion were reported to be more sensitive to nitrofurantoin (Liu *et al.*, 2010). It was hypothesised and confirmed in this study that the same principle extends to furazolidone (Table 6). Studies have reported in *ΔtolC* mutants, there is an accumulation of waste metabolites such as cysteine and porphyrins which have been noted to induce oxidative stress within cells which in turn, leads to the upregulation of the stress response systems: MarA, SoxS, Rob, Bae and CpxR (Rosner and Martin, 2013, Zgurskaya *et al.*, 2011). While the MarA, Rob, Bae and CpxR are involved in the upregulation of the efflux pump systems, the SoxRS regulon includes the *nfsA* gene that encodes for the NADPH-depenen nitroreductase, NfsA in *E. coli*, which is upregulated in response to oxidative stress (Paterson *et al.*, 2002). As more of the NfsA nitroreductase is present, this would result in greater activation of furazolidone, hence explaining why *ΔtolC* mutants are more sensitive to furazolidone (Chatterjee *et al.*, 1983, Martinez-Puchol *et al.*, 2015).

When comparing the effects of the kanamycin resistance cassette in the *ΔtolC* vs *ΔtolC::kan*, isobologram, it was observed that the deletion of the kanamycin resistance does not change the synergy or the level of individual resistance to furazolidone or vancomycin (Table 6). This suggests that the three genes downstream of *tol*C in the same operon, *ygiA*, *ygiB* and *ygiC* (Appendix 1), have no role in resistance to these antibiotics. None of these three genes are involved in the role of the efflux pumps or in the outer membrane structure (Keseler et al., 2013) .

This thesis also demonstrated a minor decrease in synergy when vancomycin and furazolidone were challenged against the mutant strain lacking the TolC channel compared to the wild-type strain (Figure 8). This suggests while there is a decrease in synergy, the TolC channel is only a minor, if any, a determinant of the synergy between vancomycin and furazolidone. Given the minor differences in synergy and no difference in the vancomycin MIC between the wild-type and *ΔtolC* mutant this may hint that vancomycin does not enter the periplasm through the TolC channel. Due to the deletion of the TolC channel and the previous studies have suggested that vancomycin may induce oxidative stress, this may act additively with the oxidative stress generated from

the accumulation of toxic metabolites to increase the activation of furazolidone through the upregulation of the NfsA nitroreductases through the SoxS stress response system (Zhou *et al.*, 2015). Overall based on the findings of this thesis, it could be concluded that the TolC channel may have only a minor involvement in vancomycin-furazolidone synergy.

Similarly to the TolC mutants, it was reported that *ΔacrA* mutants displayed a similar trend whereby the absence of the AcrA subunit caused no effect on the sensitivity or resistance of vancomycin and that the mutants were more susceptible to nitrofurantoin (Liu *et al.*, 2010). Unexpectedly the results presented in this thesis demonstrated that both the furazolidone and vancomycin MIC decreased when tested individually forthe *ΔacrA* mutant. This suggests that AcrA may play a role in the expulsion rather than internalisation of vancomycin (Table 6). The AcrA subunit has been reported to be crucial for the cycling between the open and closed state of the TolC channel (Augustus *et al.*, 2004). It was therefore hypothesised that the AcrA subunit would be required for the expulsion of vancomycin through the wild-type TolC outer membrane channel. While not a crucial component of the mechanism of action, the findings from this study suggests that the AcrA may be involved in the interaction between the two antibiotics used in this study (Figure 9).

Unlike with *ΔtolC::kan vs. ΔtolC*, that had a nearly identical isobologram, there was a noticeable decrease in the drug synergy in *ΔacrA* relative to *ΔacrA::kan* and showing a "reverse" polar effect on the downstream gene expression (Baba *et al.*, 2006) (Figure 8). Upon closer inspection of the operon containing *acrA* (Appendix 2), it was found that the *acrB* gene was immediately downstream of *acrA*. While *acrB* encodes the AcrB subunit of the AcrAB-TolC efflux system, it works with AcrA in its efflux role thus suggesting that differences in the drug synergy between *ΔacrA* and *ΔacrA::kan* were most likely due to experimental variation. This is further supported by the notion that when comparing the *ΔacrA* to *ΔacrA::kan*, no changes in the MICs for both vancomycin and furazolidone was observed similarly to the *ΔtolC* mutants (Table 6).

It is known that the TolC channel serves as the outer membrane component for 8 other inner membrane efflux pump systems besides AcrAB. Of those, mutations of genes encoding the *macAB* and *mdtEF* efflux pumps result in decrease of vancomycin, but not furazolidone MIC, when the two antibiotics are tested individually (Table 6). Based on

the results found in this thesis, given the minor differences in the decrease in the synergy between the *ΔtolC* and *ΔacrA* mutants, suggests that the other efflux pump systems such as MacAB-TolC are not involved in the interaction between vancomycin and furazolidone.

4.2.2 Enterobactin synthesis and transport

Enterobactin is a siderophore that is synthesised and excreted into the medium by *E. coli* in response to iron starvation; it serves to sequester iron when it is present in the medium at a very low concentration. Due to their large size (716 Da), enterobactin molecules cannot diffuse through the porins and are exported from the periplasm through the TolC channels (Bleuel *et al.*, 2005, Vega and Young, 2014). Prior work has found that in TolC mutants, enterobactin accumulates in the periplasm and is unable to internalise iron, which results in altered physiological states and growth inhibition (Adler *et al.*, 2014). It has also been reported that the synthesis of enterobactin is induced under the condition of oxidative stress. The synthesis and export of enterobactin, as well as the import of iron-loaded enterobactin, may be used by the enzymes in the reactions that detoxify oxidative stress (Adler *et al.*, 2014, Cornelis *et al.*, 2011, Peralta *et al.*, 2016). Consistent with what was observed in previous studies, mutants containing deletion of a gene encoding the enzyme that catalyses the first committed step in enterobactin biosynthesis EntC, were found to be more sensitive to vancomycin in comparison to the wild-type parent (Table 7). This hints at a potential secondary mechanism of vancomycin action wherein it induces oxidative stress in addition to disrupting peptidoglycan synthesis, resulting in enterobactin synthesis (Zhou *et al.*, 2015). Interestingly, the *ΔentC* mutant did not display any differences in the MIC for furazolidone (Table 7), contradicting the findings that furazolidone may induce oxidative stress (Chatterjee *et al.*, 1983). It is important to note that while enterobactin may act as a protector against oxidative stress, it cannot induce expression of the oxidative stress response genes such as superoxide dismutase and catalase, hence this is possibly why there were no profound effects on the reported MICs. It was hypothesised by (Adler *et al.*, 2014) that the role of enterobactin protection of *E. coli* from oxidative stress would only be applicable at lower cell densities of less than 10^3 CFU/mL. This hypothesis was supported by the results obtained in this study where the starting cell titre was 10^6 CFU/mL at which there was no reported increased sensitivity to furazolidone in the *ΔentC* mutant.

Prior work has demonstrated that in response to oxidative stress, transcription and biosynthesis of enterobactin is upregulated even in the presence of excess iron (Bleuel *et al.*, 2005, Peralta *et al.*, 2016, Vega and Young, 2014). It was proposed that both furazolidone and vancomycin would induce oxidative stress in the *E. coli* cells, hence upregulating enterobactin biosynthesis. The increased levels of enterobactin in the cell would allow for the export of enterobactin through the TolC channel (Augustus *et al.*, 2004, Bleuel *et al.*, 2005, Vega and Young, 2014).

In the terms of the synergy, a slight decrease in the synergy of the *ΔentC* mutant without the *kan* cassette was observed in this thesis compared to that of the wild- type strain (Figure 10), although the MICs of the two strains were identical for both antibiotics. These findings suggest that enterobactin was marginally it at all involved in the mechanism of the vancomycin-furazolidone interaction. A double *ΔtolC ΔentC* mutant was constructed and was subsequently challenged by the vancomycin-furazolidone combination. The double mutant displayed little to no difference in the synergy compared to that of the wild-type strain, BW25113 (Figure 11). The *ΔtolC* and *ΔentC* mutants individually showed minor decrease of the synergy of the vancomycin-furazolidone combination which suggests that while these two different components in *E. coli* may individually be involved in the interaction between the two antibiotics, they may cancel each other's effect on synergy.

Disparities in the results between the *ΔentC* with and without the kanamycin resistance cassette (Figure 10) were hard to reconcile with biological explanations given above. They could either be due to sample variability or differences in the polar effects on the expression of downstream genes in the operons.

EntC catalyses isomerisation of chorismate to isochorismate, the first step in the enterobactin synthesis pathway. However, EntC is not the only chorismate isomerase in *E. coli*; the second one (MenF) catalyses the same reaction in the menaquinone biosynthesis pathway (Buss, 2001, Sridharan *et al.*, 2010). Given that the *entC* open reading frame is at the 5' end of the enterobactin biosynthesis operon, *entCEBAH,* the *kan* cassette may prevent the production of downstream genes (Appendix 3). This would result in the channelling of chorismate into menaquinone synthesis, while the *kan* cassette removal could increase the expression of four downstream genes in the enterobactin synthesis operon (*entEBAH*), thus resulting in less menaquinone synthesis.

Therefore, the *kan* cassette presence *vs.* removal may result in more or less menaquinone production in the cells, converse to the less or more enterobactin, respectively. Interestingly small amounts of "crosstalk" of isochorismate between the enterobactin and menaquinone biosynthesis pathways have been reported, of which 1.9% of enterobactin is produced from MenF and 4% of menaquinone is produced from EntC. This shows that despite the deletion of the *entC* gene, residual amounts of enterobactin is still being produced (Buss, 2001). Nevertheless, it is hard to rationalise a stronger effect of "clean" *entC* deletion relative to the one containing the *kan* insert. The opposite activity of the double *ΔtolC ΔentC* vs *ΔtolC ΔentC::kan* in terms of the effect of the *kan* cassette, relative to the effect of the *kan* cassette in the single *ΔentC* mutant is again hard to rationalise and argues in favour of experimental variability.

4.2.3 DNA as a target

Bacteria face many threats to their DNA and so they possess several DNA repair systems in order to mitigate the damage. In *E. coli*, the UvrABC nucleotide excision repair (NER) system is a key DNA repair system which can eliminate DNA lesions without introducing errors in the sequence (Pakotiprapha *et al.*, 2012, Smith *et al.*, 2002). As previous studies have shown that furazolidone exhibits its antibacterial effects by targeting DNA and that vancomycin may cause DNA damage through oxidative stress, it was hypothesised in this thesis that vancomycin and furazolidone may synergise by enhancing each other's effect on DNA damage (Chatterjee *et al.*, 1983). In order to explore this hypothesis, a mutant lacking the UvrA protein of the UvrABC NER pathway was tested against the antibiotic combination. Consistent with previous studies, our results showed increased sensitivity to both vancomycin (2-fold decrease in MIC) and furazolidone (8-fold decrease in MIC). As expected, this mutant was especially sensitive to furazolidone given its primary target is DNA. In a reported Keio collection mutant screen (Ayhan *et al.*, 2016, Liu *et al.*, 2010), it was found that there was no effect in the deletion of the UvrA subunit against vancomycin. Findings in this thesis contradict the screen cited above and support the hypothesis that vancomycin induces DNA damage through oxidative stress as a secondary action.

Continuing on from the MICs, it was thought that there would be a large effect on the synergy for the *ΔuvrA* mutant, however, the results from the checkerboard assay showed

DNA repair mechanisms were not involved at all in the mechanism of synergy (Figure 12). This does not necessarily disprove the hypothesis, but rather points to the synergistic effect on other responses, e.g. base excision repair (BER), DNA mismatch repair (MMR) or the SOS response in contrast to the UvrABC repair pathway. Both vancomycin and furazolidone have been reported to induce the SOS response. While vancomycin may induce the SOS response via peptidoglycan disruption, which was found to be one of the SOS-inducing signals (Kreuzer, 2013, Rahman *et al.*, 1993), furazolidone is expected to induce the SOS response through its effect on DNA. The SOS response system is regulated by RecA (inducer of the SOS response) and LexA (repressor of the SOS response) proteins. During normal growth conditions, the LexA protein represses the SOS system, however, in response to DNA damage, RecA is upregulated and cleaves LexA, thus inducing the SOS response (Kreuzer, 2013, Zgur-Bertok, 2013). The induction of the SOS response, in turn activates pathways for the cells such as cell division arrest, cell death or induce viable but non-cultivable state (McKenzie *et al.*, 2000, Zgur-Bertok, 2013). As both antibiotics are inducers of SOS at the sub-lethal concentrations, it is possible that their synergistic effect may be downstream of the SOS response system mentioned above. This involvement of complex physiological responses is hinted by the time-kill curves where both the drug combination and furazolidone treatment alone resulted in a drop of the titre within 6 hours, followed by an increase after a 24-hour incubation (Figure 7).

In order to determine whether and what pathways of SOS-dependent cell death are induced by the vancomycin-furazolidone combination it is necessary to expand the analysis to the mutants of the key proteins of the SOS and associated pathways that trigger the cell cycle arrest, non-culturable state or death of *E. coli* in order to identify the points at which the two antibiotics synergise. The use of specific inhibitors to block the SOS response could determine whether the vancomycin-furazolidone interaction is truly due to the downstream effects of the SOS response. However, complications may arise if these molecules were to interact with vancomycin and furazolidone in an SOS-unrelated manner (Baharoglu and Mazel, 2014, Mo *et al.*, 2016).

Furthermore, while the isobologram implied that DNA was not a target of the vancomycin-furazolidone combination, we cannot completely eliminate the hypothesis that DNA is a target. While DNA may not be the point at which vancomycin and furazolidone interact synergistically, it is possible that they could both be co-targeting

DNA. A key limitation in the use of isobolograms is that they cannot distinguish the co-targeting of the two antibiotics (Breitinger, 2012) and so it would be impossible to determine whether DNA is a target or if the point of synergy is downstream of the SOS response.

4.3 Biofilms

The presence of biofilms poses problems to many different fields such as in hospitals or in industries. Primarily this is due to the biofilms' remarkable resistance to antibiotics in comparison to that of planktonic bacteria and as such is far more difficult to eliminate (Dufour, 2010, Dunne, 2002, Vasudevan, 2014). Antibiotics are usually much less effective at treating the biofilm-based infections in comparison to those that involve planktonic cells. In order to eliminate biofilms, very high concentrations beyond the planktonic MICs have to be used, reaching the levels that are often toxic to the patients (Abedon, 2015). In agreement with these biofilm properties, the concentrations required to inhibit the growth and cause eradication (killing) of *E. coli* in biofilms observed in this thesis work are greater than those of planktonic bacteria. Interestingly, vancomycin displayed a bimodal curve for its biofilm eradication (killing) activity, with a peak (maximum eradication) at 500 mg/L; with the survival increasing at higher concentrations (1000 – 32000 mg/L) after 24 hours incubation (Figure 13A). Bacteria were eradicated to below the detection level only at 64 000 mg/L. It is possible that there was a positive selection for vancomycin-resistant mutants due to vancomycin not eradicating completely the biofilm in the early hours of incubation at those concentrations and providing high enough selective pressure. Induction of mutagenic SOS DNA repair has been found to induce an increase in mutation rate, resulting in the emergence of resistant bacteria in Staphylococcus (Cirz *et al.*, 2007, Dufour, 2010, Vasudevan, 2014). The significance of the bimodal behaviour of vancomycin-treated biofilms remains to be investigated.

For furazolidone, the MBIC and MBEC were higher by a factor of ~10 in the biofilms relative to the planktonic state. However, unlike vancomycin, there was no bimodal behaviour in the MBEC dose-response analysis (Figure 13B). Consistent with our findings, another study demonstrated similar MICs for nitrofurantoin against *E. coli* biofilms (Gandee *et al.*, 2015). The analysis in this thesis showed that the furazolidone MIC was not much decreased by vancomycin (two-fold at 500 mg/L).

Therefore, furazolidon-vancomycin antibiotic combination is far less effective against biofilm-based system as opposed to planktonic culture. These findings are to be expected as it is known that bactericidal drugs such as vancomycin and furazolidone are far more effective against fast growing cells as opposed to the slow growing cells within the biofilm (Stewart, 2015). In addition to the difference in the physiological states, other factors such as penetration of the biofilm and antibiotic depletion would have also contributed to the decreased efficacy (Stewart, 2015). Based on the findings from the biofilm eradication assay, it was suggested that the eradicating vancomycin and furazolidone concentration combination was not suitable for the treatment of *E. coli* infections due to the vancomycin concentration (62 mg/L) that is above nephrotoxic level (30 mg/L). The biofilm eradicating vancomycin concentration in the most effective combination with furazolidone was 250 mg/L in combination with 39 mg/L furazolidone, as for the planktonic cultures. This vancomycin concentration required to eradicate biofilms are much higher in comparison to the toxic dose and are not suitable for systemic use on humans (Figure 14).

Although too toxic to use as a systemic treatment, this antibiotic combination could potentially be used as a viable option for the coating of catheters in a hospital setting. Strategies that are currently used for prevention of the biofilm formation on catheters include the coating with silver or antibiotics (Chen *et al.*, 2013, Trautner and Darouiche, 2004). The use of silver to coat the surface of biofilms while successful at preventing *E. coli* biofilm formation at high concentrations, it is toxic to humans and has been linked to increased risks of thrombosis (Roe *et al.*, 2008, Jena *et al.*, 2012, Stevens *et al.*, 2009). Besides the silver, antibiotics that are used for the treatment of catheter surfaces from biofilms include, quinolones, fusidic acid, nitroimidazole, triclosan and a nitrofuran, nitrofurazone (Wu *et al.*, 2015, Soto, 2014, Williams and Stickler, 2008). While they are successful at protecting against biofilms, due to the extensive use of these antibiotics, it was thought that resistances to these antibiotics may emerge. Furthermore, it was reported that, once bacteria acquire partial resistance to therapeutic doses, and possibly even promote the induction of new biofilms (Soto, 2014, Hoffman *et al.*, 2005). While the use of antibiotic combinations was successful in eradicating biofilms, there is a possibility that the use of antibiotic combinations may speed up the emergence of resistant mutants by developing resistance to both antibiotics in a stepwise manner (Hegreness *et al.*, 2008, Pena-Miller *et al.*, 2013). This could be possible to mitigate by

using increased antibiotic concentrations within the combination (Pena-Miller *et al.*, 2013).

4.4 Effects of DOC on the vancomycin-furazolidone synergy

In this thesis, a triple antibiotic combination containing vancomycin, furazolidone and DOC was characterised against the wild-type strain, BW25113. Based on the lower concentrations of vancomycin and furazolidone required to inhibit bacterial growth, we can infer that in the presence of DOC at all three concentrations used stimulates the vancomycin and furazolidone combination. Previous studies were done to characterise the synergy between furazolidone and DOC against strain BW25113 found that there this strain was highly resistant to high concentrations of DOC (Vuong Le, unpublished data). Based on the observations in this thesis, the addition of DOC enhances the interaction between vancomycin and furazolidone. It has been proposed that DOC exhibits it antibacterial effects through DNA damage and it has been reported that DOC induces the SOS response in *E. coli* (Kandell and Bernstein, 1991, Merritt and Donaldson, 2009). Based on this it could be deduced, in terms of synergy with vancomycin and furazolidone, that the interaction may occur downstream of the SOS response.

At the lowest concentration of DOC added (1.25 g/L) to the vancomycin-furazolidone combination, this thesis showed even sub-nephrotoxic levels of vancomycin (< 30 mg/L) could inhibit the growth of *E. coli* cells. This opens up many different applications as to where this triple combination could be used. Normally vancomycin is taken orally in order to treat bacterial infections that occur in the intestines. While successful at treating infections caused by Gram-positive bacteria, is largely ineffective against Gram-negative bacteria such as the foodborne pathogen *E. coli* O157:H7 at safe sub-nephrotoxic concentrations (Alvarez *et al.*, 2016, Isaac *et al.*, 2017). Even when combined with furazolidone, the concentration of vancomycin in combination was considered to be too high and to be too risky for use in humans, however in the presence of DOC which is normally found in the gut, this treatment may be a viable option (Shefer *et al.*, 1995). As there is already a very high concentration of 40 mM of bile salts found in the human hepatic bile, adding more DOC into patients without bile salts synthesising disorders could be dangerous due to its carcinogenic activity at high concentrations (Begley *et al.*, 2005, Bernstein *et al.*, 2011). However, the addition of DOC at lower concentrations along with vancomycin and furazolidone could potentially be used as an effective

treatment against Gram-negative intestinal infections for patients that have disorders in synthesising bile salts.

5 Conclusions

In agreement with the primary hypothesis, this study has confirmed that there is a synergistic interaction between vancomycin and furazolidone against *E. coli* which may allow for potential applications of vancomycin against Gram-negative bacteria. It was also shown that by adding DOC at 2.5 g/L, the concentration of vancomycin that inhibits *E. coli* is reduced to sub-toxic concentrations. In terms of the bacterial proteins involved in the interaction between vancomycin and furazolidone, there is evidence that the TolC channel plays a minor role, whereas the main synergy mechanism remains to be elucidated. It is possible that this interaction could incorporate many different mechanisms as opposed to one main mechanism. While too toxic for use as a treatment against biofilm-based infections, this combination may be a plausible coating of catheters to prevent the formation of biofilms. Additionally, the use of the triple combination consisting of vancomycin, furazolidone and DOC displayed greater synergy and potentially opens up potential treatments for more practical applications in the future.

6 Future directions

6.1 Synergy

This work only confirmed vancomycin-furazolidone synergy in *E. coli* K-12 laboratory strains BW25113 and K1508. Previous unpublished work showed that this combination is also synergistic in growth inhibition of pathogenic *E. coli* strains including uropathogenic strains and *E. coli* O157:H7, as well as Salmonella and Citrobacter natural isolates. The synergy was not observed in Klebsiella isolates or *P. aeruginosa* (Carel Jobsis and Jasna Rakonjac, unpublished). Synergy against other Gram-negative pathogens such as *Acinetobacter baumanii*, *Francisella tularensis*, *Vibrio cholerae* and Campylobacter remains to be investigated. Doing so would allow for assessment of more practical applications for this combination.

Given that the concentration of DOC used in this work is quite high, future analysis will be required to determine minimal DOC concentration that will allow sub-nephrotoxic vancomycin application for *E. coli* growth inhibition in triple combination. The relatively high DOC concentration is tolerated for topical and oral applications, the latter for the treatment of enteric infections. Furthermore, to determine whether the triple combination could be used in wound dressings or for the coating of catheters would have to be tested against biofilms.

6.2 Furazolidone mechanism of action

In order to fully elucidate the mechanism of interaction between vancomycin and furazolidone, it is necessary to characterise the mechanism of action for furazolidone. While is it known that furazolidone is reduced by the nitroreductases, NfsA and NfsB, the current targets and the exact mechanism are not fully understood. It was proposed by (Grigor'ev, 1999) that all nitrofurans can produce NO as a by-product of their reduction. By assessing the generation of NO through the reduction of furazolidone, we can gain further insights into potential targets. One can test for NO production by overexpressing the Hmp gene which encodes a flavohaemoglobin which possesses nitric oxide dioxygenase activity which detoxifies NO during aerobic conditions (Gardner and Gardner, 2002, Gardner, 2012). If a decrease in synergy is observed, this would indicate that NO is produced during the reduction of furazolidone.

6.3 Inhibition of biofilms

Given the problems posed by the presence of biofilms on catheters, it would be important to gain insights into the inhibition of biofilm on catheters (Gandee *et al.*, 2015). As found in this study, concentrations of vancomycin and furazolidone required to eradicate biofilms are higher than those that are effective against the planktonic cultures. If the strategy is applied to coat the catheters containing this antibiotic combination before biofilm formation, then it may be possible to prevent the seeding of the biofilm. The inhibition of bacterial growth and biofilm formation by coating of catheters will have to be assayed in the future, as described by Gandee *et al.* (2015).

7 References

1. Abedon, S. T. 2015. Ecology of Anti-Biofilm Agents I: Antibiotics versus Bacteriophages. *Pharmaceuticals (Basel),* 8**,** 525-58. Available: DOI 10.3390/ph8030525.
2. Adler, C., Corbalan, N. S., Peralta, D. R., Pomares, M. F., De Cristobal, R. E. & Vincent, P. A. 2014. The alternative role of enterobactin as an oxidative stress protector allows *Escherichia coli* colony development. *PLoS One,* 9**,** e84734. Available: DOI 10.1371/journal.pone.0084734.
3. Alvarez, R., Lopez Cortes, L. E., Molina, J., Cisneros, J. M. & Pachon, J. 2016. Optimizing the Clinical Use of Vancomycin. *Antimicrob Agents Chemother,* 60**,** 2601-9. Available: DOI 10.1128/AAC.03147-14.
4. Augustus, A. M., Celaya, T., Husain, F., Humbard, M. & Misra, R. 2004. Antibiotic-Sensitive TolC Mutants and Their Suppressors. *Journal of Bacteriology,* 186**,** 1851-1860. Available: DOI 10.1128/jb.186.6.1851-1860.2004.
5. Ayhan, D. H., Tamer, Y. T., Akbar, M., Bailey, S. M., Wong, M., Daly, S. M., Greenberg, D. E. & Toprak, E. 2016. Sequence-Specific Targeting of Bacterial Resistance Genes Increases Antibiotic Efficacy. *PLoS Biol,* 14**,** e1002552. Available: DOI 10.1371/journal.pbio.1002552.
6. Baba, T., Ara, T., Hasegawa, M., Takai, Y., Okumura, Y., Baba, M., Datsenko, K. A., Tomita, M., Wanner, B. L. & Mori, H. 2006. Construction of *Escherichia coli* K-12 in-frame, single-gene knockout mutants: the Keio collection. *Mol Syst Biol,* 2**,** 2006 0008. Available: DOI 10.1038/msb4100050.
7. Baharoglu, Z. & Mazel, D. 2014. SOS, the formidable strategy of bacteria against aggressions. *FEMS Microbiol Rev,* 38**,** 1126-45. Available: DOI 10.1111/1574-6976.12077.
8. Baneyx, F. G. G. 1991. Construction and characterization of *Escherichia coli* strains deficient in multiple secreted proteases: protease III degrades high-molecular-weight substrates in vivo. *Journal of Bacteriology,* 173**,** 2696-2701.
9. Begley, M., Gahan, C. G. & Hill, C. 2005. The interaction between bacteria and bile. *FEMS Microbiol Rev,* 29**,** 625-51. Available: DOI 10.1016/j.femsre.2004.09.003.

10. Bernstein, C., Bernstein, H., Payne, C. M., Beard, S. E. & Schneider, J. 1999. Bile salt activation of stress response promoters in *Escherichia coli*. *Curr Microbiol,* 39**,** 68-72.
11. Bernstein, C., Holubec, H., Bhattacharyya, A. K., Nguyen, H., Payne, C. M., Zaitlin, B. & Bernstein, H. 2011. Carcinogenicity of deoxycholate, a secondary bile acid. *Arch Toxicol,* 85**,** 863-71. Available: DOI 10.1007/s00204-011-0648-7.
12. Bleuel, C., Grosse, C., Taudte, N., Scherer, J., Wesenberg, D., Krauss, G. J., Nies, D. H. & Grass, G. 2005. TolC is involved in enterobactin efflux across the outer membrane of *Escherichia coli*. *J Bacteriol,* 187**,** 6701-7. Available: DOI 10.1128/JB.187.19.6701-6707.2005.
13. Berenbaum, M. C. 1989. What is synergy? *Pharmacological Reviews,* 43**,** 93-114.
14. Blair, J. M. & Piddock, L. J. 2009. Structure, function and inhibition of RND efflux pumps in Gram-negative bacteria: an update. *Curr Opin Microbiol,* 12**,** 512-9. Available: DOI 10.1016/j.mib.2009.07.003.
15. Bliss, C. I. 1939. The toxicity of poisons applied jointly. *Annals of Applied Biology,* 26**,** 585–615.
16. Bollenbach, T. 2015. Antimicrobial interactions: mechanisms and implications for drug discovery and resistance evolution. *Curr Opin Microbiol,* 27**,** 1-9. Available: DOI 10.1016/j.mib.2015.05.008.
17. Breitinger, H.-G. 2012. Drug synergy - mechanisms and methods of analysis. *Toxicity and Drug Testing***,** 143-166.
18. Buss, K., R. Muller, C. Dahm, N. Gaitatzis, E. Skrzypczak-Pietraszek, S. Lohmann, M. Gassen, and E. Leistner 2001. Clustering of isochorismate synthase genes menF and entC and channeling of isochorismate in *Escherichia coli*. *Biochimica et Biophysica Acta (BBA) - Gene Structure and Expression,* 1522**,** 151-157.
19. Campbell, J. 2010. High-throughput assessment of bacterial growth inhibition by optical density measurements. *Curr Protoc Chem Biol,* 2**,** 195-208. Available: DOI 10.1002/9780470559277.ch100115.
20. Carey, D. E. & Mcnamara, P. J. 2014. The impact of triclosan on the spread of antibiotic resistance in the environment. *Front Microbiol,* 5**,** 780. Available: DOI 10.3389/fmicb.2014.00780.

21. Chatterjee, S. N., Banerjee, S. K., Pal, A. K. & Basak, J. 1983. DNA damage, prophage induction and mutation by furazolidone. *Chem Biol Interact,* 45**,** 315-26.
22. Chen, M., Yu, Q. & Sun, H. 2013. Novel strategies for the prevention and treatment of biofilm related infections. *Int J Mol Sci,* 14**,** 18488-501. Available: DOI 10.3390/ijms140918488.
23. Cirz, R. T., Jones, M. B., Gingles, N. A., Minogue, T. D., Jarrahi, B., Peterson, S. N. & Romesberg, F. E. 2007. Complete and SOS-mediated response of *Staphylococcus aureus* to the antibiotic ciprofloxacin. *J Bacteriol,* 189**,** 531-9. Available: DOI 10.1128/JB.01464-06.
24. Coenye, T. & Nelis, H. J. 2010. In vitro and in vivo model systems to study microbial biofilm formation. *J Microbiol Methods,* 83**,** 89-105. Available: DOI 10.1016/j.mimet.2010.08.018.
25. Cornelis, P., Wei, Q., Andrews, S. C. & Vinckx, T. 2011. Iron homeostasis and management of oxidative stress response in bacteria. *Metallomics,* 3**,** 540-9. Available: DOI 10.1039/c1mt00022e.
26. Cosgrove, S. E. & Carmeli, Y. 2003. The impact of antimicrobial resistance on health and economic outcomes. *Clin Infect Dis,* 36**,** 1433-7. Available: DOI 10.1086/375081.
27. Courvalin, P. 2006. Vancomycin resistance in gram-positive cocci. *Clin Infect Dis,* 42 Suppl 1**,** S25-34. Available: DOI 10.1086/491711.
28. Cremers, C. M., Knoefler, D., Vitvitsky, V., Banerjee, R. & Jakob, U 2014. Bile salts act as effective protein-unfolding agents and instigators of disulfide stress in vivo. *PNAS,* 111**,** 1610-1619.
29. D'mello, A. & Yotis, W. W. 1987. The action of sodium deoxycholate on *Escherichia coli*. *Appl Environ Microbiol,* 53**,** 1944-6.
30. Datsenko, K. A. & Wanner, B. L. 2000. One-step inactivation of chromosomal genes in *Escherichia coli* K-12 using PCR products. *Proc Natl Acad Sci U S A,* 97**,** 6640-5. Available: DOI 10.1073/pnas.120163297.
31. Davies, J. 2006. Where have All the Antibiotics Gone? *Journal of Infectious Diseases and Medical Microbiology,* 17**,** 287-290.
32. Davis, B. D. 1982. Bactericidal synergism between beta-lactams and aminoglycosides: mechanism and possible therapeutic implications. *Rev Infect Dis,* 4**,** 237-45.

33. Delcour, A. H. 2009. Outer membrane permeability and antibiotic resistance. *Biochim Biophys Acta,* 1794**,** 808-16. Available: DOI 10.1016/j.bbapap.2008.11.005.
34. Dufour, D., Leung, V., and Lévesque, C.M. 2010. Bacterial biofilm: structure, function, and antimicrobial resistance. 22**,** 2-16.
35. Dunne, W. M. 2002. Bacterial Adhesion: Seen Any Good Biofilms Lately? *Clinical Microbiology Reviews,* 15**,** 155-166. Available: DOI 10.1128/cmr.15.2.155-166.2002.
36. Eady, E. A., Coates, P., Ross, J. I., Ratyal, A. H. & Cove, J. H. 2000. Antibiotic resistance patterns of aerobic coryneforms and furazolidone-resistant Gram-positive cocci from the skin surface of the human axilla and fourth toe cleft. *J Antimicrob Chemother,* 46**,** 205-13.
37. Elyasi, S., Khalili, H., Dashti-Khavidaki, S. & Mohammadpour, A. 2012. Vancomycin-induced nephrotoxicity: mechanism, incidence, risk factors and special populations. A literature review. *Eur J Clin Pharmacol,* 68**,** 1243-55. Available: DOI 10.1007/s00228-012-1259-9.
38. Fernandez-Recio, J., Walas, F., Federici, L., Venkatesh Pratap, J., Bavro, V. N., Miguel, R. N., Mizuguchi, K. & Luisi, B. 2004. A model of a transmembrane drug-efflux pump from Gram-negative bacteria. *FEBS Lett,* 578**,** 5-9. Available: DOI 10.1016/j.febslet.2004.10.097.
39. Foucquier, J. & Guedj, M. 2015. Analysis of drug combinations: current methodological landscape. *Pharmacol Res Perspect,* 3**,** e00149. Available: DOI 10.1002/prp2.149.
40. Gandee, L., Hsieh, J. T., Sperandio, V., Moreira, C. G., Lai, C. H. & Zimmern, P. E. 2015. The efficacy of immediate versus delayed antibiotic administration on bacterial growth and biofilm production of selected strains of uropathogenic *Escherichia coli* and *Pseudomonas aeruginosa*. *Int Braz J Urol,* 41**,** 67-77. Available: DOI 10.1590/S1677-5538.IBJU.2015.01.10.
41. Gardner, A. M. & Gardner, P. R. 2002. Flavohemoglobin detoxifies nitric oxide in aerobic, but not anaerobic, *Escherichia coli*. Evidence for a novel inducible anaerobic nitric oxide-scavenging activity. *J Biol Chem,* 277**,** 8166-71. Available: DOI 10.1074/jbc.M110470200.
42. Gardner, P. R. 2012. Hemoglobin: a nitric-oxide dioxygenase. *Scientifica (Cairo),* 2012**,** 683729. Available: DOI 10.6064/2012/683729.

43. Grigor'ev, N. B., Chechekin, G. V., Arzamaztsev, A. P., Levina, V. I. & Granik, V. G. 1999. Nitrogen oxide generation during reduction of nitrofuran antibacterial drugs. *Chemistry of Heterocyclic Compounds,* 35**,** 788-791.
44. Hall-Stoodley, L., Costerton, J. W. & Stoodley, P. 2004. Bacterial biofilms: from the natural environment to infectious diseases. *Nat Rev Microbiol,* 2**,** 95-108. Available: DOI 10.1038/nrmicro821.
45. Hegreness, M., Shoresh, N., Damian, D., Hartl, D. & Kishony, R. 2008. Accelerated evolution of resistance in multidrug environments. *Proc Natl Acad Sci U S A,* 105**,** 13977-81. Available: DOI 10.1073/pnas.0805965105.
46. Hoffman, L. R., D'argenio, D. A., Maccoss, M. J., Zhang, Z., Jones, R. A. & Miller, S. I. 2005. Aminoglycoside antibiotics induce bacterial biofilm formation. *Nature,* 436**,** 1171-5. Available: DOI 10.1038/nature03912.
47. Hoiby, N., Bjarnsholt, T., Givskov, M., Molin, S. & Ciofu, O. 2010. Antibiotic resistance of bacterial biofilms. *Int J Antimicrob Agents,* 35**,** 322-32. Available: DOI 10.1016/j.ijantimicag.2009.12.011.
48. Holmes, N. E., Johnson, P. D. & Howden, B. P. 2012. Relationship between vancomycin-resistant *Staphylococcus aureus*, vancomycin-intermediate *S. aureus*, high vancomycin MIC, and outcome in serious *S. aureus* infections. *J Clin Microbiol,* 50**,** 2548-52. Available: DOI 10.1128/JCM.00775-12.
49. Ip, H., Stratton, K., Zgurskaya, H. & Liu, J. 2003. pH-induced conformational changes of AcrA, the membrane fusion protein of *Escherichia coli* multidrug efflux system. *J Biol Chem,* 278**,** 50474-82. Available: DOI 10.1074/jbc.M305152200.
50. Isaac, S., Scher, J. U., Djukovic, A., Jimenez, N., Littman, D. R., Abramson, S. B., Pamer, E. G. & Ubeda, C. 2017. Short- and long-term effects of oral vancomycin on the human intestinal microbiota. *J Antimicrob Chemother,* 72**,** 128-136. Available: DOI 10.1093/jac/dkw383.
51. Jacobsson, K., Rosander, A., Bjerketorp, J. & Frykberg, L. 2003. Shotgun Phage Display - Selection for Bacterial Receptins or other Exported Proteins. *Biol Proced Online,* 5**,** 123-135. Available: DOI 10.1251/bpo54.
52. Jena, N. R. 2012. DNA damage by reactive species: Mechanisms, mutation and repair. *Journal of Biosciences,* 37**,** 503-517. Available: DOI 10.1007/s12038-012-9218-2.

53. Jena, P., Mohanty, S., Mallick, R., Jacob, B. & Sonawane, A. 2012. Toxicity and antibacterial assessment of chitosan-coated silver nanoparticles on human pathogens and macrophage cells. *Int J Nanomedicine,* 7**,** 1805-18. Available: DOI 10.2147/IJN.S28077.
54. Jin, X., Tang, S., Chen, Q., Zou, J., Zhang, T., Liu, F., Zhang, S., Sun, C. & Xiao, X. 2011. Furazolidone induced oxidative DNA damage via up-regulating ROS that caused cell cycle arrest in human hepatoma G2 cells. *Toxicol Lett,* 201**,** 205-12. Available: DOI 10.1016/j.toxlet.2010.12.021.
55. Kandell, R. L. & Bernstein, C. 1991. Bile salt/acid induction of DNA damage in bacterial and mammalian cells: implications for colon cancer. *Nutr Cancer,* 16**,** 227-38. Available: DOI 10.1080/01635589109514161.
56. Keseler, I.M., Mackie, A., Peralta-Gil, M., Santos-Zavaleta, A., Gama-Castro, S., Bonavides-Martinez, C., Fulcher, C., Huerta, A.M., Kothari, A., Krummenacker, M., Latendresse, M., Muniz-Rascado, L., Ong, Q., Paley, S., Schroder, I., Shearer, A., Subhraveti, P., Travers, M., Weerasinghe, D., Weiss, V., Collado-Vides, J., Gunsalus, R.P., Paulsen, I., and Karp, P.D. 2013. EcoCyc: fusing model organism databases with systems biology. *Nucleic Acids Res,* 41, 605-612. Available: DOI 10.1093/nar/gks1027.
57. Khong, S. P., Gremaud, E., Richoz, J., Delatour, T., Guy, P. A., Stadler, R. H. & Mottier, P. 2004. Analysis of matrix-bound nitrofuran residues in worldwide-originated honeys by isotope dilution high-performance liquid chromatography-tandem mass spectrometry. *J Agric Food Chem,* 52**,** 5309-15. Available: DOI 10.1021/jf0401118.
58. Korobko, V. M., Melnikova, N. B., Panteleev, D. A., Martusevich, A. K. & Peretyagin, S. P. 2014. The study of the complexes of nitromedicine with cytochrome c and NO-containing aqueous dosage form in the wound treatment of rats. *Nitric Oxide,* 42**,** 62-9. Available: DOI 10.1016/j.niox.2014.08.001.
59. Koronakis, V., Sharff, A., Koronakis, E., Luisi, B. & Hughes, C. 2000. Crystal structure of the bacterial membrane protein TolC central to multidrug efflux and protein export. *Nature,* 405**,** 914-9. Available: DOI 10.1038/35016007.
60. Kreuzer, K. N. 2013. DNA damage responses in prokaryotes: regulating gene expression, modulating growth patterns, and manipulating replication forks. *Cold Spring Harb Perspect Biol,* 5**,** a012674. Available: DOI 10.1101/cshperspect.a012674.

61. Lee, S. I. 2010. Drug interaction: focusing on response surface models. *Korean J Anesthesiol,* 58**,** 421-34. Available: DOI 10.4097/kjae.2010.58.5.421.
62. Levine, D. P. 2006. Vancomycin: a history. *Clin Infect Dis,* 42 Suppl 1**,** S5-12. Available: DOI 10.1086/491709.
63. Littmann, J. & Viens, A. M. 2015. The Ethical Significance of Antimicrobial Resistance. *Public Health Ethics,* 8**,** 209-224. Available: DOI 10.1093/phe/phv025.
64. Liu, A., Tran, L., Becket, E., Lee, K., Chinn, L., Park, E., Tran, K. & Miller, J. H. 2010. Antibiotic sensitivity profiles determined with an *Escherichia coli* gene knockout collection: generating an antibiotic bar code. *Antimicrob Agents Chemother,* 54**,** 1393-403. Available: DOI 10.1128/AAC.00906-09.
65. Martinez-Puchol, S., Gomes, C., Pons, M. J., Ruiz-Roldan, L., Torrents De La Pena, A., Ochoa, T. J. & Ruiz, J. 2015. Development and analysis of furazolidone-resistant *Escherichia coli* mutants. *APMIS,* 123**,** 676-81. Available: DOI 10.1111/apm.12401.
66. Mccollister, B. D., Hoffman, M., Husain, M. & Vazquez-Torres, A. 2011. Nitric oxide protects bacteria from aminoglycosides by blocking the energy-dependent phases of drug uptake. *Antimicrob Agents Chemother,* 55**,** 2189-96. Available: DOI 10.1128/AAC.01203-10.
67. Mckenzie, G. J., Harris, R. S., Lee, P. L. & Rosenberg, S. M. 2000. The SOS response regulates adaptive mutation. *Proc Natl Acad Sci U S A,* 97**,** 6646-51. Available: DOI 10.1073/pnas.120161797.
68. Meletiadis, J., Pournaras, S., Roilides, E. & Walsh, T. J. 2010. Defining fractional inhibitory concentration index cutoffs for additive interactions based on self-drug additive combinations, Monte Carlo simulation analysis, and in vitro-in vivo correlation data for antifungal drug combinations against Aspergillus fumigatus. *Antimicrob Agents Chemother,* 54**,** 602-9. Available: DOI 10.1128/AAC.00999-09.
69. Merritt, M. E. & Donaldson, J. R. 2009. Effect of bile salts on the DNA and membrane integrity of enteric bacteria. *J Med Microbiol,* 58**,** 1533-41. Available: DOI 10.1099/jmm.0.014092-0.
70. Mikolosko, J., Bobyk, K., Zgurskaya, H. I. & Ghosh, P. 2006. Conformational flexibility in the multidrug efflux system protein AcrA. *Structure,* 14**,** 577-87. Available: DOI 10.1016/j.str.2005.11.015.

71. Mitosch, K. & Bollenbach, T. 2014. Bacterial responses to antibiotics and their combinations. *Environmental Microbiology Reports,* 6**,** 545-557. Available: DOI 10.1111/1758-2229.12190.
72. Mo, C. Y., Manning, S. A., Roggiani, M., Culyba, M. J., Samuels, A. N., Sniegowski, P. D., Goulian, M. & Kohli, R. M. 2016. Systematically Altering Bacterial SOS Activity under Stress Reveals Therapeutic Strategies for Potentiating Antibiotics. *mSphere,* 1. Available: DOI 10.1128/mSphere.00163-16.
73. Moskowitz, S. M., Foster, J. M., Emerson, J. & Burns, J. L. 2004. Clinically Feasible Biofilm Susceptibility Assay for Isolates of *Pseudomonas aeruginosa* from Patients with Cystic Fibrosis. *Journal of Clinical Microbiology,* 42**,** 1915-1922. Available: DOI 10.1128/jcm.42.5.1915-1922.2004.
74. Murakami, S., Nakashima, R., Yamashita, E., Matsumoto, T. & Yamaguchi, A. 2006. Crystal structures of a multidrug transporter reveal a functionally rotating mechanism. *Nature,* 443**,** 173-9. Available: DOI 10.1038/nature05076.
75. Nakashima, R., Sakurai, K., Yamasaki, S., Nishino, K. & Yamaguchi, A. 2011. Structures of the multidrug exporter AcrB reveal a proximal multisite drug-binding pocket. *Nature,* 480**,** 565-9. Available: DOI 10.1038/nature10641.
76. Nicolle, L. E. 2014. Catheter associated urinary tract infections. *Antimicrobial Resistance & Infection Control,* 3**,** 1-8.
77. Nikaido, H. 2005. Restoring permeability barrier function to outer membrane. *Chem Biol,* 12**,** 507-9. Available: DOI 10.1016/j.chembiol.2005.05.001.
78. Nishino, Y., Takemura, S., Minamiyama, Y., Hirohashi, K., Ogino, T., Inoue, M., Okada, S. & Kinoshita, H. 2009. Targeting Superoxide Dismutase to Renal Proximal Tubule Cells Attenuates Vancomycin-induced Nephrotoxicity in Rats. *Free Radical Research,* 37**,** 373-379. Available: DOI 10.1080/1071576031000061002.
79. O'Toole, G., Kaplan, H.B., and Kolter, R. 2000. Biofilm Formation as Microbial Development. *Annual Review of Microbiology,* 54**,** 49-79.
80. Ocampo, P. S., Arnoldini, M., Fekete, G., Ackermann, M., and Bonhoeffer, S. 2014. Antagonism between Bacteriostatic and Bactericidal Antibiotics Is Prevalent. *Antimicrobial Agents and Chemotherapy,* 58**,** 4573-4582.
81. Oktem, F., Arslan, M. K., Ozguner, F., Candir, O., Yilmaz, H. R., Ciris, M. & Uz, E. 2005. In vivo evidences suggesting the role of oxidative stress in

pathogenesis of vancomycin-induced nephrotoxicity: protection by erdosteine. *Toxicology,* 215**,** 227-33. Available: DOI 10.1016/j.tox.2005.07.009.

82. World Health Organization. 2014. Antimicrobial Resistance: Global Report on Surveillance. *World Health Organization* 1–256.
83. Pakotiprapha, D., Samuels, M., Shen, K., Hu, J. H. & Jeruzalmi, D. 2012. Structure and mechanism of the UvrA-UvrB DNA damage sensor. *Nat Struct Mol Biol,* 19**,** 291-8. Available: DOI 10.1038/nsmb.2240.
84. Pankey, G. A. & Sabath, L. D. 2004. Clinical relevance of bacteriostatic versus bactericidal mechanisms of action in the treatment of Gram-positive bacterial infections. *Clin Infect Dis,* 38**,** 864-70. Available: DOI 10.1086/381972.
85. Paterson, E. S., Boucher, S. E. & Lambert, I. B. 2002. Regulation of the nfsA Gene in *Escherichia coli* by SoxS. *Journal of Bacteriology,* 184**,** 51-58. Available: DOI 10.1128/jb.184.1.51-58.2002.
86. Pena-Miller, R., Laehnemann, D., Jansen, G., Fuentes-Hernandez, A., Rosenstiel, P., Schulenburg, H. & Beardmore, R. 2013. When the most potent combination of antibiotics selects for the greatest bacterial load: the smile-frown transition. *PLoS Biol,* 11**,** e1001540. Available: DOI 10.1371/journal.pbio.1001540.
87. Peralta, D. R., Adler, C., Corbalan, N. S., Paz Garcia, E. C., Pomares, M. F. & Vincent, P. A. 2016. Enterobactin as Part of the Oxidative Stress Response Repertoire. *PLoS One,* 11**,** e0157799. Available: DOI 10.1371/journal.pone.0157799.
88. Petersen, P. J., Labthavikul, P., Jones, C. H. & Bradford, P. A. 2006. In vitro antibacterial activities of tigecycline in combination with other antimicrobial agents determined by chequerboard and time-kill kinetic analysis. *J Antimicrob Chemother,* 57**,** 573-6. Available: DOI 10.1093/jac/dki477.
89. Planta, M. B. 2007. The role of poverty in antimicrobial resistance. *J Am Board Fam Med,* 20**,** 533-9. Available: DOI 10.3122/jabfm.2007.06.070019.
90. Raczkowska, A., Trzos, J., Lewandowska, O., Nieckarz, M. & Brzostek, K. 2015. Expression of the AcrAB Components of the AcrAB-TolC Multidrug Efflux Pump of *Yersinia enterocolitica* Is Subject to Dual Regulation by OmpR. *PLoS One,* 10**,** e0124248. Available: DOI 10.1371/journal.pone.0124248.
91. Rahal, J. J. 2006. Novel Antibiotic Combinations against Infections with Almost Completely Resistant *Pseudomonas aeruginosa* and *Acinetobacter* Species. *Clinical Infectious Diseases,* 43**,** 95-99.

92. Rahman, M. S., Pal, A. K. & Chatterjee, S. N. 1993. Induction of SOS like responses by nitrofurantoin in *Vibrio cholerae* el tor cells. *Arch Microbiol,* 159**,** 98-100.

93. Rendueles, O. & Ghigo, J. M. 2012. Multi-species biofilms: how to avoid unfriendly neighbors. *FEMS Microbiol Rev,* 36**,** 972-89. Available: DOI 10.1111/j.1574-6976.2012.00328.x.

94. Roe, D., Karandikar, B., Bonn-Savage, N., Gibbins, B. & Roullet, J. B. 2008. Antimicrobial surface functionalization of plastic catheters by silver nanoparticles. *J Antimicrob Chemother,* 61**,** 869-76. Available: DOI 10.1093/jac/dkn034.

95. Roldan, M. D., Perez-Reinado, E., Castillo, F. & Moreno-Vivian, C. 2008. Reduction of polynitroaromatic compounds: the bacterial nitroreductases. *FEMS Microbiol Rev,* 32**,** 474-500. Available: DOI 10.1111/j.1574-6976.2008.00107.x.

96. Rosner, J. L. & Martin, R. G. 2013. Reduction of cellular stress by TolC-dependent efflux pumps in *Escherichia coli* indicated by BaeSR and CpxARP activation of spy in efflux mutants. *J Bacteriol,* 195**,** 1042-50. Available: DOI 10.1128/JB.01996-12.

97. Shefer, S., Kren, B. T., Salen, G., Steer, C. J., Nguyen, L. B., Chen, T., Tint, G. S. & Batta, A. K. 1995. Regulation of bile acid synthesis by deoxycholic acid in the rat: Different effects on cholesterol 7α-hydroxylase and sterol 27-hydroxylase. *Hepatology,* 22**,** 1215-1221. Available: DOI http://dx.doi.org/10.1016/0270-9139(95)90631-2.

98. Seeger, M. A., Schiefner, A., Eicher, T., Verrey, F., Diederichs, K. & Pos, K. M. 2006. Structural asymmetry of AcrB trimer suggests a peristaltic pump mechanism. *Science,* 313**,** 1295-8. Available: DOI 10.1126/science.1131542.

99. Shlaes, D. M., Shlaes, J. H., Davies, J. & Williamson, R. 1989. *Escherichia coli* susceptible to glycopeptide antibiotics. *Antimicrob Agents Chemother,* 33**,** 192-7.

100. Singh, A. P., Prabha, V. & Rishi, P. 2013. Value addition in the efficacy of conventional antibiotics by Nisin against Salmonella. *PLoS One,* 8**,** e76844. Available: DOI 10.1371/journal.pone.0076844.

101. Smith, B. T., Grossman, A. D. & Walker, G. C. 2002. Localization of UvrA and Effect of DNA Damage on the Chromosome of *Bacillus subtilis*. *Journal of Bacteriology,* 184**,** 488-493. Available: DOI 10.1128/jb.184.2.488-493.2002.

102. Soto, S. M. 2014. Importance of Biofilms in Urinary Tract Infections: New Therapeutic Approaches. *Advances in Biology*, 2014**,** 1-13. Available: DOI 10.1155/2014/543974.

103. Spagnuolo, J., Opalka, N., Wen, W. X., Gagic, D., Chabaud, E., Bellini, P., Bennett, M. D., Norris, G. E., Darst, S. A., Russel, M. & Rakonjac, J. 2010. Identification of the gate regions in the primary structure of the secretin pIV. *Mol Microbiol,* 76**,** 133-50. Available: DOI 10.1111/j.1365-2958.2010.07085.x.

104. Sridharan, S., Howard, N., Kerbarh, O., Blaszczyk, M., Abell, C. & Blundell, T. L. 2010. Crystal structure of *Escherichia coli* enterobactin-specific isochorismate synthase (EntC) bound to its reaction product isochorismate: implications for the enzyme mechanism and differential activity of chorismate-utilizing enzymes. *J Mol Biol,* 397**,** 290-300. Available: DOI 10.1016/j.jmb.2010.01.019.

105. Stevens, K. N., Crespo-Biel, O., Van Den Bosch, E. E., Dias, A. A., Knetsch, M. L., Aldenhoff, Y. B., Van Der Veen, F. H., Maessen, J. G., Stobberingh, E. E. & Koole, L. H. 2009. The relationship between the antimicrobial effect of catheter coatings containing silver nanoparticles and the coagulation of contacting blood. *Biomaterials,* 30**,** 3682-90. Available: DOI 10.1016/j.biomaterials.2009.03.054.

106. Stewart, P. S. 2015. Antimicrobial Tolerance in Biofilms. *Microbiol Spectr,* 3. Available: DOI 10.1128/microbiolspec.MB-0010-2014.

107. Sun, J., Deng, Z. & Yan, A. 2014. Bacterial multidrug efflux pumps: mechanisms, physiology and pharmacological exploitations. *Biochem Biophys Res Commun,* 453**,** 254-67. Available: DOI 10.1016/j.bbrc.2014.05.090.

108. Takatsuka, Y. & Nikaido, H. 2009. Covalently linked trimer of the AcrB multidrug efflux pump provides support for the functional rotating mechanism. *J Bacteriol,* 191**,** 1729-37. Available: DOI 10.1128/JB.01441-08.

109. Tamae, C., Liu, A., Kim, K., Sitz, D., Hong, J., Becket, E., Bui, A., Solaimani, P., Tran, K. P., Yang, H. & Miller, J. H. 2008. Determination of antibiotic hypersensitivity among 4,000 single-gene-knockout mutants of *Escherichia coli*. *J Bacteriol,* 190**,** 5981-8. Available: DOI 10.1128/JB.01982-07.

110. Tang, J., Wennerberg, K. & Aittokallio, T. 2015. What is synergy? The Saariselka agreement revisited. *Front Pharmacol,* 6**,** 181. Available: DOI 10.3389/fphar.2015.00181.

111. Tangden, T. 2014. Combination antibiotic therapy for multidrug-resistant Gram-negative bacteria. *Ups J Med Sci,* 119**,** 149-53. Available: DOI 10.3109/03009734.2014.899279.

112. Thomas, M. G., Smith, A. J. & Tilyard, M. 2014. Rising antimicrobial resistance: a strong reason to reduce excessive antimicrobial consumption in New Zealand. *N Z Med J,* 127**,** 72-84.

113. Trautner, B. W. & Darouiche, R. O. 2004. Role of biofilm in catheter-associated urinary tract infection. *Am J Infect Control,* 32**,** 177-83. Available: DOI 10.1016/j.ajic.2003.08.005.

114. Tuomanen, E., Cozens, R., Tosch, W., Zak, O., and Tomasz, A. 1986. The rate of killing of *Escherichia coli* by β-lactam antibiotics is strictly proportional to the rate of bacterial growth. *Journal of General Microbiology,* 132**,** 1297-1304.

115. Vass, M., Hruska, K., and Franet, M. 2008. Nitrofuran antibiotics: a review on the application, prohibition and residual analysis. *Veterinarni Medicina,* 53**,** 469-500.

116. Vasudevan, R. 2014. Biofilms: Microbial Cities of Scientific Significance. *Journal of Microbiology & Experimentation,* 1. Available: DOI 10.15406/jmen.2014.01.00014.

117. Vega, D. E. & Young, K. D. 2014. Accumulation of periplasmic enterobactin impairs the growth and morphology of *Escherichia coli* tolC mutants. *Mol Microbiol,* 91**,** 508-21. Available: DOI 10.1111/mmi.12473.

118. Ventola, C. L. 2015. The antibiotic resistance crisis: part 1: causes and threats. *P T,* 40**,** 277-83.

119. Walzer, P. D., Kim, C. K., Foy, J. & Zhang, J. L. 1991. Furazolidone and nitrofurantoin in the treatment of experimental *Pneumocystis carinii pneumonia*. *Antimicrob Agents Chemother,* 35**,** 158-63.

120. Webber, M. A. 2002. The importance of efflux pumps in bacterial antibiotic resistance. *Journal of Antimicrobial Chemotherapy,* 51**,** 9-11. Available: DOI 10.1093/jac/dkg050.

121. Weeks, J. W., Celaya-Kolb, T., Pecora, S. & Misra, R. 2010. AcrA suppressor alterations reverse the drug hypersensitivity phenotype of a TolC mutant by inducing TolC aperture opening. *Mol Microbiol,* 75**,** 1468-83. Available: DOI 10.1111/j.1365-2958.2010.07068.x.

122. Whiteway, J., Koziarz, P., Veall, J., Sandhu, N., Kumar, P., Hoecher, B. & Lambert, I. B. 1998. Oxygen-insensitive nitroreductases: analysis of the roles of nfsA and nfsB in development of resistance to 5-nitrofuran derivatives in *Escherichia coli*. *J Bacteriol,* 180**,** 5529-39.

123. Williams, G. J. & Stickler, D. J. 2008. Effect of triclosan on the formation of crystalline biofilms by mixed communities of urinary tract pathogens on urinary catheters. *J Med Microbiol,* 57**,** 1135-40. Available: DOI 10.1099/jmm.0.2008/002295-0.

124. Worthington, R. J. & Melander, C. 2013. Combination approaches to combat multidrug-resistant bacteria. *Trends Biotechnol,* 31**,** 177-84. Available: DOI 10.1016/j.tibtech.2012.12.006.

125. Wright, G. D. 2007. The antibiotic resistome: the nexus of chemical and genetic diversity. *Nat Rev Microbiol,* 5**,** 175-86. Available: DOI 10.1038/nrmicro1614.

126. Wright, G. D. 2011. Molecular mechanisms of antibiotic resistance. *Chem Commun (Camb),* 47**,** 4055-61. Available: DOI 10.1039/c0cc05111j.

127. Wu, H., Moser, C., Wang, H. Z., Hoiby, N. & Song, Z. J. 2015. Strategies for combating bacterial biofilm infections. *Int J Oral Sci,* 7**,** 1-7. Available: DOI 10.1038/ijos.2014.65.

128. Xie, J., Pierce, J. G., James, R. C., Okano, A. & Boger, D. L. 2011. A redesigned vancomycin engineered for dual D-Ala-D-ala And D-Ala-D-Lac binding exhibits potent antimicrobial activity against vancomycin-resistant bacteria. *J Am Chem Soc,* 133**,** 13946-9. Available: DOI 10.1021/ja207142h.

129. Yarlagadda, V., Manjunath, G. B., Sarkar, P., Akkapeddi, P., Paramanandham, K., Shome, B. R., Ravikumar, R. & Haldar, J. 2016. Glycopeptide Antibiotic To Overcome the Intrinsic Resistance of Gram-Negative Bacteria. *ACS Infect Dis,* 2**,** 132-9. Available: DOI 10.1021/acsinfecdis.5b00114.

130. Yu, H., Sato, E. F., Nagata, K., Nishikawa, M., Kashiba, M., Arakawa, T., Kobayashi, K., Tamura, T. & Inoue, M. 1997. Oxygen-dependent regulation of the respiration and growth of *Escherichia coli* by nitric oxide. *FEBS Letters,* 409**,** 161-165. Available: DOI 10.1016/s0014-5793(97)00494-8.

131. Zgur-Bertok, D. 2013. DNA damage repair and bacterial pathogens. *PLoS Pathog,* 9**,** e1003711. Available: DOI 10.1371/journal.ppat.1003711.

132. Zgurskaya, H. I., Krishnamoorthy, G., Ntreh, A. & Lu, S. 2011. Mechanism and Function of the Outer Membrane Channel TolC in Multidrug Resistance and Physiology of Enterobacteria. *Front Microbiol,* 2**,** 189. Available: DOI 10.3389/fmicb.2011.00189.

133. Zhou, A., Kang, T. M., Yuan, J., Beppler, C., Nguyen, C., Mao, Z., Nguyen, M. Q., Yeh, P. & Miller, J. H. 2015. Synergistic interactions of vancomycin with different antibiotics against *Escherichia coli*: trimethoprim and nitrofurantoin display strong synergies with vancomycin against wild-type *E. coli*. *Antimicrob Agents Chemother,* 59**,** 276-81. Available: DOI 10.1128/AAC.03502-14.

8 Appendix 1. *tolC* operon

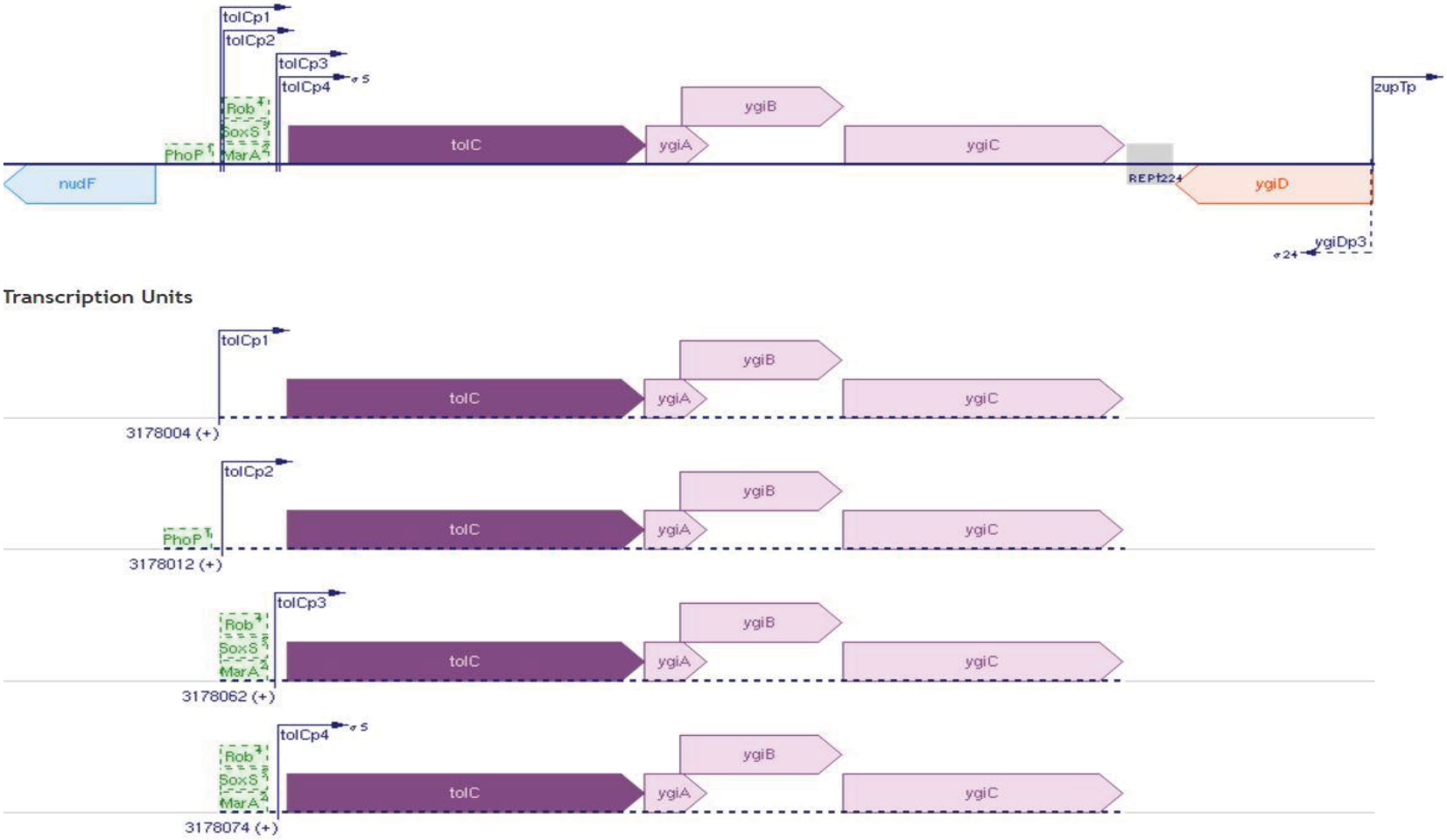

(Keseler et al., 2013)

9 Appendix 2. *acrA* operon

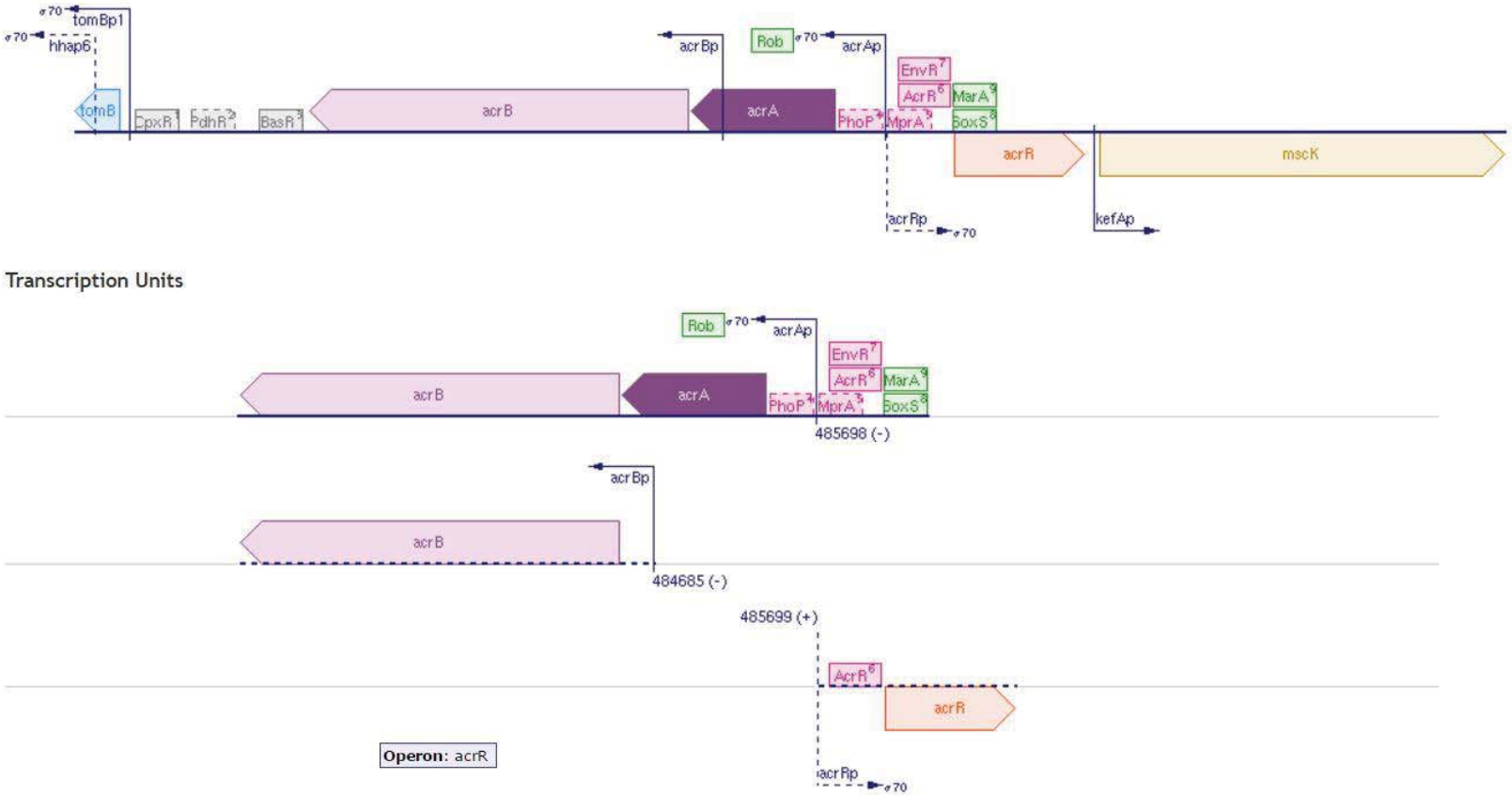

(Keseler et al., 2013)

10 Appendix 3. *entC* operon

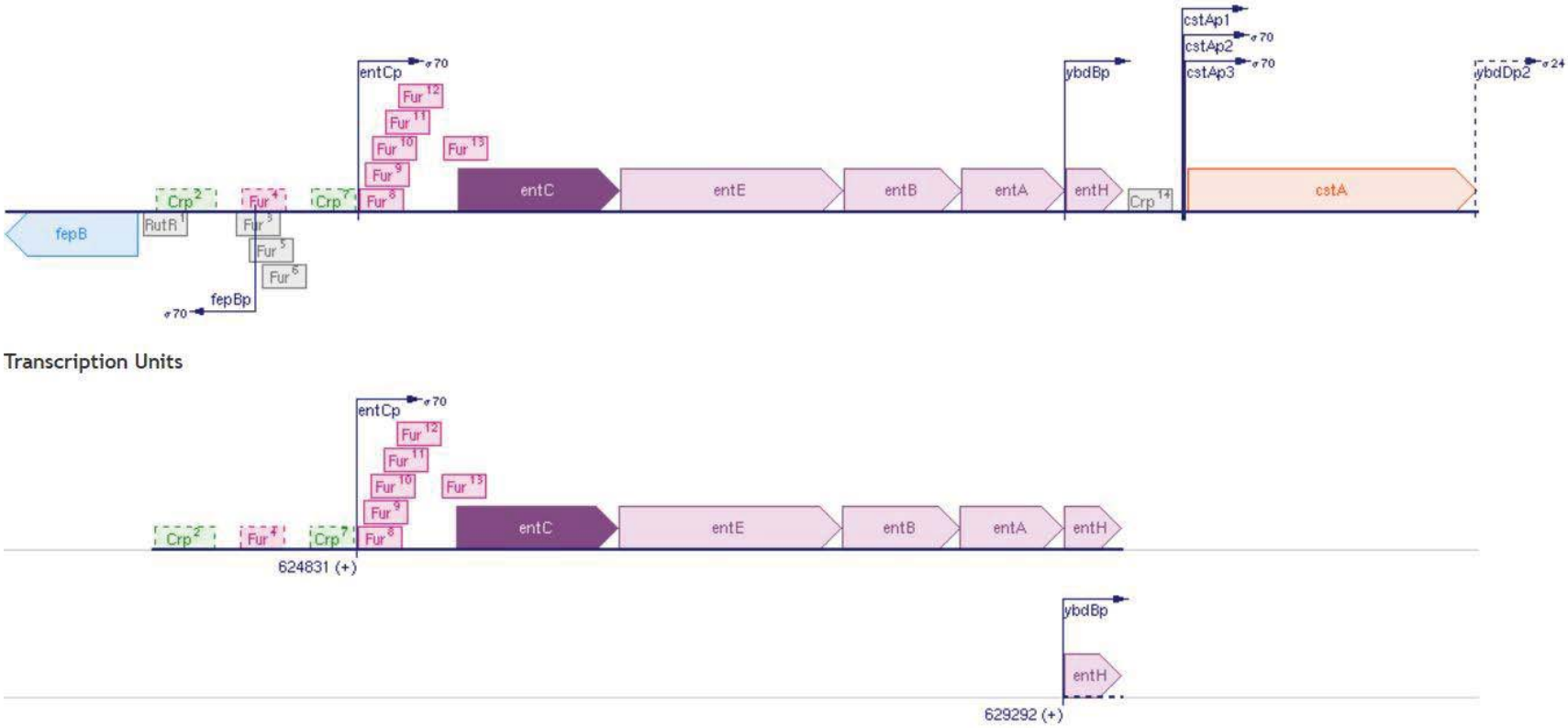

(Keseler et al., 2013)